Control of protein degradation pathways by BAG proteins and changes during aging

Dissertation zur Erlangung des Grades
"Doktor der Naturwissenschaften"

am Fachbereich Biologie der
Johannes Gutenberg-Universität
in Mainz

vorgelegt von
Martin Gamerdinger
geb. am 07. April 1978 in Horb am Neckar

Mainz, 2009

A SUMMARY

Many age-related neurodegenerative disorders such as Alzheimer's disease, Parkinson's disease, amyotrophic lateral sclerosis and polyglutamine disorders, including Huntington's disease, are associated with the aberrant formation of protein aggregates. These protein aggregates and/or their precursors are believed to be causally linked to the pathogenesis of such protein conformation disorders, also referred to as proteinopathies. The accumulation of protein aggregates, frequently under conditions of an age-related increase in oxidative stress, implies the failure of protein quality control and the resulting proteome instability as an upstream event of proteinopathies. As aging is a main risk factor of many proteinopathies, potential alterations of protein quality control pathways that accompany the biological aging process could be a crucial factor for the onset of these disorders.

The focus of this dissertation lies on age-related alterations of protein quality control mechanisms that are regulated by the co-chaperones of the BAG (Bcl-2-associated athanogene) family. BAG proteins are thought to promote nucleotide exchange on Hsc/Hsp70 and to couple the release of chaperone-bound substrates to distinct down-stream cellular processes. The present study demonstrates that BAG1 and BAG3 are reciprocally regulated during aging leading to an increased BAG3 to BAG1 ratio in cellular models of replicative senescence as well as in neurons of the aging rodent brain. Furthermore, BAG1 and BAG3 were identified as key regulators of protein degradation pathways. BAG1 was found to be essential for effective degradation of polyubiquitinated proteins by the ubiquitin/proteasome system, possibly by promoting Hsc/Hsp70 substrate transfer to the 26S proteasome. In contrast, BAG3 was identified to stimulate the turnover of polyubiquitinated proteins by macroautophagy, a catabolic process mediated by lysosomal hydrolases. BAG3-regulated protein degradation was found to depend on the function of the ubiquitin-receptor protein SQSTM1 which is known to sequester polyubiquitinated proteins for macroautophagic degradation. It could be further demonstrated that SQSTM1 expression is tightly coupled to BAG3 expression and that BAG3 can physically interact with SQSTM1. Moreover, immunofluorescence-based microscopic analyses revealed that BAG3 co-localizes with SQSTM1 in protein sequestration structures suggesting a direct role of BAG3 in substrate delivery to SQSTM1 for macroautophagic degradation. Consistent with these findings, the age-related switch from BAG1 to BAG3 was found to determine that aged cells use the macroautophagic system more intensely for the turnover of polyubiquitinated proteins, in particular of insoluble, aggregated quality control substrates. Finally, *in vivo* expression analysis of macroautophagy markers in young and old mice as well as analysis of the lysosomal enzymatic activity strongly indicated that the macroautophagy pathway is also recruited in the nervous system during the organismal aging process.

Together these findings suggest that protein turnover by macroautophagy is gaining importance during the aging process as insoluble quality control substrates are increasingly produced that cannot be degraded by the proteasomal system. For this reason, a switch from the proteasome regulator BAG1 to the macroautophagy stimulator BAG3 occurs during cell aging. Hence, it can be concluded that the BAG3-mediated recruitment of the macroauto-phagy pathway is an important adaptation of the protein quality control system to maintain protein homeostasis in the presence of an enhanced pro-oxidant and aggregation-prone milieu characteristic of aging. Future studies will explore whether an impairment of this adaptation process may contribute to age-related proteinopathies.

B INTRODUCTION

In biological systems proteins serve a wide variety of functions, such as building structure and mediating transport, signalling and metabolism. The specific function of a protein is defined by the unique three-dimensional folding structure which is encoded in the amino-acid sequence. The structural integrity of proteins is permanently challenged and must be maintained in the cellular environment to avoid protein misfolding and aggregation. For this reason, efficient adapting protein homeostasis (proteostasis) mechanisms have evolved that assist proper protein folding and eliminate irreversibly damaged proteins. Nevertheless, proteins with aberrant conformations accumulate in many age-related human degenerative diseases, implicating the loss of proteostatic control during aging as a central factor of pathogenesis. In the aging cellular environment the proteome is increasingly challenged by accumulating oxidative damage to which quality control systems must adapt. Understanding the accurate adaptation of the proteostasis network in aged cells is of fundamental relevance to combat age-associated protein conformational disorders.

B.1 Protein quality control (PQC)

Proteostasis is a term encompassing the right balance between protein synthesis, folding, refolding and degradation (Balch et al, 2008). This balance is maintained by fine-tuned protein quality control (PQC) pathways that can adapt to environmental changes. The intracellular PQC system basically consists of a molecular chaperone network that is tightly linked to protein biosynthesis and degradation machineries. These quality control mechanisms are essential to maintain protein function and to avoid protein misfolding and aggregation as specified in the following paragraphs.

B.1.1 Protein folding, misfolding and aggregation

Newly translated polypeptide chains must fold into distinct three-dimensional structures to become functional proteins. The native folding state of a protein is encoded in and determined by its amino-acid sequence, involves specific covalent or non-covalent intra- and sometimes intermolecular interactions and constitutes an energetically favourable state (Dobson & Karplus, 1999; Anfinsen, 1973). The current protein folding hypothesis states that a polypeptide bears a globally "funnelled energy landscape" that is largely directed towards the native conformation (Figure 1) (Dill et al, 2008). According to this model, a polypeptide chain could fold spontaneously to its biologically active state under appropriate conditions in

an adequate time period. However, the intracellular environment is disadvantageous for unassisted folding of proteins, in particular of large multi-domain proteins. Until a protein with a high structural complexity reaches its native conformation, it undergoes multiple metastable folding states (Figure 1). Proteins in intermediate folding states can expose hydrophobic amino-acid residues, which are buried in the native state inside the core of the protein, to the solvent (Dill et al, 2008). Such proteins are prone to aggregate due to unspecific hydrophobic interactions and hydrogen-bonding with other macromolecules. The tendency of a protein to interact unspecifically is increased in the highly crowded cytosol, which contains up to 400 mg/ml of proteins and other macromolecules (Hartl & Hayer-Hartl, 2002).

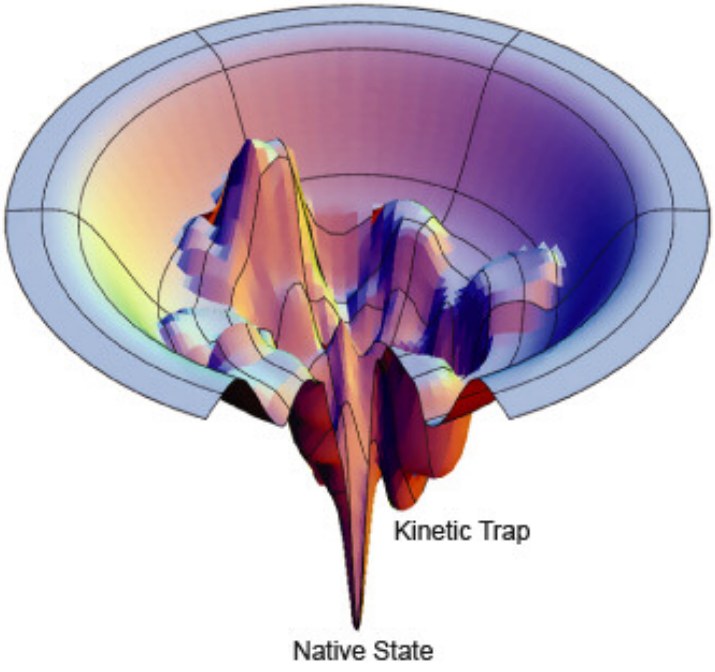

Figure 1: Folding funnel of a polypeptide chain. The folding funnel represents the whole energy landscape that can be explored by a protein as it folds into the native state. The native conformation is the most favourable energy state, but on the path to this conformation the polypeptide must get over some kinetic traps. In these metastable folding states proteins often expose hydrophobic surfaces to the solvent which allow unspecific intermolecular interactions and aggregation. Figure adapted from http://www.dillgroup.ucsf.edu.

The native conformation of a protein is an energetically favourable state, but it is by no means a solid structure. The functional state of a protein is in a dynamic equilibrium with metastable intermediate states (Ferreira et al, 2006). This means that in the crowded cellular environment also natively folded proteins can spontaneously unfold and tend to aggregate. Moreover, the protein aggregation potential critically increases, in particular, under stressful

conditions that lead to protein denaturation like heat and oxidative stress (Ferreira et al, 2006).

For the above-mentioned reasons, efficient PQC pathways have evolved in prokaryotic and eukaryotic cells. To control protein quality cells employ a large arsenal of molecular chaperones (for overview see Figure 5) and protein degradation systems that specifically eliminate irreversibly damaged proteins. These systems are highly effective to maintain proteostasis under normal conditions and can adapt to environmental perturbations that increase the amount of aggregate-prone protein species, as described consecutively.

B.1.2 Protein degradation systems

To maintain proteostasis, irreversibly damaged proteins must be detected and transferred to protein degradation systems for elimination. Regulated protein turnover in cells is mainly achieved by selective attachment of a degradation signal to damaged proteins. The degradation signal is then bound either directly by the degradation complex or by receptor proteins which direct the quality control substrate to intracellular protein turnover pathways. For the degradation of defective proteins cells use mainly two different degradation systems: the proteasome and the autophagy machinery.

B.1.2.1 Ubiquitination as a degradation signal

Misfolded proteins are directed to intracellular protein degradation systems when a native folding state cannot be reached. In this case the damaged protein is generally marked for degradation by covalent attachment of multiple ubiquitin moieties. Ubiquitin, a highly conserved and ubiquitously expressed protein with low molecular weight (8 kDa), is transferred to a substrate by forming an isopeptide bond between a lysine residue of the target protein and the glycine at the exposed C-terminal tail of ubiquitin (Figure 2). The ubiquitination reaction is performed by the sequential action of an E1 ubiquitin-activating enzyme, an E2 ubiquitin-conjugating enzyme and, finally, an E3 ubiquitin-ligase which covalently links the ubiquitin molecule directly to the target substrate or to an already attached ubiquitin molecule for polyubiquitin chain elongation (Sowa & Harper, 2006). Generally, a polyubiquitin chain consisting of at least four moieties is sufficient for labelling a target protein for degradation (Thrower et al, 2000).

Ubiquitin has a total of seven lysine residues that all can be used to form isopeptide linkages to the C-terminal glycine of a second ubiquitin molecule (Figure 2) (Sowa & Harper, 2006).

The best studied are K48- and K63-linked polyubiquitin chains and it has been shown that these different chain types may determine in which way a target substrate is preferentially degraded (Tan et al, 2008; Thrower et al, 2000). Furthermore, differently linked polyubiquitin chains and mono-ubiquitination serve, in addition to a degradation signal, to regulate diverse other cellular processes such as gene activity, DNA repair, protein transport and many signalling pathways (Marx, 2002; Tenno et al, 2004).

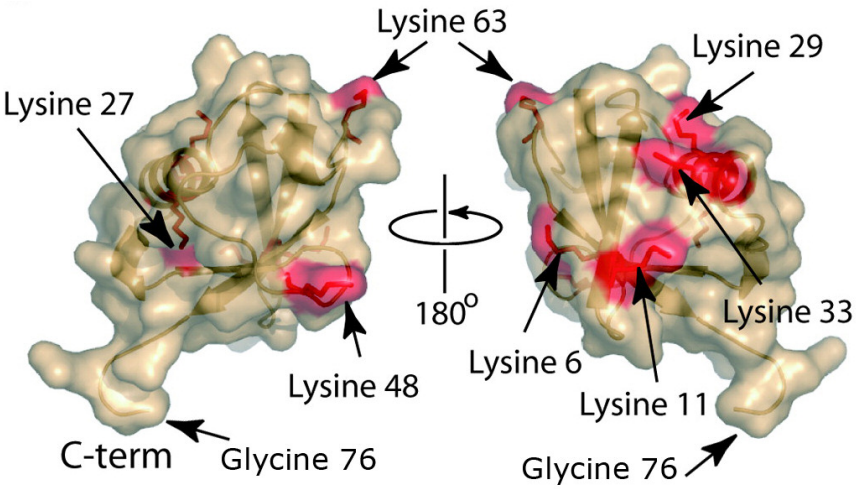

Figure 2: Structure of Ubiquitin. Ubiquitin is small protein consisting of 76 amino-acids and has a compact structure. At the exposed C-terminal tail a glycine residue is found, which is used to form an isopeptide linkage with a lysine of either a substrate or a second ubiquitin molecule. Ubiquitin has seven lysine residues (K6, K11, K27, K29, K33, K48 and K63), which can be used as linkage points for polyubiquitin chain elongation. Figure adapted from Mathew and Wade (2006).

B.1.2.2 The ubiquitin/proteasome system

The ubiquitin/proteasome system is the main degradation pathway for polyubiquitinated proteins (consecutively referred to as polyUb-proteins). In this pathway polyUb-proteins are transferred to and degraded by the proteasome, a ~2000 kDa large barrel-shaped protein complex located in the cytoplasm and nucleus that performs fast proteolysis reactions (Reits et al, 1997; Yoshimura et al, 1993). The 26S (*S* denotes Svedberg sedimentation coefficient) proteasome is formed by two subcomponents: the 20S core particle and the regulatory 19S subunit (Figure 3). The barrel-shaped 20S core complex consists of four stacked rings and each ring is composed of seven individual protein subunits. The two structure-giving outer rings are formed by seven α-subunits whereas the two catalytic inner rings are assembled by seven β-subunits. The β-subunits contain the proteolytic active sites which are exposed to the interior surface of the rings and line the central pore (Baumeister et al, 1998). Thus, a protein must enter the central cavity of the proteasome before it can be degraded. The inner chamber of the proteasome is at most 53 Å wide, but the entrance channel can be as narrow

as 13 Å (Nandi et al, 2006), suggesting that only unfolded proteins can be degraded by the proteasome since a folded globular protein would not fit through the narrow entrance channel.

Unfolding of proteasome substrates is regulated by the 19S particle (Navon & Goldberg, 2001). The 19S particle consists of at least nineteen different subunits that form an asymmetrical structure composed of two sub-components, the base and the lid (Figure 3) (Sharon et al, 2006). The base binds to the outer α-ring of the 20S particle, whereas the lid is thought to bind polyubiquitin chains. The base contains several ATPase units which stimulate assembly of the 26S proteasome complex upon ATP binding (Liu et al, 2006). ATP hydrolysis is required for substrate unfolding. During or after substrate unfolding, the 19S particle relocates and opens the gate to the destruction chamber. The proteasome substrate is then deubiquitinated and translocates into the proteolytic core, where the substrate is fragmented to peptides of about seven to eight amino-acids in length (Zhu et al, 2005). These peptides are then further degraded into single amino-acids by cytosolic peptidases.

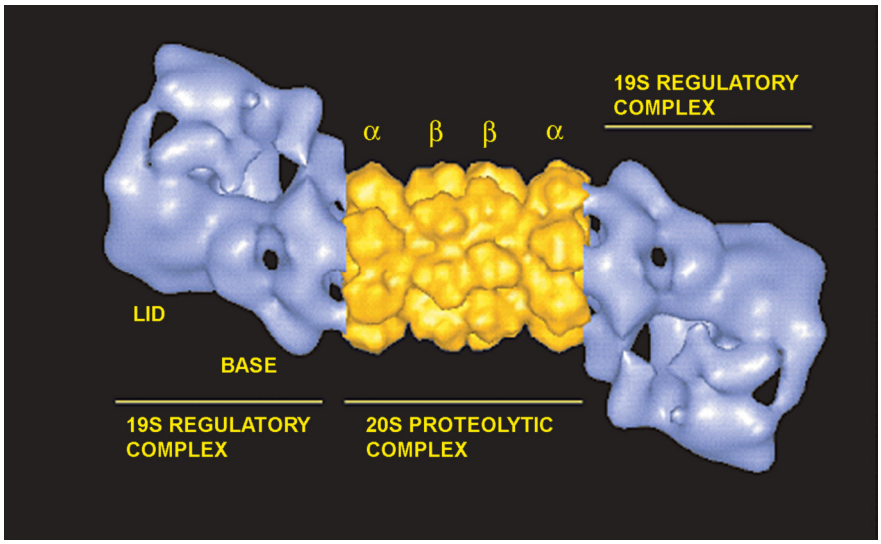

Figure 3: Structure of the 26S proteasome. The 26S proteasome is composed of the 20S core complex and two 19S regulatory complexes. The barrel-shaped 20S complex consists of four stacked rings and each ring is composed of seven subunits. The inner two rings are formed by β-subunits which expose the proteolytic active sites to the interior surface. The two outer rings are assembled by α-subunits and interact with the base, a sub-component of the 19S regulatory complex. In addition to the base, the 19S complex is formed by the lid sub-component, which interacts with polyubiquitin chains. Figure adapted from Baumeister et al, 1998.

It has been proposed that the 19S particle in particular has a high affinity to polyubiquitin chains linked via K48 of ubiquitin, suggesting that K48-polyUb-proteins are the preferred substrates of the proteasome (Schmidt et al, 2005). The 19S particle represents not only the

docking site for polyUb-proteins but also for ubiquitin-receptor proteins. Ubiquitin-receptor proteins possess ubiquitin-like domains (UBL) which enables their binding to the 19S particle of proteasomes without being self degraded. Several studies suggest that such ubiquitin-receptor proteins escort polyUb-proteins to the proteasome (Elsasser & Finley, 2005). Such an “escort service” is thought to prevent protein aggregation while substrates are en route to the proteasome. However, these pathways are poorly understood and it is unknown whether distinct sets of proteins or even all proteasome substrates are transferred to the proteasome by escorting proteins.

B.1.2.3 Autophagy

Besides the ubiquitin/proteasome system cells employ different autophagy (from the Greek, meaning “self-eating”) pathways for degradation of quality control substrates. The main characteristic of autophagic processes is the involvement of lysosomes in the degradation process. Lysosomes are acidic organelles with pH 4.5 - 4.8 that contain a wide variety of digestive enzymes including proteases, carbohydrases, lipases and nucleases that all show a work-optimum at acidic pH (Kurz et al, 2008). The term autophagy encompasses three different catabolic pathways in which the degradation of cytoplasmic components occurs through the lysosomal machinery: macroautophagy, microautophagy and chaperone-mediated autophagy (Mizushima, 2007).

B.1.2.3.1 Macroautophagy

In the macroautophagy pathway damaged proteins are handled and degraded in a way distinct from the ubiquitin/proteasome system. Proteins, but also other cytoplasmic constituents like lipids and whole organelles, are first engulfed by a double-layered membrane, called the isolation membrane. The resultant cargo containing vesicle, the autophagosome, then fuses with lysosomes whereupon the content is degraded by lysosomal hydrolases (Figure 4) (Mizushima, 2007). This special degradation pathway can also cope with insoluble and aggregated proteins. This is a great advantage over the ubiquitin/proteasome pathway in which substrates must be in soluble form and unfolded before degradation (Ding & Yin, 2008).

The exact origin of the isolation membrane is still a matter of discussion, but it is likely that the endoplasmic reticulum could be the source (Touret et al, 2005). The initiation of autophagosome formation in eukaryotes is primarily regulated by the class III phospho-

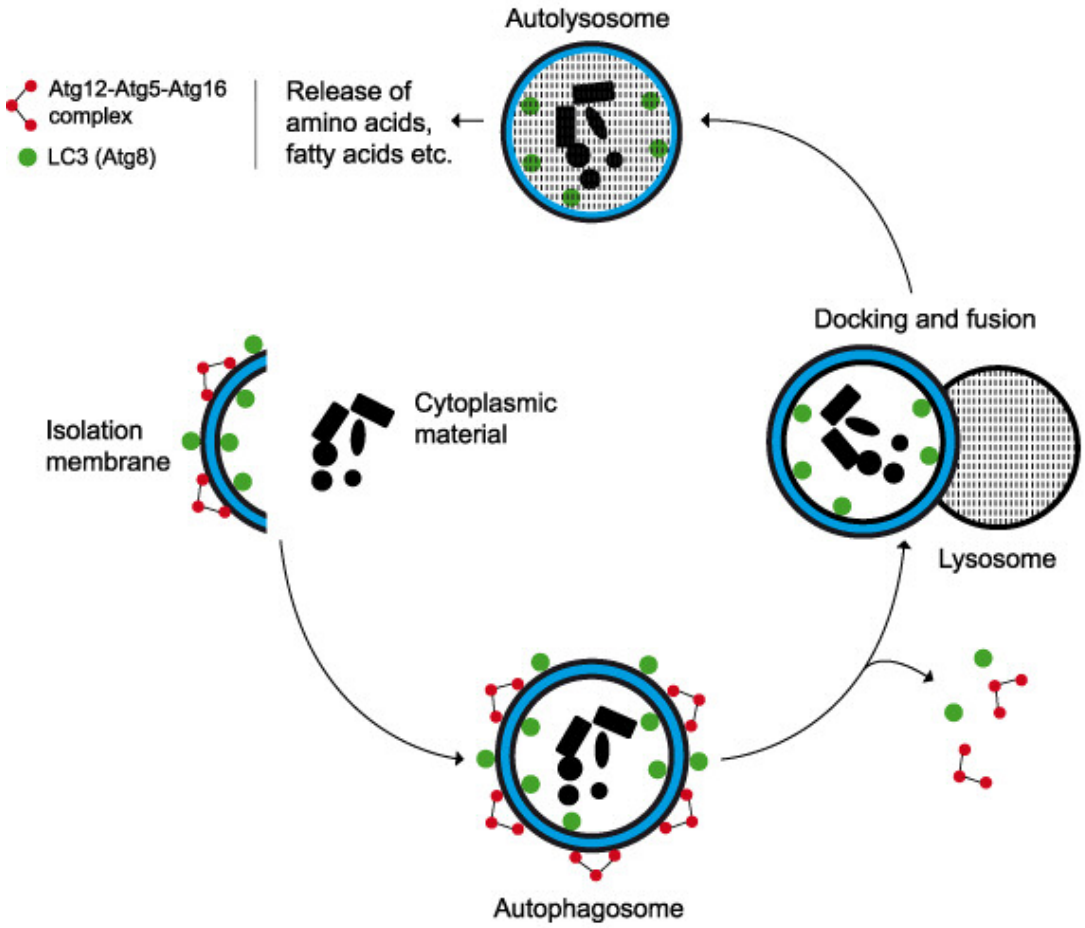

Figure 4: Macroautophagy. In the macroautophagy pathway cytoplasmic constituents are first engulfed by a double-layered isolation membrane. Recruitment of the isolation membrane and maturation of the autophagosome depends on association of LC3 and a complex consisting of Atg12-Atg5-Atg16 with the membrane. Upon completion of the autophagosome, the Atg12-Atg5-Atg16 complex and LC3 dissociate from the exterior membrane, whereas LC3 remains associated with the interior membrane. The mature autophagosome then fuses with lysosomes to autolysosomes, where the cargo together with the interior membrane is degraded by lysosomal hydrolases.

inositide 3-kinase beclin-1 (also termed autophagy-related gene 6, Atg6) which activates several macroautophagy-related proteins (Pattingre et al, 2008). The molecular machinery involved in autophagosome formation is evolutionarily conserved from yeast to higher eukaryotes (Yorimitsu & Klionsky, 2005). LC3 (also known as Atg8), a key protein involved in the assembly of autophagosomes, is first cleaved by the cysteine protease Atg4 resulting in the cytosolic form LC3-I. When macroautophagy is induced, LC3-I is lipidated to LC3-II by an Atg7- and Atg3-driven ubiquitin-like conjugation system which attaches phosphatidylethanolamine (PE) to LC3-I. LC3-II then strongly associates with the exterior and the interior membrane of autophagosomes. Functional analysis of LC3-II suggested an important function, in particular, in the completion of autophagosome formation (Fujita et al, 2008). For expansion of the autophagosome membrane a multimeric complex composed of Atg12-Atg5-Atg16 is required. Although the Atg12-Atg5-Atg16 complex has been shown to

be essential for autophagosome formation, the molecular function of this complex is still unknown. Once the autophagosome is completed, the Atg12-Atg5-Atg16 complex dissociates from the isolation membrane. LC3-II from the exterior lipid layer can be released by Atg4-mediated PE deconjugation. In contrast, LC3-II bound at the interior membrane remains associated with the mature autophagosome and is degraded together with the cargo upon fusion with lysosomes. Thus, LC3-II itself constitutes a substrate of the macroautophagy pathway and is therefore widely used to monitor macroautophagy activity (Mizushima & Yoshimori, 2007; Yorimitsu & Klionsky, 2005).

Macroautophagy was thought for a long time to be merely an unspecific general bulk degradation process in which cytoplasmic components are randomly engulfed by a membrane and transferred to lysosomes for degradation (Yorimitsu & Klionsky, 2005). Furthermore, as macroautophagy is induced upon starvation, it has been suggested that the sole physiological role of macroautophagy is to supply the cell with amino-acids, lipids and energy substrates under conditions of nutrient deprivation. However, in recent years it has been demonstrated that constitutive basal activity of macroautophagy is indispensable for maintenance of protein homeostasis. The fact that macroautophagy has essential functions in PQC was shown by tissue-specific ablation of Atg5 or Atg7, two essential genes for macroautophagy, in the central nervous system and the liver of mice (Komatsu et al, 2006; Hara et al, 2006; Komatsu et al, 2005). In these tissues, suppression of macroautophagy resulted in severe degenerative phenotypes involving the accumulation of ubiquitin-positive protein aggregates. In accord with these findings, recent work demonstrated that polyUb-proteins can be degraded selectively by macroautophagy involving the ubiquitin-receptor protein SQSTM1 (Bjørkøy et al, 2009; Pankiv et al, 2007). Interestingly, it has been shown that SQSTM1 preferentially binds K63-linked polyubiquitin chains, suggesting that substrate specificity of the ubiquitin/proteasome system and macroautophagy might be determined by different ubiquitin linkages (Tan et al, 2008). Together these observations led to the current hypothesis that in addition to the ubiquitin/proteasome system cells employ the macroautophagy pathway for degradation of ubiquitinated quality control substrates and that both degradation pathways complement one another and are both essential to sustain proteostasis.

B.1.2.3.2 Microautophagy

In the microautophagy pathway lysosomes directly engulf portions of cytoplasm or of organelles either by invagination of the lysosomal membrane or by septation or protrusion of arm-like structures (Uttenweiler & Mayer, 2008). Thus, in contrast to macroautophagy the

sequestration process during microautophagy proceeds without formation of transport vesicles and their fusion with lysosomes. Microautophagy has been observed in a large number of cell types from a variety of eukaryotic organisms. However, the molecular details and physiological importance of this pathway have not yet been elucidated in detail.

B.1.2.3.3 Chaperone-mediated autophagy

Chaperone-mediated autophagy (CMA) is a selective form of autophagy involving the lysosomal membrane-associated receptor LAMP2A. This receptor binds preferentially proteins that contain a penta-peptide lysosome-targeting motif with the consensus sequence KFERQ. After binding of KFERQ-like proteins to LAMP2A the substrate is unfolded and translocates across the lysosomal membrane to reach the lysosomal matrix where it is degraded (Massey et al, 2006). Substrate unfolding is mediated in a concerted action involving the intralysosomal heat-shock cognate 73 (lyHsc73) and a cytosolic chaperone/co-chaperone complex which has been shown to contain Hsp90, Hsc/Hsp70, Hsp40, Hop, Hip, and BAG1 (these chaperones and co-chaperones are described below) (Majeski & Dice, 2004). However, whether all these chaperones and co-chaperones participate in the CMA pathway has so far not been investigated in detail. Also the physiological role of CMA is largely unknown. The CMA pathway is activated upon nutrient starvation, but only in late stages of starvation. In early stages, macroautophagy is activated and CMA is suppressed (Finn & Dice, 2006). However, the molecular basis and physiological role of the switch from macroautophagy to CMA in late stages of starvation is unknown. Furthermore, CMA is up-regulated under mild oxidative stress conditions and has been implicated in the removal of oxidized KFERQ-like proteins (Kiffin et al, 2004). This finding may suggest a function also for CMA in PQC in addition to the ubiquitin/proteasome system and the macroautophagy pathway.

B.1.3 Chaperone networks

Above described protein turnover pathways are essential to maintain the cellular proteostasis as they eliminate irreversibly damaged proteins. As discussed, protein turnover can be carried out in a selective manner by attaching ubiquitin degradation signals specifically to misfolded proteins. But how are misfolded proteins recognized, and what is the molecular basis for discriminating irreversibly damaged proteins from transiently unfolded ones? Detailed analysis of protein folding mechanisms demonstrated that molecular chaperones have a major role in this discrimination process.

Molecular chaperones are specialized proteins capable to prevent non-native intra- and intermolecular interactions of unfolded proteins. Chaperones bind with high affinity to solvent-exposed, unstructured and hydrophobic regions of non-native proteins (Hartl & Hayer-Hartl, 2002). Through this binding chaperones shield cohesive-hydrophobic surfaces of an unfolded polypeptide from other macromolecules and prevent protein aggregation. The chaperoned substrate is thereby enabled to fold properly into the native three-dimensional structure. Substrate binding and release by chaperones is regulated by an ATP-consuming cycle which regulates the affinity of a chaperone to its substrate (Hartl & Hayer-Hartl, 2002). A main characteristic of many molecular chaperones is their up-regulation under protein denaturating conditions like heat stress. For this reason, many chaperones are referred to as heat-shock proteins (Hsp) (for overview see Chang et al, 2007; Tang et al, 2007).

	Chaperone	Localization	Co-chaperone/Co-factor
Hsp70 System	Hsc/Hsp70	Cytosol	Hsp40, Hop, Hip, BAG1-6, Hsp110, CHIP, HspBP1, SGT, TPR1, Tom70
	Hsp110	Cytosol	Hsc/Hsp70
	Grp78/Bip	ER	Grp170, Sil1
	mtHsp70	Mitochondria	
Hsp90	Hsp90	Cytosol	Hsc/Hsp70, Hop, Hip, p50, p23, CHIP, HspBP1, Sgt1, TPR2, Immunophilins
	Grp94	ER	Grp78
Hsp40	Hsp40	Cytosol	Hsc/Hsp70, Hip
	Hdj2	Cytosol	Hsc/Hsp70, Hip
	Auxilin	Cytosol	Hsc/Hsp70
Chaperonins	Group I mtHsp60	Mitochondria	Hsp10
	Group II TRiC/CCT	Cytosol	Prefoldin/GimC, PhLP
small Hsp	Hsp27	Cytosol	
	α-crystallin	Cytosol (lens)	
others	Calnexin	ER	ERp57, EDEM
	Calreticulin	ER	ERp57, EDEM
	Hsp47	ER	P4H

Figure 5: Overview of molecular chaperone systems in mammals. Molecular chaperones interact with a large group of co-chaperones as well as other co-factors. Together these proteins form a close-meshed chaperone network that affords correct protein folding and protein homeostasis. Figure adapted from Chang et al, 2007 and Tang et al, 2007.

B.1.3.1 Chaperone-assisted protein folding pathways

Several distinct chaperone classes exist in eukaryotes, including the Hsp families Hsp40, Hsp70 and Hsp90 (for overview see Figure 5). In addition to these protein families, the chaperone network encompasses a diverse group of small Hsps (12 to 43 kDa in size), ribosome-associated chaperones (e.g. NAC) and two groups of multimeric cylindrical chaperone complexes referred to as chaperonins (Chang et al, 2007, Tang et al, 2007). Together with multiple binding factors and co-chaperones, a fine-meshed and functional chaperone network is formed which supports the folding and refolding of proteins. Analysis of chaperone-assisted folding of model substrates revealed that different chaperone pathways exist that cope with the folding diversity of proteins. The majority of small proteins may fold without assistance of molecular chaperones. About 15 to 20% of proteins are thought to be folded by assistance of Hsc/Hsp70 and Hsp40. A small fraction of these proteins, mostly larger proteins composed of multiple domains require additional folding assistance by Hsp90. About 10 to 15% of total proteins are slow-folding and aggregation-sensitive proteins which require the action of chaperonins for native folding (Hartl & Hayer-Hartl, 2002).

B.1.3.2 Chaperone-assisted protein degradation pathways

The main chaperone systems (Hsc/Hsp70, Hsp90, chaperonins) are interconnected by a large group of co-chaperones and co-regulators (prefoldin, Hop, small heat-shock proteins etc.). By coordinated substrate transfer between the different chaperone systems a close-meshed cellular chaperone network is formed that afford productive folding pathways for the diversity of cellular proteins. However, in addition to support protein folding, the molecular chaperone network is thought to regulate also substrate transfer to protein degradation systems. In this context, molecular chaperones are thought to sense damaged proteins and direct them to protein degradation systems when refolding fails (Arndt et al, 2007). How chaperones regulate this triage decision between substrate folding and degradation is poorly understood. However, recent studies of eukaryotic Hsc/Hsp70 activity suggested that co-chaperones of the BAG family and other co-factors may play an important role in regulating the degradation activity of the chaperone (Höhfeld et al, 2001).

B.1.3.3 The Hsc/Hsp70 System

Hsc/Hsp70 chaperones have two functionally coupled domains, a 44 kDa N-terminal ATPase domain and a 27 kDa C-terminal substrate binding domain (Bukau & Horwich, 1998). The affinity of the C-terminal domain to a substrate is regulated by binding and hydrolysis of ATP by the N-terminal domain (Figure 6). In the ATP bound state, Hsc/Hsp70 shows rapid

substrate association and dissociation kinetics. Hydrolysis of the bound ATP to ADP stabilizes the interaction of Hsc/Hsp70 with a substrate. Release of bound ADP from Hsc/Hsp70 and rebinding of ATP triggers the dissociation of the chaperone-substrate complex and the release of the substrate (Frydman, 2001). The polypeptide chain then may fold to the native state, undergo another Hsc/Hsp70 reaction cycle or is directed to degradation. Through such ATP-controlled cycles of substrate binding and release, potential aggregate-prone proteins are shielded until a proper folding state or, when folding fails, protein degradation is reached. The cycles of substrate binding and release are regulated in addition to ATP by a divergent class of co-chaperones which stimulate ATP hydrolysis and nucleotide exchange, as described in the following sections.

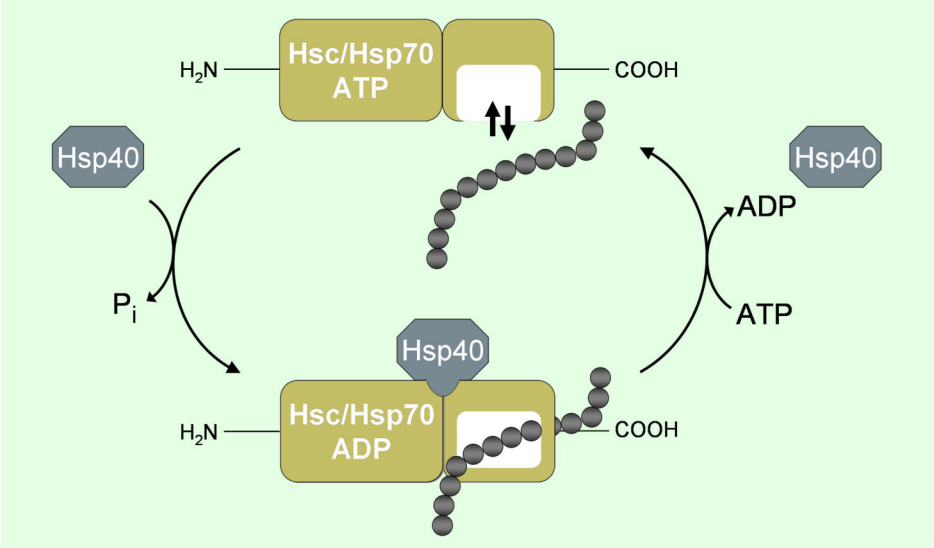

Figure 6: Hsc/Hsp70 folding cycle in eukaryotes. Hsc/Hsp70 chaperones have two functionally coupled domains, an N-terminal ATPase domain and a C-terminal substrate binding domain. In the ATP-bound conformation Hsc/Hsp70 exhibits rapid substrate association and dissociation kinetics. Binding of Hsp40 to Hsc/Hsp70 stimulates hydrolysis of bound ATP to ADP resulting in an Hsc/Hsp70 conformation with high substrate affinity. ADP to ATP exchange triggers dissociation of the Hsc/Hsp70-substrate complex and the release of the substrate. The substrate then may fold or undergo another Hsc/Hsp70 reaction cycle. Although nucleotide exchange on Hsc/Hsp70 in eukaryotes can occur in the absence of co-factors, several co-chaperones exist that modulate this process.

B.1.3.4 Hsc/Hsp70 co-chaperones

Although Hsp40 is sufficient to drive the Hsc/Hsp70 reaction cycle in the eukaryotic cytosol there are several other regulatory factors that modulate Hsc/Hsp70 chaperone function. For example, the Hsc/Hsp70 co-factor Hip binds to the ATPase domain of Hsc/Hsp70 and stabilizes the ADP-bound state of Hsc/Hsp70, thereby preventing substrate release from the chaperone (Höhfeld & Jentsch, 1997). Hip belongs to a group of chaperone modulators

which possess a characteristic chaperone-binding motif known as the tetratricopeptide repeats (TPR). Another member of the TPR family of co-chaperones is Hop. The TPR domain of Hop allows binding to the eukaryote-specific EEVD sequence located at the C-terminus of Hsc/Hsp70 (Figure 7) (Hartl & Hayer-Hartl, 2002). Hop possesses two TPR motifs that enable simultaneous binding to Hsc/Hsp70 and Hsp90 thereby facilitating substrate transfer between the two chaperone systems (Chen & Smith, 1998; Johnson et al, 1998). A further co-factor which binds the EEVD sequence of Hsc/Hsp70 via the TPR motif is the E3 ubiquitin ligase CHIP (C-terminus of Hsc/Hsp70-interacting protein). CHIP is the first discovered E3 ubiquitin ligase that binds to chaperones showing that the chaperone network is directly linked to the protein degradation machinery (Demand et al, 2001; Connell et al, 2001).

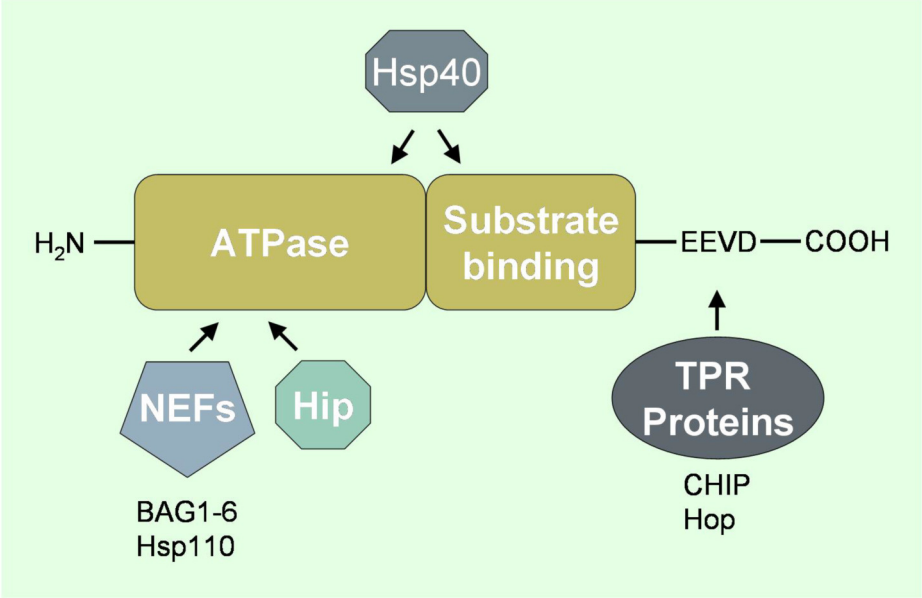

Figure 7: Eukaryotic Hsc/Hsp70 chaperone activity is modulated by diverse co-chaperones and co-regulators. Domain organization of eukaryotic cytosolic Hsc/Hsp70 chaperones. Interaction sites with co-chaperones and co-regulators are shown schematically. Nucleotide exchange factors (NEFs), such as the BAG proteins, bind to the ATPase domain of Hsc/Hsp70 and mediate ADP to ATP exchange. Binding of Hsp40 to Hsc/Hsp70 stimulates ATP hydrolysis resulting in the ADP-bound state of Hsc/Hsp70. The C-terminal EEVD sequence is specific for eukaryotic Hsc/Hsp70s and is involved in binding of a group of Hsc/Hsp70 co-regulators possessing the TPR domain like the E3 ubiquitin ligase CHIP.

Furthermore, several TPR-independent acting co-chaperones exist in the eukaryotic cytosol which can modulate Hsc/Hsp70 function. One such group is the Hsp110 family. These proteins bind to the ATPase domain of Hsc/Hsp70 and stimulate ADP to ATP exchange on Hsc/Hsp70 (Polier et al, 2008; Dragovic et al, 2006). Hsp110 proteins themselves are Hsc/Hsp70 homologues with chaperoning activity containing an ATPase domain and a

substrate binding domain. The dual activity of Hsp110 to chaperone as well as to catalyze nucleotide exchange on Hsc/Hsp70 suggests that Hsp110 forms a high-efficient chaperoning complex in conjunction with Hsc/Hsp70 in which substrates are efficiently folded or even disaggregated by cycling between both chaperones. Another important group of Hsc/Hsp70 co-chaperones are proteins of the BAG (Bcl-2-associated athanogene) protein family. BAG proteins are thought to mediate nucleotide exchange on Hsc/Hsp70 thereby targeting chaperone substrates to downstream cellular processes (Takayama & Reed, 2001; Höhfeld & Jentsch, 1997). The human BAG family and their known functions are summarized in the following paragraphs.

B.1.3.5 The BAG protein family of Hsc/Hsp70 co-regulators

BAG (Bcl-2-associated athanogene) proteins are characterized by their eponymous BAG domains which allow them to interact with and regulate Hsc/Hsp70. The BAG domain is evolutionary conserved and BAG homologues are found in yeast (*Saccharromyces cerevisiae*, *Schizosaccharromyces pombe*), invertebrates (*Caenorhabditis elegans*, *Drosophila melanogaster*), amphibians (*Xenopus laevis*), mammals (human, mouse, rat) and plants (*Arabidopsis thaliana*, *Oryza sativa*) (Takayama & Reed, 2001). Several BAG proteins were identified to promote survival under stress conditions, suggesting that the BAG family generally constitute an evolutionary conserved group of proteins acting as anti-apoptotic and pro-survival factors (Kabbage & Dickman, 2008).

The human BAG family contains at least six members (for overview see Figure 8A) (Takayama & Reed, 2001). The BAG domain is located near the C-terminus of human BAG family members, except BAG5 which contains four putative BAG domains distributed throughout the protein. Co-crystallization analysis of the eukaryotic Hsc70 ATPase domain and the BAG domain of BAG1 revealed that BAG binding remodels Hsc70 ATPase domain into a conformation incompatible for nucleotide binding (Figure 8B) (Sondermann et al, 2001). The structural data together with chaperone substrate release studies strongly suggest that binding of BAG proteins to Hsc/Hsp70 promotes nucleotide exchange on Hsc/Hsp70 and the dissociation of the chaperone-substrate complex. This raises the possibility that the BAG-mediated release of chaperone substrates is coupled to downstream cellular processes (Takayama & Reed, 2001). In other words, BAG proteins could modulate different chaperone-dependent cellular processes by determining the subcellular location of chaperone substrate release. According to a function in targeting molecular chaperones and their substrates to different cellular processes, BAG proteins possess different interaction

motifs in their N-terminal region which confer distinct localization or specific protein interactions (Figure 8).

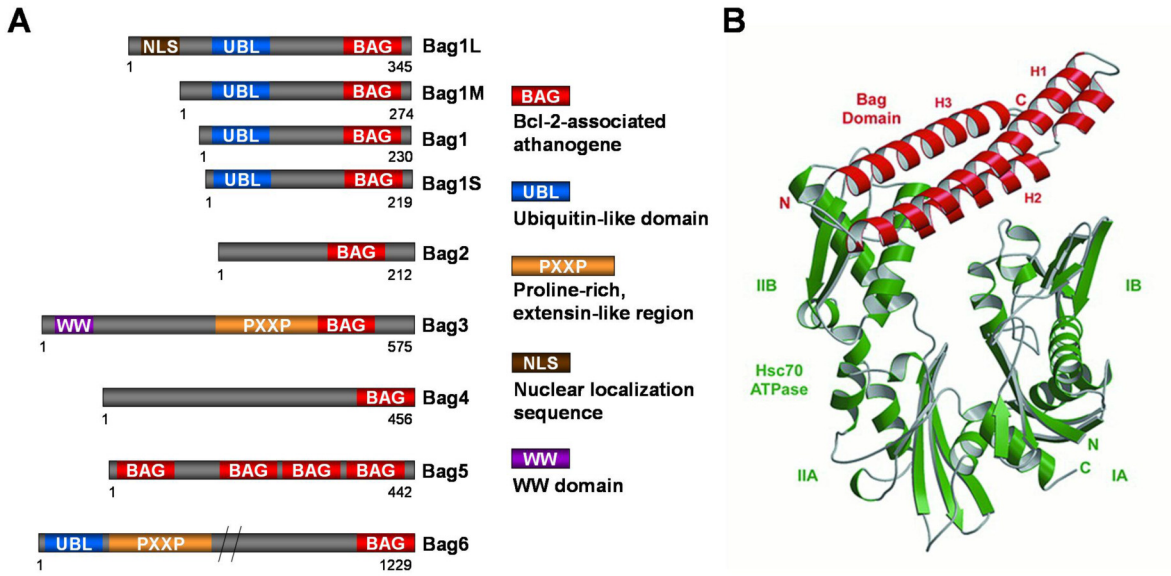

Figure 8: The human family of BAG (Bcl-2-associated athanogene) proteins. (**A**) In humans at least six genes coding for proteins containing a BAG domain were identified. BAG1 is expressed as four isoforms that differ in their N-terminal region. In addition to the BAG domain, which confers binding to Hsc/Hsp70, several other protein interaction motifs were found in human BAG proteins. The UBL (ubiquitin-like domain) is thought to mediate linkage of BAG protein to the proteasome. The PXXP (proline-rich region) found on BAG3 and BAG6 is a candidate docking site for interaction with SH3 domain proteins like PLCγ. BAG1L features a NLS (nuclear localization sequence) which determines predominant localization of this BAG1 isoform within the nucleus. A WW domain, which generally binds proline-rich ligands, is found on BAG3. (**B**) Co-crystallization of the eukaryotic Hsc70 ATPase domain and the BAG domain of human BAG1. Binding of the BAG domain (red) to the ATPase domain of Hsc70 (green) results in a nucleotide binding incompatible conformation of Hsc70 by a 14° rotation of subdomain IIB relative to the nucleotide-bound conformation. Figure adapted from Sondermann et al, 2001.

B.1.3.5.1 BAG1

BAG1, the founding member of the BAG protein family, was originally identified by Reed and colleagues as a strong anti-apoptotic Bcl-2 interacting factor (Takayama et al, 1995). By alternative translation initiation from one mRNA, human BAG1 is expressed as four isoforms which differ in their N-terminal extensions (Takayama & Reed, 2001). Homozygous *bag1* gene knockout is embryonic lethal in mice. BAG1-/- embryos show massive apoptosis in the fetal liver and the developing nervous system, suggesting that BAG1 is an important survival factor of haematopoietic and neuronal progenitor cells during mouse development (Götz et al, 2005).

On the cellular level, BAG1 has been described to exert multiple functions by binding to Hsc/Hsp70. It has been shown that BAG1 catalyzes nucleotide exchange on Hsc/Hsp70, thereby contributing to dissociation of the chaperone-substrate complex and the release of the substrate (Höhfeld & Jentsch, 1997; Sondermann et al, 2001). However, contradictory to this observation, it has been also demonstrated that BAG1 can act as a negative regulator of Hsc/Hsp70 by uncoupling nucleotide exchange from substrate release (Bimston et al, 1998). With respect to molecular chaperone targeting, BAG1 has been shown to couple Hsc/Hsp70 chaperones to proteasomes via its ubiquitin-like (UBL) domain (Lüders et al, 2000a), suggesting a function of BAG1 in chaperone-assisted 26S proteasomal protein degradation.

B.1.3.5.2 BAG2

BAG2 contains no known protein motif besides the BAG domain and is functionally less characterized. BAG2 was identified independently by two research groups as a specific inhibitor of CHIP (Arndt et al, 2005; Dai et al, 2005). As aforementioned, CHIP is an Hsc/Hsp70-associated E3 ubiquitin ligase that is thought to ubiquitinate chaperone-bound substrates for their subsequent degradation. As an inhibitor of CHIP, BAG2 could modulate protein triage decisions that regulate the balance between protein folding and degradation of Hsc/Hsp70 substrates. Thus, BAG2 may support the folding activity of Hsc/Hsp70 by inhibiting ubiquitination reactions of CHIP. However, a recent study showed that BAG2 along with Hsc/Hsp70 promote protein degradation by the ubiquitin-independent acting 20S proteasomal degradation pathway (Carrettiero et al, 2009). These findings implicate that BAG2 negatively regulates the ubiquitin-dependent 26S proteasome degradation pathway but promotes 20S proteasomal degradation of Hsc/Hsp70 substrates.

B.1.3.5.3 BAG3

BAG3 (also known as CAIR-1 and Bis) is widely expressed in mouse tissues with highest expression levels found in striated muscles and heart (Homma et al, 2006). Homozygous *bag3* gene knockout mice are growth retarded and show a severe myopathy characterized by massive myofibrillar degeneration with apoptotic features (Homma et al, 2006). However, the cellular functions of BAG3 are mostly unknown. Expression of BAG3 is up-regulated upon proteasome inhibition and under protein-denaturating conditions, suggesting a role of BAG3 in the cellular anti-stress response (Pagliuca et al, 2003; Wang et al, 2008). BAG3 contains a WW domain near the N-terminus and a proline-rich region with several PXXP motifs next to the C-terminal BAG domain (Takayama & Reed, 2001). The WW domain is a protein-protein interaction module that binds proline-rich ligands. However, an interaction

partner binding to the WW domain has not been found yet. The PXXP motif has been described as a candidate docking site for interaction with SH3 (Src homology 3) domains often found in proteins of signalling pathways. Indeed, it has been shown that BAG3 binds to PLCγ, a SH3 domain containing protein involved in growth signal transduction (Takayama & Reed, 2001). More recently, BAG3 has been described to decrease aggregation of an overexpressed mutant huntingtin-derived peptide and to increase macroautophagy activity (Carra et al, 2008a). For both effects, the proline-rich domain of BAG3 was required but the BAG domain was dispensable. Furthermore, BAG3 overexpression was reported to inhibit 26S proteasomal degradation of Hsp90 client proteins leading to their accumulation in a polyubiquitinated state (Doong et al, 2003). This function of BAG3 was shown to depend on the BAG domain and the binding to Hsc/Hsp70.

B.1.3.5.4 BAG4

BAG4, also known as silencer of death domains (SODD), possesses like BAG2 no known protein motif except the BAG domain. It has been reported that BAG4 binds to death domains found in several members of the tumour necrosis factor (TNF) receptor superfamily such as tumour necrosis factor receptor 1 (TNFR1) and death receptor 3 (DR3) (Jiang et al, 1999). These receptors are activated by ligand-induced receptor oligomerization. BAG4 is supposed to suppress spontaneous death receptor activation by targeting Hsc/Hsp70 to these receptors. The chaperoning activity of Hsc/Hsp70 then prevents ligand-independent receptor self-aggregation and activation (Tschopp et al, 1999).

B.1.3.5.5 BAG5

BAG5 is unique in the human BAG protein family in that it contains four putative BAG domains. Little is known about the cellular functions of BAG5. In a previous study, BAG5 was identified as an inhibitor the E3 ubiquitin ligase parkin (Kalia et al, 2004). Parkin has attracted a lot of attention since loss of function mutations in the parkin gene cause early-onset Parkinson's disease (PD). The potential suppression of parkin activity by BAG5 suggests a role of BAG5 in the pathogenesis of PD. In this context, it has been shown that BAG5 enhance dopaminergic neurodegeneration in an *in vivo* model of PD (Kalia et al, 2004). Thus, BAG5 seems to be also functionally unique since it contrasts the pro-survival function ascribed generally to BAG proteins. Recently, BAG5 expression has been shown to decrease upon proteasome inhibition showing a regulation inverse to that of BAG3 which is up-regulated under these conditions (Sarközi et al, 2008).

B.1.3.5.6 BAG6

BAG6 (also known as BAT3 and Scythe) is the longest human BAG isoform. BAG6 is located predominantly in the nucleus but was also found in the cytoplasm and mitochondria. BAG6 is an anti-apoptotic protein that binds to the *Drosophila* killer protein Reaper (Thress et al, 1998, Thress et al, 2001). In this context, BAG6 acts together with Hsc/Hsp70 to sequestrate an unknown apoptosis inducer that, when released, induce apoptosis by cytochrome c release from mitochondria. Binding of Reaper to BAG6 is supposed to result in the release of this unknown pro-apoptotic molecule (Thress et al, 2001). More recently, an association of BAG6 with the mitochondrial intermembrane protein AIF (apoptosis-inducing factor) was reported (Desmots et al, 2008). In addition to these apoptosis-related functions, BAG6 contains a UBL domain like BAG1, suggesting that BAG6 targets Hsc/Hsp70 substrates to the proteasome. However, involvement of BAG6 in proteasomal protein degradation remains to be elucidated.

B.2 Aging

Aging is generally characterized by gradual changes in the structure and function of an organism, organs or of single cells that occur with the passage of time. This mostly irreversible process is genetically determined and environmentally modulated. In most cases the aging process leads to increased probability of organismal death (Troen, 2003).

Improvements in health services and living conditions over the past few centuries have contributed to aging of the world human population. Future projections on aging of the human population suggest a further severe demographic redistribution towards older age groups (Lutz et al, 2008). As the increase in longevity will be followed by a higher incidence of age-related disorders, research on aging and age-related disorders as well as the linkage of both research disciplines is gaining importance (Hayflick, 2000; Hebert et al). Although biological aging is an irreversible process, the detailed examination of the aging process can promote the understanding of causal relationships between age-related changes in biochemistry and age-related disorders and could lead to development of therapies that increase the rate of healthy aging.

B.2.1 Theories of aging

The “rate of living” theory of aging, perhaps the oldest explanation of aging, originates from the beginning of the 20th century and means that lifespan is an inverse function of the metabolic rate (Lints, 1989). The theory states that organisms possess a certain amount of

energy and when all of that energy is used up, the organism dies. Hence, organisms with a high metabolic rate have short life spans while organisms with a lower metabolic rate tend to have longer life spans. Nevertheless, although true for many species in the animal kingdom, the discovery of several exceptions to this empirical rule strongly challenged the “rate of living” hypothesis.

The “free radical theory of aging” proposed first by Denham Harman 1956 states that aging is caused by the progressive accumulation of free radical damage to macromolecules (Harman, 1956). A free radical is a chemical reactive molecule that has one unpaired electron in an outer atomic shell. The most prominent biological free radicals are oxygen species. These radicals but also other reactive oxygen species (ROS) are primarily produced by mitochondria during normal oxidative metabolism. According to Harman’s theory, continuous production of ROS and accumulation of oxidative damage is crucial and limits the resting life span.

The “Hayflick concept” from 1965 states that cultured normal human cells have a limited capacity to divide, after which they become senescent - a phenomenon referred to as the “Hayflick limit” (Shay & Wright, 2000). Hayflick also discovered that the finite replicative capacity of normal human cells is genetically pre-determined. Thus, an organism ages because the mitotic clock runs down in every cell and the self-renewal capacity of organs and tissues progressively decreases.

Today these originally independently of each other stated theories of aging can be combined in parts. A higher metabolic rate is often associated with higher oxidative damage due to increased oxidative respiration and the production of ROS (Sohal, 2002). Moreover, exposing cells to oxidative stress inducing agents leads to premature cellular senescence showing a direct impact of ROS on replicative capacity and aging (Dumont et al, 2000). Furthermore, the aging process can be slowed by modulating the balance between ROS producing and ROS scavenging mechanisms, either by caloric restriction or overexpression of anti-oxidative enzymes (Sohal & Weindruch, 1996). Together these findings lead to the current theory that the driving force of aging is the progressive damage of macromolecules caused by the continuous flux of free radicals and other ROS. Importantly, it has been shown that ROS can stimulate their own production since oxidative damage of the mitochondrial respiratory chain can lead to increased production of ROS (Sanz et al, 2006). This vicious cycle theory implies that once an imbalance between ROS producing and scavenging pathways manifests, the aging ball gets rolling faster and faster due to the exponentially growing production of ROS. Interestingly, in a recent study the content of the oxidation-

sensitive amino-acid cysteine in mitochondrial respiratory chain proteins has been correlated with the life span of aerobic animals (Moosmann & Behl, 2008). This study strongly suggested that depletion of cysteine in respiratory chain complexes during evolution promotes longevity of aerobic animals. These data are consistent with the “free radical theory of aging” and support a possible central role of ROS-mediated mitochondrial dysfunction in aging and age-related disorders.

The model of mitochondrial dysfunction as a primary cause of aging implies that oxidative damage increases with age. Indeed, the occurrence of oxidized cellular macromolecules is a hallmark of aging in a large number of cell types and tissues from a wide variety of organisms (Brunk & Terman, 2002; Sohal, 2002). Protein oxidation and associated protein misfolding events are a main characteristic of age-related human disorders, as described in the following paragraph.

B.2.2 Age-related proteinopathies

Many human degenerative diseases are associated with age. Among them are many devastating neurodegenerative disorders with high incidence such as Alzheimer’s disease, Parkinson’s disease and amyotrophic lateral sclerosis (ALS). A main characteristic of these age-related human disorders is the accumulation of aberrant protein aggregates in disease-affected tissues (Paulson, 1999; Rubinsztein, 2006). Generally, these age-related degenerative diseases are sporadic, but also few familiar forms are known. The hereditary forms are frequently caused by mutant proteins that exhibit instable conformations and are thus prone to aggregate (Paulson, 1999; Forman et al, 2004). The familial forms usually show an earlier onset than the sporadic forms. Nevertheless, although mutant aggregate-prone proteins are present already early in life, many familial forms, such as mutant SOD1-linked ALS and mutant α-synuclein-linked Parkinson’s disease, are nonetheless age-related.

Aberrant protein aggregation is a key hallmark of several age-related diseases. As specified in the above sections, proteins exhibiting non-native conformations tend to aggregate due to unspecific interactions with other macromolecules. For this reason, disorders associated with protein aggregates are also designated as protein conformational/misfolding diseases or proteinopathies (Paulson, 1999). Although all proteinopathies are characterized by aberrant protein aggregates, it becomes increasingly clear that in most cases protein aggregation *per se* does not ultimately contribute to disease pathology (Ross & Poirier, 2005). The proposed underlying upstream pathological events for proteinopathies are highly diverse. The conformational change assumed for disease-related aggregate-prone proteins can result in

loss of their biological functions or, more frequently, in a gain of toxic function (Rubinsztein, 2006). Gain of toxic functions could be simply due to unspecific interactions of a misfolded protein with other macromolecules. Such unspecific protein-protein interactions could lead to a diverse spectrum of aberrations including protein mislocation and abnormal enzymatic activity. Moreover, the toxic properties of instable proteins could also underlie the capacity to silence the function of another protein by "protein-entrapping", which means that cellular proteins are hindered in their function by sequestration via unspecific complex formation with the disease-related aggregate-prone protein (Taylor et al, 2002). As aggregate-prone proteins very likely exhibit multiple altered interaction characteristics, it is hard to find those who are causally linked to disease onset. Therefore, it is important to investigate the upstream events that lead to failure of proteostatic control and the accumulation of misfolded proteins. Since many proteinopathies occur in an age-related altered biochemical background, the impact of aging and age-related biochemical changes like accumulating oxidative stress on PQC mechanisms, in particular on chaperone systems and protein degradation pathways, should be investigated to understand the causal events leading to these pathologies.

B.3 Aim of the project

Many age-related neurodegenerative disorders such as Alzheimer's disease, Parkinson's disease and ALS are associated with the aberrant formation of protein aggregates. These aggregates and/or their precursors have been causally linked to the pathogenesis of these neurodegenerative diseases. The accumulation of protein aggregates implies the failure of proteostatic control as a possible causal factor of disease pathology. As the main risk factor of these disorders is age, analysis of PQC pathways in the context of aging is of fundamental relevance for understanding the causal events leading to onset of these disorders.

The central goal of the present study was to analyze and discover potential alterations of PQC pathways during the biological aging process. Therefore, based on cellular *in vitro* aging models, an initial comparative expression analysis of diverse chaperones and co-chaperones was performed in young and old cells. This screening revealed a reciprocal regulation of the Hsc/Hsp70 co-chaperones BAG1 and BAG3 during the aging process of cells. Based on these findings the specific function of BAG1 and BAG3 in PQC pathways was to be elucidated by knock-down and overexpression studies. Once BAG-controlled pathways were identified, potential BAG interaction partners, in addition to Hsc/Hsp70, should be identified to get a mechanistic insight into the function of BAG1 and BAG3 in PQC. As soon as a strong hypothesis about the function of BAG1 and BAG3 was developed from

the functional analyses, this hypothesis should be tested in the context of aging using the *in vitro* aging models. Finally, these findings were to be continued in a model of organismal aging, in particular, of the aging central nervous system by comparing potentially BAG-controlled pathways in rodent brain tissues as well as primary cell cultures from young and old animals.

C RESULTS

C.1 Regulation of BAG levels during aging and oxidative stress

C.1.1 Characterization of the cellular aging models

To analyze possible age-related alterations of PQC mechanisms a well-established cellular *in vitro* aging model based on the human cell line IMR-90 (I90) was employed. I90 cells are primary human diploid fibroblasts which exhibit the hallmarks of aging over time and become senescent after a finite number of divisions in culture, a process referred to as the replicative senescence (Nichols et al, 1977; Shay & Wright, 2000). Growth analysis revealed that I90 cells became senescent after population doubling (PD) 60 (Figure 9A). Consecutively, pre-senescent I90 cells with PD 52-58 were considered to be old whereas cells with PD below 30 were considered as young. Besides the growth rate analysis, aged cells were also identified microscopically by the typical large and flat cell morphology (Figure 9B). In addition, a biochemical characterization of young and old cells was performed as well by showing the induction of the aging marker caveolin1 by Western-blot analyses (Figure 9C). Caveolin1 is up-regulated during cellular aging and has been associated with the transition from proliferation to senescence (Linge et al, 2007). For analysis of *in vitro* aging effects, the primary human fibroblast cell line, WI38, distinct from the I90 cell model was employed as well. Similarly to I90 cells, aging of WI38 cells was accompanied by a morphological change as well as the up-regulation of caveolin1 (data not shown). Transition from growth to senescence in WI38 cells occurred at PD 54 (data not shown), thus, pre-senescent WI38 cells with PD 46-52 were considered as old whereas cells with PD below 30 were assigned to be young.

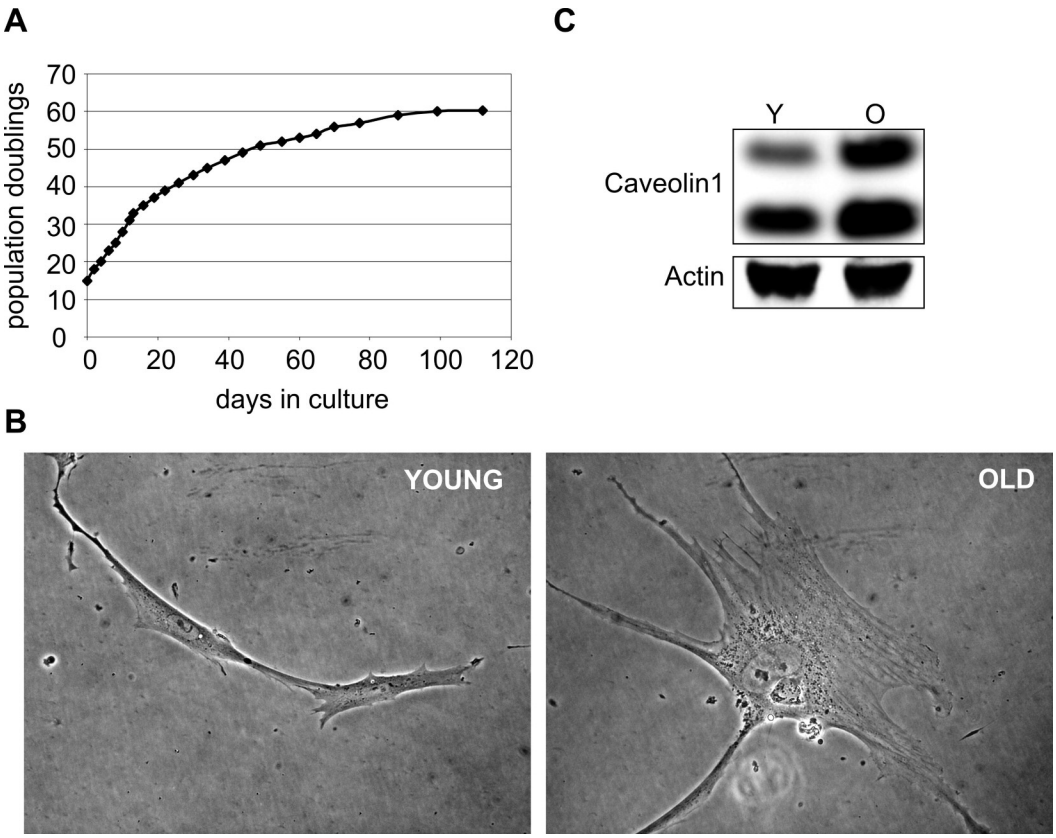

Figure 9: (**A**) Growth curve analysis of I90 cells. Growth rate of I90 cells progressively declined with age and cells became senescent at population doubling (PD) 60. I90 cells with PD 52-58 were considered as old whereas cells with PD below 30 were assigned to be young. (**B**) Microscopic analysis of cell morphology of young and old I90 cells. Aged cells showed the typical large and flat morphology in contrast to the spindle-shaped morphology of young cells. (**C**) Immunoblot analysis of the aging marker caveolin1 in young (Y) and old (O) I90 cells. Actin was used as loading control.

C.1.2 BAG1 and BAG3 are reciprocally regulated during cellular aging

Earlier studies implicated the Hsc/Hsp70 co-chaperones of the BAG protein family in modulation of cellular PQC systems (Lüders et al, 2000a; Carrettiero et al, 2009; Carra et al, 2008a). To investigate potential alterations of BAG-controlled quality control pathways during aging, BAG expression was investigated in young and old I90 cells. Real-time PCR-based expression profiling of the six human BAG family members revealed a significant down-regulation of BAG1 and BAG2 as well as an up-regulation of BAG3 mRNA levels during cellular aging (Figure 10A). Transcript levels of other BAG isoforms were unchanged. Furthermore, protein expression levels of BAG family members were investigated by immunoblot analysis using a polyclonal antibody (*cBAG*) directed against the BAG domain which is highly conserved among human BAG family members. Strong immunoreactivity of the *cBAG* antibody was observed with BAG1 and BAG3 (Figure 10B), indicating predominant expression of these BAG isoforms in I90 cells.

It should be noted here that human BAG1 is expressed as four isoforms by alternative translation initiation from one mRNA (Takayama & Reed, 2001). These isoforms are referred to as BAG1L, BAG1M, BAG1 and BAG1S and have an apparent molecular weight of 50 kDa, 46 kDa, 36 kDa and 29 kDa, respectively. Weak bands were observed for BAG1M and BAG1S, but strong signals for BAG1L and BAG1 (Figure 10B). Consistent with the real-time PCR analysis decreased levels of BAG1 isoforms and increased BAG3 protein levels were found in old I90 cells (Figure 10B). A similar regulation of BAG1 and BAG3 was also observed during aging of WI38 cells (Figure 10C), indicating that the shift from BAG1 to BAG3 is a general effect of cellular aging. As a next step the expression levels of Hsc/Hsp70 and Hsp90 were analyzed, which are known to be functionally modulated by BAG1 and BAG3 (Doong et al, 2003; Höhfeld & Jentsch, 1997). Protein levels of Hsp90 were slightly down-regulated during aging in both cell lines (Figure 10B, C). Hsc/Hsp70 levels were moderately reduced in old I90 cells, but remained unchanged in WI38 cells during aging. Transcript levels of Hsp90 were moderately down-regulated, whereas Hsc70 mRNA levels were unchanged during aging of I90 cells (Figure 10A).

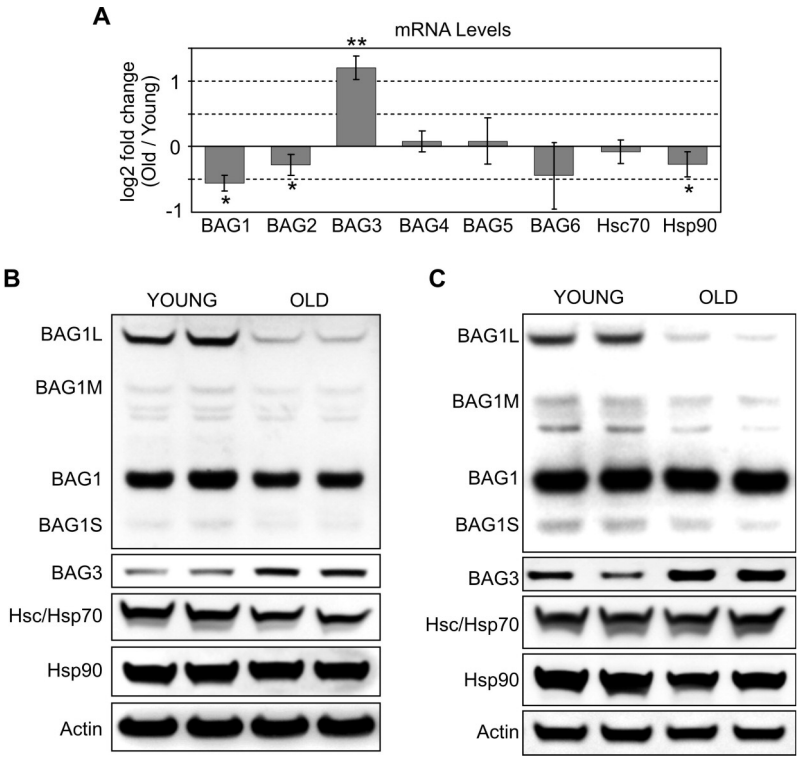

Figure 10: (**A**) Real-time PCR analysis of human BAG family members and Hsc70 and Hsp90 in young and old I90 cells. Depicted is the expression ratio (log2) ± SEM of target genes in old cells relative to young cells. *P<0.05 and **P<0.01 versus young, n=3. (**B**) and (**C**) Immunoblot analysis of BAG1, BAG3, Hsc/Hsp70 and Hsp90 in young and old I90 and WI38 cells, respectively. For detection of BAG proteins, a polyclonal antibody directed against the conserved BAG domain (*cBAG*) was used. Detection of Actin served to ensure equal protein loading.

C.1.2 The interaction of Hsc/Hsp70 with BAG proteins is altered during cellular aging

The altered BAG expression profile suggested a potentially altered interaction of BAG proteins with Hsc/Hsp70 in aged cells. To test this hypothesis, co-immunoprecipitation (Co-

IP) studies of Hsc/Hsp70 and BAG3 were performed in young and old I90 cells. These studies revealed that more BAG3 was associated with Hsc/Hsp70 in old cells compared to young cells (Figure 11). In contrast, association of BAG1 with Hsc/Hsp70 was decreased in old cells. It should be noted that the BAG1L isoform could not be appropriately analyzed because of cross-reactivity of the secondary antibody with the IgG heavy chain of the Hsc/Hsp70 antibody that co-migrated exactly with BAG1L. Furthermore, when BAG3 was directly immunoprecipitated higher levels of Hsc/Hsp70 co-precipitated in lysates from old cells (Figure 11). These data suggested that, based on the altered BAG expression, the interaction of Hsc/Hsp70 with BAG proteins is shifted from BAG1 to BAG3 during cellular aging.

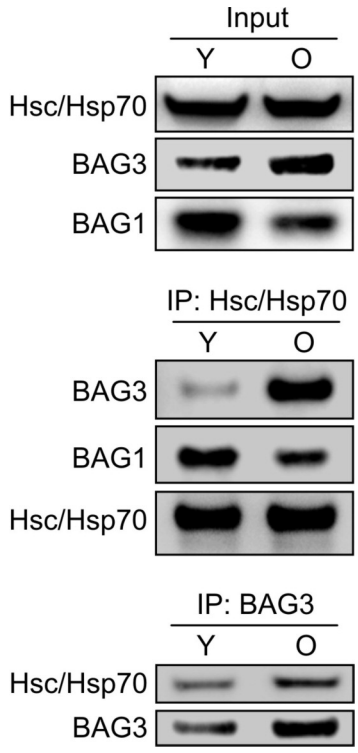

Figure 11: Co-immunoprecipitation (Co-IP) analysis testing the interaction of BAG1 and BAG3 with Hsc/Hsp70 in young (Y) and old (O) I90 cells. Upper panel shows relative amounts of proteins in cell lysates used for Co-IP (Input). Middle panel shows levels of BAG1 and BAG3 found in Hsc/Hsp70 immunocomplexes. Lower panel shows levels of Hsc/Hsp70 co-sedimented upon immunoprecipitation of BAG3.

C.1.3 Oxidative stress induces a shift from BAG1 to BAG3

Oxidative stress and the occurrence of oxidized, cross-linked proteins is a hallmark of aging (Brunk & Terman, 2002). For this reason, it was of interest whether also oxidative stress alters the chaperone network including the shift from BAG1 to BAG3 as observed in the cellular aging models. To analyze this aspect the well-established human cell line HEK293 originating from a human embryonic kidney was employed. HEK293 cells (293 cells) were treated with the lipid peroxidation product 4-hydroxy-2-nonenal and H_2O_2 to induce oxidative stress. Strikingly, when these oxidative stress-inducing agents were applied to cells in concentrations that caused the accumulation of polyUb-proteins, BAG3 was up-regulated

whereas BAG1 was down-regulated (Figure 12A, B). The accumulation of polyUb-proteins indicated that under the oxidative stress conditions the cellular PQC system was strongly challenged. Together, these data could suggest that the shift from BAG1 to BAG3 is an adaptation of the cellular PQC system to cope with elevated levels of oxidized and cross-linked proteins.

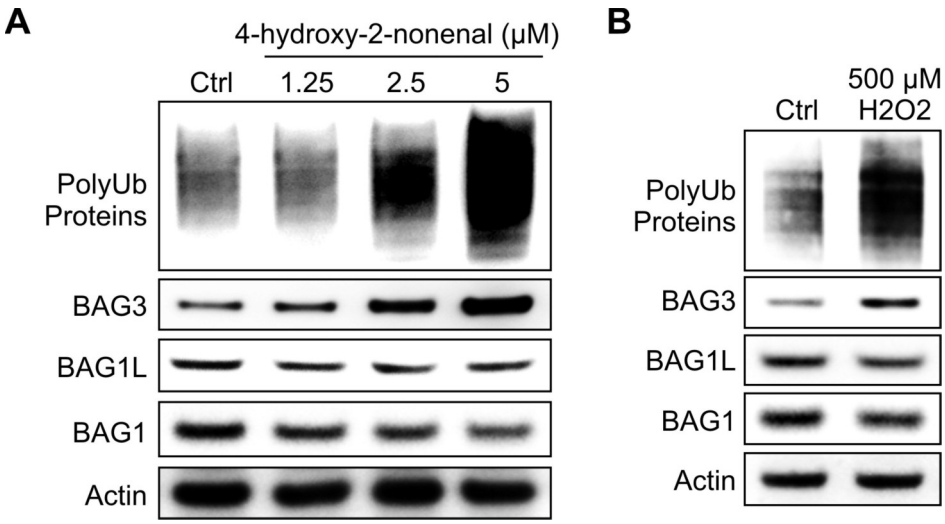

Figure 12: (**A**) and (**B**) 293 cells were treated with 4-hydroxy-2-nonenal or H_2O_2 in the indicated concentrations for 8 h. Thereafter, levels of polyUb-proteins, BAG3 and BAG1 were detected by Western-blot analysis. Detection of Actin served as loading control.

C.1.4 Overexpression of mutant huntingtin does not induce a shift in BAG expression

It was also of interest to investigate whether the shift from BAG1 to BAG3 could be observed upon overexpression of a mutant, aggregate-prone protein that is causally linked to an age-related disorder. Huntington's disease is caused by CAG repeat expansions of the huntingtin gene. These mutations lead to polyglutamine (polyQ)-extensions in the huntingtin protein. PolyQ-extensions reaching over a disease-causing threshold of 35–40 glutamines are crucial for the onset of Huntington's disease (Duyao et al, 1993). Mutant huntingtin proteins show strong aggregation properties which directly correlate with the length of the polyQ-extensions (Krobitsch & Lindquist, 2000). To investigate whether BAG levels are altered in the presence of such an aggregate-prone protein, EGFP fused to huntingtin exon 1 containing a pathological 103Q-extension (103QHtt.EGFP) was overexpressed in 293 cells. As a control, 293 cells were transfected either with EGFP fused to huntingtin bearing a non-pathological 25Q-extension (25QHtt.EGFP) or EGFP alone. These studies showed that BAG1 and BAG3 levels remained unchanged in the presence of 103QHtt.EGFP although the mutant protein strongly aggregated 45-96 hours post-transfection (Figure 13, see EGFP-signal in the stacking gel and direct fluorescence pictures). These data suggested that the presence of a

single aggregate-prone protein, although overexpressed and heavily aggregated, cannot induce the BAG shift in 293 cells. However, only about ~15% of total cells (transfected plus non-transfected) showed EGFP-positive inclusions in these transient overexpression experiments with 103QHtt.EGFP. Thus, it cannot be ruled out that in immunoblot analysis a potential BAG-shift in cells containing polyQ-inclusions is masked by the other ~85% of cells bearing no polyQ-inclusions.

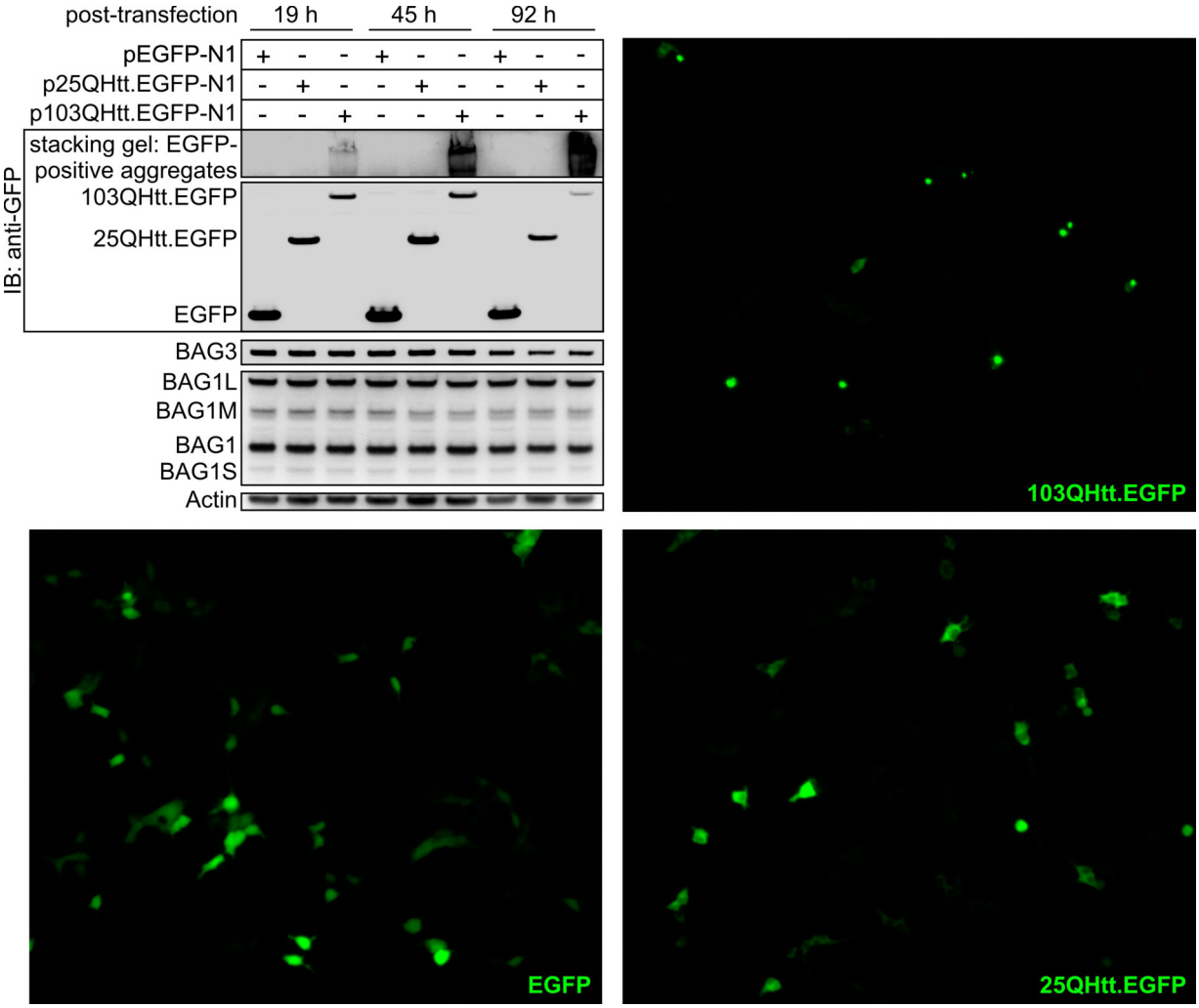

Figure 13: 293 cells were transfected for the indicated time periods with an EGFP expression plasmid (pEGFP-N1) or huntingtin exon 1-EGFP fusion constructs with polyglutamine-repeats of 25 glutamines (p25QHtt.EGFP-N1) and pathological 103 glutamines (p103QHtt.EGFP-N1). Upper left panel shows immunoblot analysis of EGFP-positive proteins and BAG proteins. Note, in lysates from p103QHtt.EGFP-N1-transfected cells EGFP-positive insoluble protein aggregates of high molecular weight were present that remained in the stacking gel. The microscopic pictures show direct EGFP fluorescence of living 293 cells transfected as indicated for 45 h. Only p103QHtt.EGFP-N1-transfected cells showed EGFP-positive inclusion bodies.

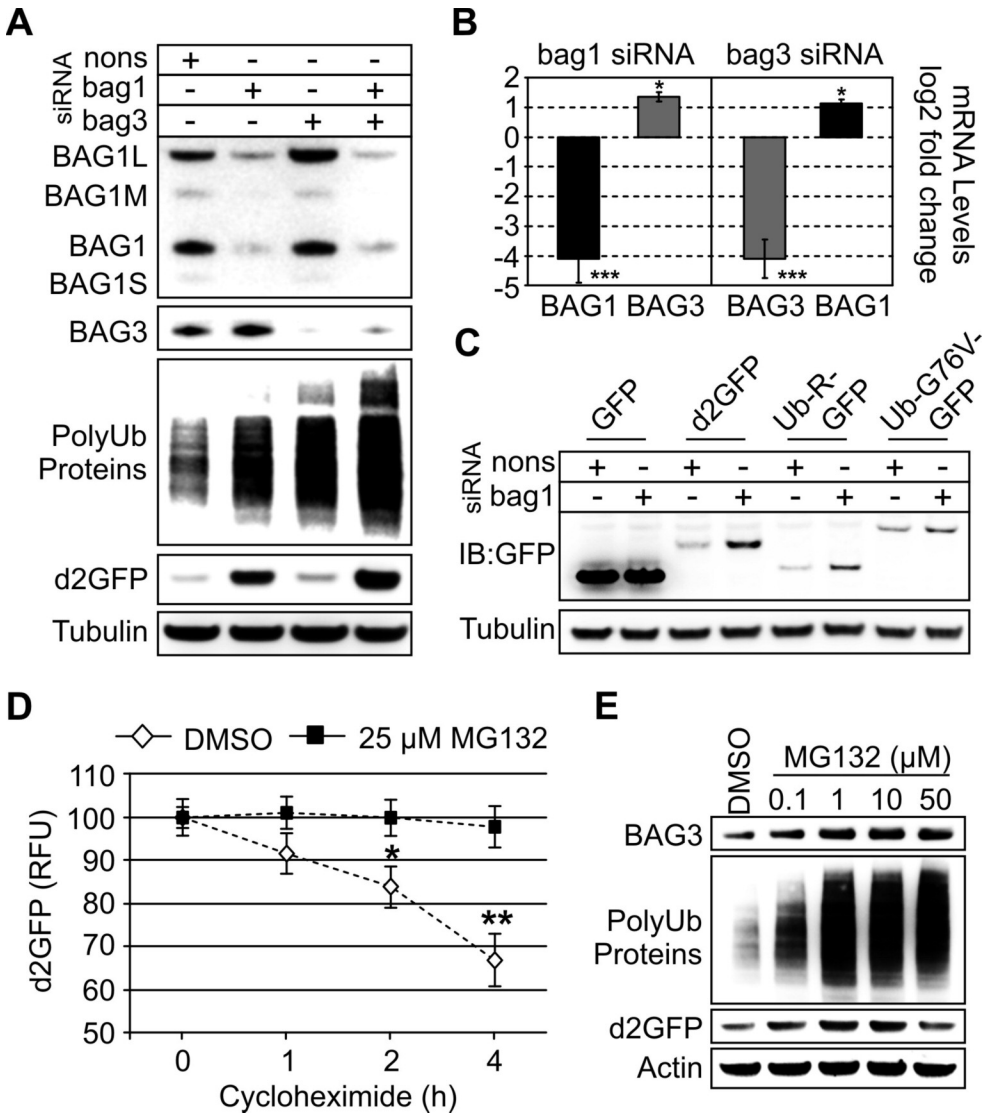

Figure 14: (**A**) 293 cells were transfected with bag1, bag3 or nonsense (nons) siRNAs, as indicated. After 48 h, cells were transfected with a proteasome reporter plasmid (d2GFP) together with half the amounts of the indicated siRNAs. After additional 24 h, levels of indicated proteins were detected by immunoblot analysis. Detection of Tubulin served as loading control. (**B**) 293 cells were transfected with indicated siRNAs for 48 h followed by real-time PCR analysis of BAG1 and BAG3 mRNA levels. Depicted is the mean relative expression ratio (log2) ± SEM. *P<0.05 and ***P<0.001 versus nons, n=3. (**C**) BAG1 knockdown was performed in 293 cells for 48 h. Thereafter, cells were transfected with GFP or different GFP-based proteasome reporter plasmids as indicated. After additional 24 h, levels of GFP-positive proteins were detected by Western-blot analysis using a GFP antibody. Tubulin levels were used to ensure equal protein loading. (**D**) 293 cells were transfected with the proteasome reporter d2GFP for 24 h. Thereafter, protein translation was inhibited with cycloheximide (500 µM) in the absence (DMSO) or the presence of the proteasome inhibitor MG132 (25 µM). GFP fluorescence was recorded during a time period of 4 h. Values expressed are mean relative fluorescence units (RFU) ± SEM. *P<0.05 and **P<0.01 versus DMSO-treated cells, n=3. (**E**) 293 cells stably transfected with d2GFP (d2HEK) were treated with different concentrations of MG132 for 5 h. Thereafter, immunoblot analysis of indicates proteins were performed. Actin served as loading control.

C.2 Specific roles of BAG1 and BAG3 in PQC pathways

The present findings so far indicated that BAG1 and BAG3 are reciprocally regulated during cellular aging and under oxidative stress conditions. This raised the question for the

functional consequence and the significance of this molecular switch. To elucidate the specific roles of BAG1 and BAG3 in PQC in detail, BAG1 and BAG3 levels were depleted in 293 cells by siRNA-mediated knock-down. Western-blot analysis confirmed an efficient down-regulation of BAG1 and BAG3 protein levels upon transfection of cells with specific siRNAs (Figure 14A). As seen before with I90 cells, the *cBAG* antibody recognized four BAG1 isoforms with weaker labelling of BAG1M and BAG1S, but strong signals for BAG1L and BAG1. Strikingly, knock-down of BAG1 provoked an increase of BAG3 levels. Conversely, BAG1 expression, in particular the BAG1L isoform, was elevated upon depletion of BAG3 (Figure 14A). This was most likely due to altered gene expression, as real-time PCR analysis revealed up-regulated transcript levels of BAG1 as well as BAG3 upon knock-down of BAG3 and BAG1, respectively (Figure 14B). These data suggested an adaptive response of the cell where the expression of BAG1 is induced to compensate for the deprivation of BAG3, and *vice versa*. This view was strongly supported by the finding that both knock-downs resulted in the accumulation of polyUb-proteins (Figure 14B), suggesting a functional relation of both BAG isoforms in either the removal or generation of polyUb-proteins.

C.2.1 BAG1 is essential for effective proteasomal degradation

In a previous study, BAG1 has been described to act as a molecular link between the proteasome and Hsc/Hsp70 chaperones (Lüders et al, 2000a). This study showed that BAG1 overexpression can enhance the association of Hsc/Hsp70 molecules with proteasomes, suggesting a role for BAG1 in chaperone-mediated proteasomal degradation. Therefore, it is possible that polyUb-protein accumulation upon BAG1 and BAG3 knock-down was a result of an impaired ubiquitin/proteasome system. To monitor the activity of the ubiquitin/proteasome system in living cells, a GFP-based proteasome sensor (d2GFP) containing a PEST sequence was employed. The PEST sequence is supposed to give rise to polyubiquitination and subsequent proteasomal degradation of the reporter (Rechsteiner & Rogers, 1996). The functionality of d2GFP as a proteasome reporter was proven in a cycloheximide chase experiment. The degradation of d2GFP was completely blocked in the presence of the proteasome inhibitor MG132 (Figure 14D). Interestingly, when d2GFP was expressed in BAG1 or BAG3 knock-down cells, the ubiquitin/proteasome system reporter accumulated only in BAG1-depleted cells (Figure 14A). Knock-down of BAG3 resulted only in a negligible increase of d2GFP compared with the observed rise of polyUb-proteins. These results imply a role in the ubiquitin/proteasome system exclusively for BAG1. To strengthen this conclusion, the influence of BAG1 on two other ubiquitin/proteasome pathways, the “N-end rule” and the ubiquitin-fusion degradation (UFD) pathways, that use degradation signals different from the PEST sequence, was analyzed as well. The “N-end rule” states that the *in*

vivo half-life of a protein is determined by the identity of the destabilizing amino-acid residue located at the N-terminus (Varshavsky, 2000). For example, an arginine (R) residue at the N-terminus has been shown to be highly destabilizing for a protein. Thus, ubiquitin fused to GFP that exhibits an arginine at the N-terminus, Ub-R-GFP (Dantuma et al, 2000), can be used as a specific substrate for the N-end rule pathway. The UFD pathway is a proteolytic system in which an un-cleavable ubiquitin moiety fused to the N-terminus of a protein functions as a degradation signal. To analyze this pathway a GFP-based reporter fused to mutant ubiquitin with a glycine to valine substitution at position 76 (Ub-G76V-GFP; Dantuma et al, 2000) can be used since it cannot be cleaved by deubiquitinating enzymes. As seen for d2GFP, also the substrates of the “N-end rule” and UFD pathways accumulated upon knock-down of BAG1 (Figure 14C). In contrast, levels of GFP without a degradation signal were unaltered. These results strongly indicated that BAG1 knock-down impairs the ubiquitin/proteasome system.

The present results so far showed that due to proteasome inhibition, BAG1 depletion leads to the accumulation of polyUb-proteins and proteasome reporters. Moreover, BAG1 knock-down induced the up-regulation of BAG3. Therefore, it was interesting to investigate whether pharmacological inhibition of the proteasome triggers similar effects. For this purpose, a proteasome-reporter cell line was engineered that stably expresses d2GFP (d2HEK cells). These cells were treated with the proteasome inhibitor MG132 in different concentrations. Remarkably, pharmacological proteasome inhibition with MG132 fully mimicked the effects observed in BAG1 knock-down cells, including the up-regulation of BAG3 as well as the accumulation of d2GFP and polyUb-proteins (Figure 14E). Together, these results strongly indicated that BAG1 is essential for efficient degradation of polyUb-proteins by the ubiquitin/proteasome system.

C.2.2 BAG3 does not interfere with the ubiquitin/proteasome system

In a previous study, BAG3 has been described to inhibit a chaperone-associated proteasomal degradation pathway (Doong et al, 2003). According to this study, BAG3 overexpression inhibits the proteasomal degradation of Hsp90 substrates induced by inhibition of the Hsp90 chaperone with geldanamycin. Geldanamycin belongs to the group of ansamycin antibiotics which specifically inhibits Hsp90 thereby inducing the selective degradation of Hsp90-dependent proteins like the Akt kinase (Georgakis & Younes, 2005). Geldanamycin-induced Hsp90 client protein degradation seems to involve client transfer to Hsc/Hsp70 chaperones and is thus potentially modulated by BAG proteins (Doong et al, 2003). Consequently, the accumulation of the proteasome reporter d2GFP in BAG1-depleted

cells (Figure 14A) could be caused by the concomitant up-regulation of BAG3. To address this issue, the time course of BAG3 induction and d2GFP accumulation was examined following BAG1 knock-down in d2HEK cells. However, there was no temporal correlation between BAG3 induction and d2GFP accumulation (Figure 15A). Moreover, overexpression of BAG3 in d2HEK cells did not lead to accumulation of the proteasome reporter (Figure 15B). These results together with the observation that d2GFP accumulated even stronger in BAG1/BAG3 double knock-down cells than in single BAG1 knock-down cells (Figure 14A) ruled out the possibility that increased BAG3 levels were responsible for ubiquitin/proteasome system inhibition in BAG1-depleted cells and underscored an essential function of BAG1 in the ubiquitin/proteasome system.

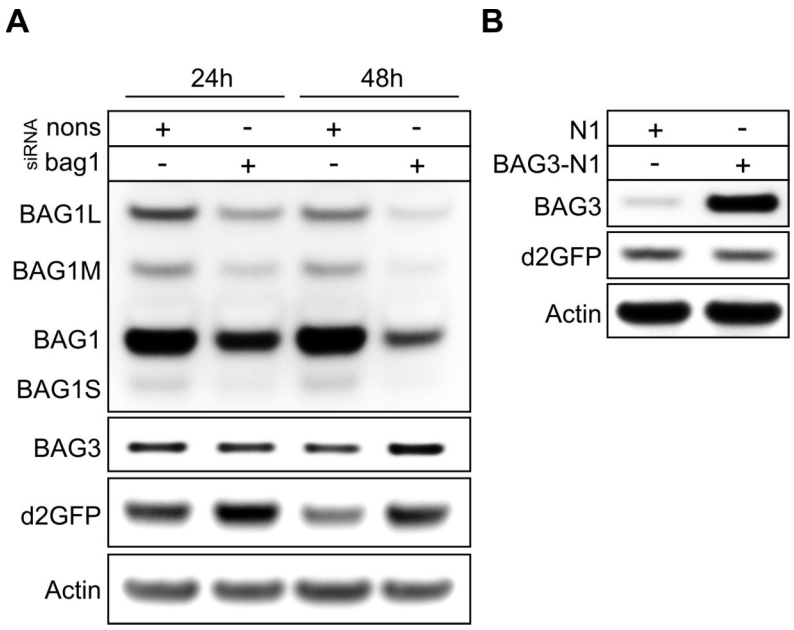

Figure 15: (**A**) 293 cells stably expressing d2GFP (d2HEK) were transfected with nonsense (nons) or bag1 siRNA. 24 and 48 h post-transfection, BAG1, BAG3 and d2GFP levels were detected by immunoblot analysis. Actin was used as loading control. (**B**) d2HEK cells were transfected with BAG3 (BAG3-N1) or control vector (N1) for 24 h followed by immunoblot analysis of BAG3 and d2GFP levels. Actin served as an internal standard.

C.2.3 BAG1 overexpression stimulates the ubiquitin/proteasome system

It was also of interest to examine whether overexpression of BAG1 can actually stimulate the activity of the ubiquitin/proteasome system. Proteasomes are located in the cytoplasm and nucleus (Breusing & Grune, 2008). To gain insight into the role of BAG1 in both compartments, overexpression studies were performed with the cytosolic isoform BAG1S as well as the predominantly nuclear-located BAG1L isoform (Takayama & Reed, 2001). BAG1S overexpression in the proteasome reporter cell line d2HEK led to decreased levels of polyUb-proteins as well as d2GFP indicating that BAG1S indeed can stimulate the

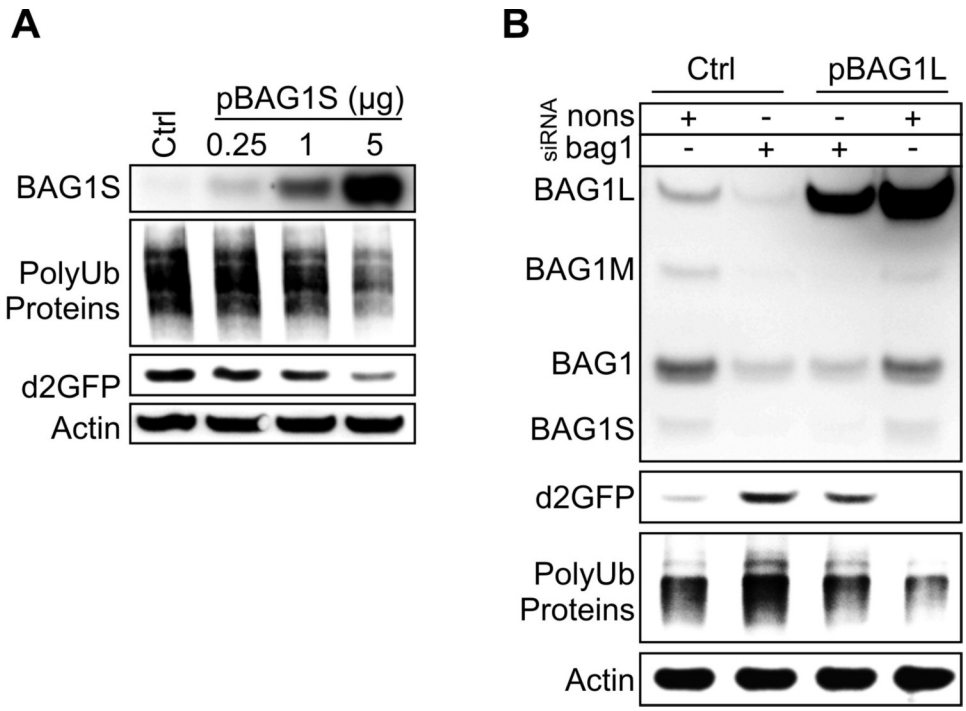

Figure 16: (**A**) d2HEK cells were transfected with indicated amounts of a BAG1S encoding expression plasmid or 5 µg of control vector (Ctrl) for 24 h. Thereafter, levels of indicated proteins were analyzed by immunoblot analysis. Actin was used as loading control. (**B**) d2HEK cells were transfected with nonsense (nons) or bag1 siRNA and additionally with BAG1L expression plasmid or vector control (Ctrl), as indicated. 48 h post-transfection, levels of indicated proteins were detected by Western-blot analysis. Actin was used to ensure equal protein loading.

ubiquitin/proteasome system (Figure 16A). However, clear effects were only observed when BAG1S was massively overexpressed. This fact could indicate that under normal conditions sufficient amounts of BAG1 are available in cells to ensure proper function and efficiency of the ubiquitin/proteasome system. According to this view, a previous study demonstrated that BAG1 promotes glucocorticoid hormone receptor (GR) degradation only when the E3 ubiquitin ligase CHIP was simultaneously overexpressed (Demand et al, 2001). For these reasons the experimental approach was extended and the effects of BAG1L overexpression was also analyzed in cells that were depleted of BAG1 before. Interestingly, overexpression of BAG1L in the BAG1 knock-down background effectively counteracted the accumulation of polyUb-proteins caused by the knock-down of the other BAG1 isoforms (Figure 16B). However, here the accumulation of d2GFP could be only partially reversed. It is possible that BAG1L, which resides to a large extent in the nucleus, exerted only a limited effect on the degradation of cytoplasmic d2GFP. These results show BAG1L overexpression cannot fully compensate for the loss of other BAG1 isoforms. Furthermore, as seen with BAG1S, ectopic expression of BAG1L in cells with unmodified BAG levels led only to a moderate reduction of polyUb-proteins and d2GFP despite massive up-regulated BAG1L levels (Figure 16B). Taken together, these data showed that under basal conditions BAG1 overexpression has

only limited stimulating effects on the ubiquitin/proteasome system. This raised the question whether BAG1 overexpression exhibits stronger stimulating effects on the ubiquitin/proteasome pathway under stress conditions when the amounts of quality control substrates increase and the cellular PQC system is challenged. Although not yet investigated in detail, interesting preliminary data indicate that recovery rates from heat-stress are strongly increased in BAG1-overexpressing cells (data not shown). Future studies are planned that address the question whether these observations and the reported strong anti-apoptotic activity of BAG1 (Kermer et al, 2003) are causally linked to a function in the ubiquitin/proteasome pathway.

C.2.4 BAG3 knock-down decreases the macroautophagic flux

What then could be the role of BAG3 in PQC? As seen for BAG1, reduced BAG3 levels also resulted in the accumulation of polyUb-proteins (Figure 14A). However, the effect on the proteasome sensor d2GFP was negligible suggesting that BAG3, if only, plays a minor role in the ubiquitin/proteasome system. Remarkably, the accumulation of d2GFP in BAG1/BAG3 double knock-down cells was even stronger than upon knock-down of BAG1 alone (Figure 14A). These observations pointed to the possibility that depletion of BAG3 caused the impairment of a protein breakdown pathway other than the ubiquitin/proteasome system. This impairment could have provoked the accumulation of polyUb-proteins which, in turn, might have led to a partial capacity overload of the proteasomal system and thus a slight increase of d2GFP levels.

BAG3 has been described to suppress aggregation of a mutant polyQ-huntingtin peptide. This effect was ascribed to involve the macroautophagy pathway (Carra et al, 2008a). Macroautophagy has been implicated in the turnover of polyUb-proteins in addition to the ubiquitin/proteasome system (Pankiv et al, 2007; Hara et al, 2006; Komatsu et al, 2006). Therefore, it was analyzed whether BAG3 is involved in macroautophagic processes that mediate polyUb-protein degradation. A well-established marker for macroautophagy is LC3. When macroautophagy is induced, the cytoplasmic LC3-I isoform is conjugated with phosphatidylethanolamine to LC3-II which then strongly associates with the membrane of autophagosomes. Due to the lipid anchor LC3-II migrates faster in SDS-PAGE and can be separated from LC3-I. Because LC3-II itself is degraded upon fusion of autophagosomes with lysosomes, LC3-II constitutes a specific substrate of the macroautophagic degradation pathway. Thus, the macroautophagic flux can be measured by monitoring LC3-II accumulation in the presence of lysosomal inhibitors (Mizushima & Yoshimori, 2007).

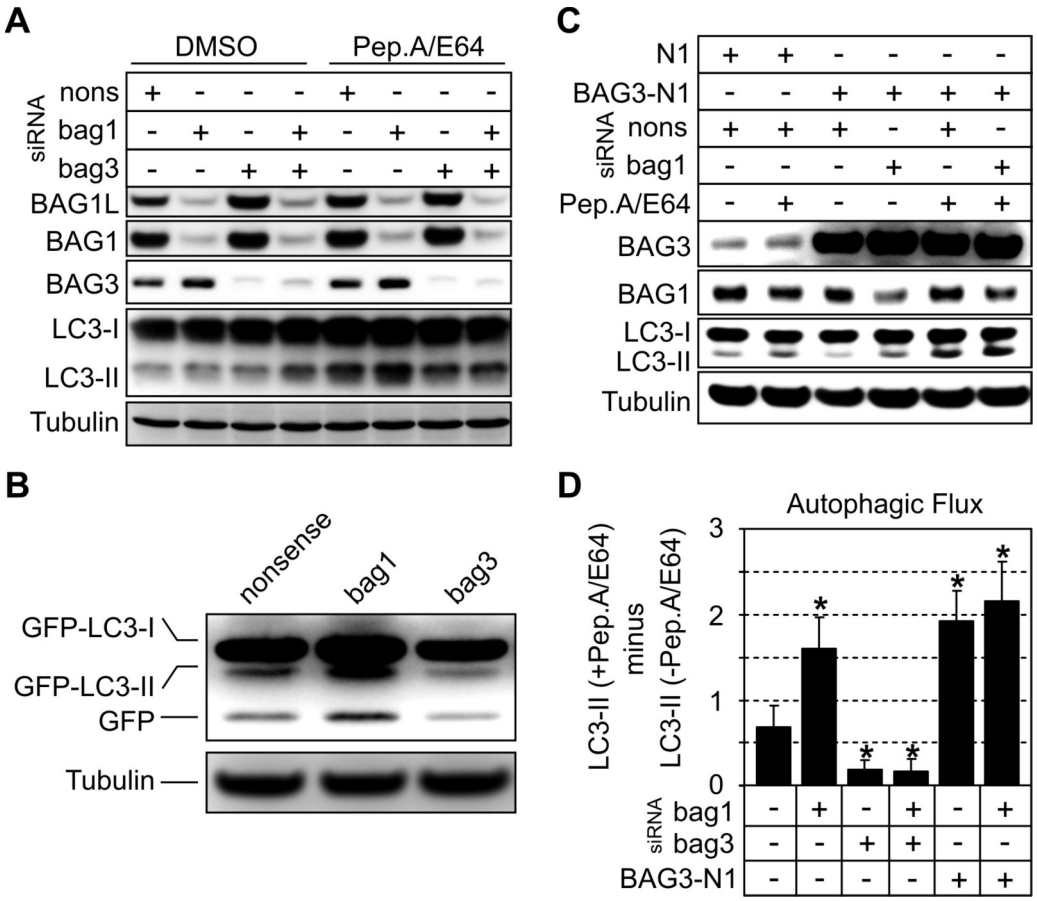

Figure 17: (**A**) 293 cells were transfected with nonsense (nons), bag1 and bag3 siRNAs, as indicated, for 48 h and then treated for 2 h with the lysosomal inhibitors Pepstatin A and E64 (both 10 µg/ml; Pep.A/E64) or DMSO as control. Thereafter, levels of the specific macroautophagy substrate LC3-II and BAG levels were detected by immunoblot analysis. Tubulin served as loading control. (**B**) 293 cells were transfected with GFP-LC3 and co-transfected either with nonsense, bag1 or bag3 siRNA. 24 h post-transfection, levels of GFP-LC3-I, GFP-LC3-II and GFP were detected by Western-blot analysis using a GFP-specific antibody. Tubulin served as loading control. (**C**) 293 cells were transfected for 48 h with the indicated siRNAs and BAG3 expression plasmid (BAG3-N1) or vector control (N1) followed by the same analysis as in (A). (**D**) Diagram shows the macroautophagic flux of 293 cells with differently modulated BAG1 and BAG3 levels as described in (A) and (B). Macroautophagic flux was determined by the strength of LC3-II accumulation in a 2 h treatment period with Pep.A/E64. Therefore, normalized LC3-II levels in the absence of inhibitors were subtracted from corresponding levels obtained in the presence of Pep.A/E64. Values are expressed as mean ± SEM. *P<0.05 versus control-transfected cells, n=3.

In BAG3 knock-down cells, accumulation of LC3-II upon lysosomal inhibition by Pepstatin A and E64 (Pep.A/E64) was significantly diminished (Figure 17A, D). This was the case when BAG3 was depleted alone or in combination with BAG1. Interestingly, knock-down of BAG1 alone, which resulted in the induction of BAG3, caused an increased accumulation of LC3-II (Figure 17A, D). It is well-acknowledged that proteasome inhibition provokes a cellular stress response involving the induction of macroautophagy (Ding & Yin, 2008). Given that BAG1 has an essential function in the ubiquitin/proteasome system (see Figure 14), an increased macroautophagic flux is reasonable upon BAG1 knock-down. The present results further suggested a role of BAG3 in this adaptation process as the increased macroautophagic flux

following BAG1 knock-down seems to depend on the presence of BAG3 (Figure 17A, D). To substantiate this view, LC3 fused to GFP (GFP-LC3) (Jackson et al, 2005) was expressed in 293 cells. On the basis of this fusion protein, the macroautophagic flux can be determined by analysis of the GFP-tag, which is relatively resistant to lysosomal degradation and is released upon GFP-LC3-II turnover (Hosokawa et al, 2006). According to a lower macroautophagic flux in BAG3 knock-down cells, Western-blot analyses revealed that steady-state levels of free GFP were decreased (Figure 17B). In contrast, when BAG1 was depleted, the steady-state levels of free GFP were elevated indicating an enhanced macroautophagic flux. Together these results showed that macroautophagy activity correlates directly with the BAG3 to BAG1 ratio expressed in cells.

C.2.5 BAG3 overexpression increases the macroautophagic flux

In the next step, it was examined whether BAG3 overexpression results in an increased activation of the macroautophagy pathway. Indeed, in 293 cells transiently transfected with BAG3, treatment with Pep.A/E64 provoked a greater increase of LC3-II levels compared with the increase in control-transfected cells (Figure 17C, D). Moreover, when BAG3 was overexpressed in a BAG1 knock-down background, a further moderate increase of lysosomal LC3-II degradation was consistently measured (Figure 17C, D). These findings showed that a higher expression of BAG3 leads to an increased lysosomal breakdown of LC3-II which strongly indicated a higher activity of the macroautophagy pathway.

C.2.6 BAG3 overexpression increases the number of autophagosomes

To strengthen the conclusion that BAG3 promotes macroautophagic processes, additional fluorescence microscopic analyses of GFP-LC3-positive autophagosomes were performed in BAG3- and control-transfected cells. However, autophagosomes could not be detected in 293 cells, which may be attributed to the high metabolic activity of 293 cells and the rapid disappearance of these transient structures. Therefore, the I90 cell model was employed, in which GFP-LC3-positive autophagosomes could be clearly detected as green fluorescent punctuated structures (Figure 18A). In BAG3-transfected cells, we observed a clear increase in the number of GFP-LC3 puncta per cell (Figure 18A, B). This observation could be corroborated by Western-blot analysis showing that BAG3 overexpression resulted in increased levels of GFP-LC3-II that further increased upon Pep.A/E64 treatment (Figure 18C). These data showed that increased BAG3 levels contribute to enhanced formation and lysosomal turnover of LC3-II-positive autophagosomes. Having in mind that BAG3 depletion resulted in polyUb-protein accumulation without altering proteasome function (Figure 14A), it

is very likely that BAG3 has a function in regulating polyUb-protein turnover by the macroautophagy pathway.

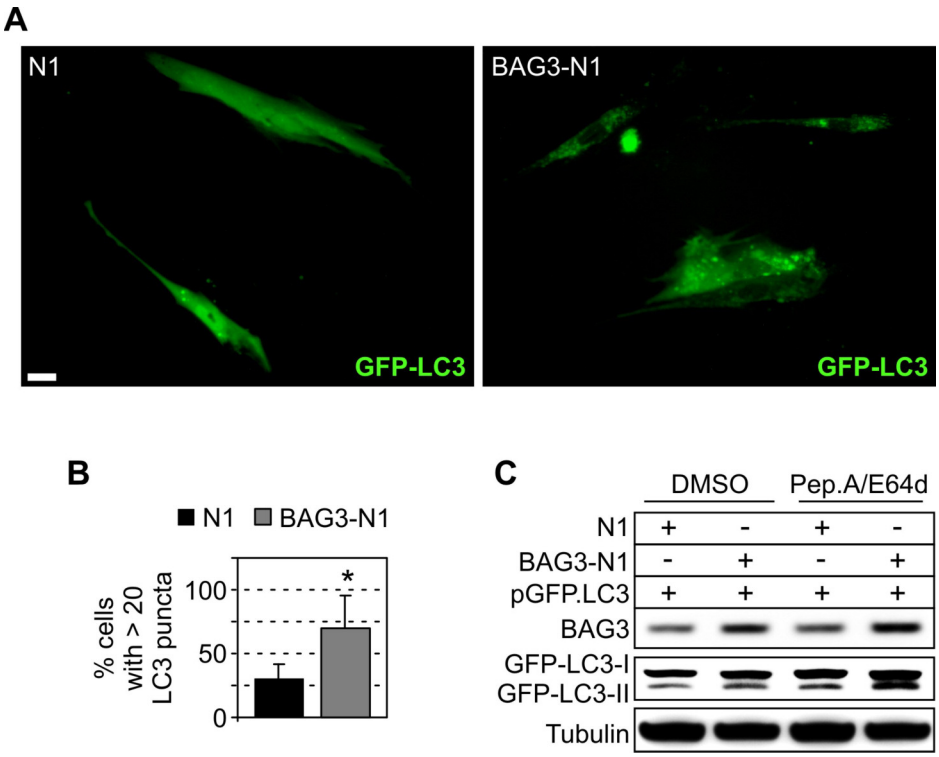

Figure 18: (**A**) I90 cells were transfected with GFP fused to LC3 (pGFP.LC3) and co-transfected either with BAG3 expression plasmid (BAG3-N1) or vector control (N1). After transfection for 24 h, cells were microscopically analyzed for GFP-LC3 fluorescence. Representative pictures are shown. Bar: 20 µm. (**B**) I90 cells were transfected as in (A). Thereafter, percentage of cells showing more than 20 clear visible GFP-LC3 positive puncta was determined. Values expressed in the diagram are mean ± SEM from three independent experiments (50 cells were counted per group per experiment). *P<0.05 versus N1, n=3. (**C**) I90 cells were transfected as in (A). After transfection for 48 h, cells were treated for 2 h with the lysosomal inhibitors Pepstatin A and E64 (both 10 µg/ml; Pep.A/E64) or DMSO as control and levels of indicated proteins were detected by immunoblot analysis. Tubulin served as loading control.

C.3 Functional relation between BAG3 and SQSTM1

The present study so far indicated that BAG3 potentially controls polyUb-protein degradation by macroautophagy. Moreover, since BAG3 is a stress-regulated protein that is typically up-regulated under protein-denaturating conditions, a function of BAG3 in stimulating polyUb-protein degradation by macroautophagy under acute stress conditions is implied as well.

To gain deeper insight into this potential function of BAG3, the ubiquitin-binding protein p62/sequestosome-1 (SQSTM1) was investigated. SQSTM1 is a key player of the macroautophagy pathway which facilitates the selective degradation of polyUb-proteins by the lysosomal system. SQSTM1 is a stress-regulated multi-adaptor protein which can bind

simultaneously LC3 and polyUb-proteins. Thus, SQSTM1 can act as an autophagosome membrane-recruiting ubiquitin-receptor protein (Figure 19). In this respect, SQSTM1 is suggested to control cytoplasmic protein sequestration by the formation of inclusion bodies which are then engulfed by the autophagosome membrane and degraded by macro-autophagy (Pankiv et al, 2007).

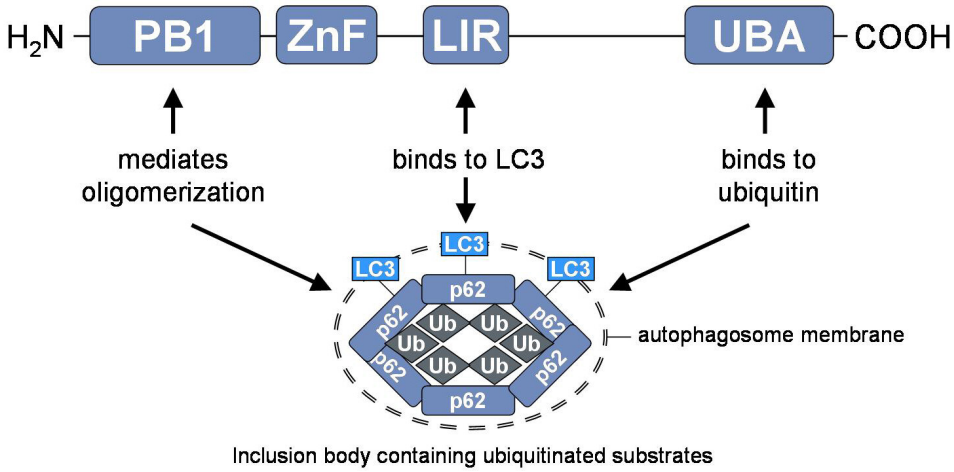

Figure 19: The ubiquitin-receptor protein p62/sequestosome-1 (SQSTM1): domain organization and proposed function in macroautophagy. SQSTM1 is a multi-functional adaptor protein comprising several conserved protein motifs. At the N-terminus SQSTM1 possesses a motif known as the Phox and Bem1p (PB1) domain which mediates SQSTM1 self-oligomerization. SQSTM1 also possesses a zinc-finger (ZnF) domain and a C-terminal ubiquitin-associated (UBA) domain. The UBA domain binds to ubiquitin with a preference for K63-linked polyUb chains. SQSTM1 also features a specific protein interaction site that binds to the autophagosome membrane-associated protein LC3 (LC3-interacting region, LIR).It has been suggested that the PB1 and UBA domains in SQSTM1 confer the ability to sequestrate ubiquitinated substrates in form of inclusion bodies. The inclusion bodies are then specifically engulfed by the autophagosome membrane by recruiting LC3 via the LIR motif in SQSTM1.

C.3.1 BAG3 and SQSTM1 are co-regulated

To examine whether SQSTM1 is involved in the BAG3-regulated macroautophagy pathway, BAG3 overexpression studies were performed in I90 cells. Strikingly, Western-blot analysis revealed increased steady-state levels of SQSTM1 in BAG3-transfected cells (Figure 20A). In addition, analysis of gene expression by real-time PCR analysis revealed significantly increased SQSTM1 mRNA levels upon BAG3 overexpression (Figure 20B). Interestingly, siRNA-mediated knock-down of BAG3 was accompanied by a down-regulation of SQSTM1 mRNA (Figure 20B) as well as protein levels (Figure 20A). The same experiments were also performed in 293 cells. As seen with I90 cells, also in 293 cells SQSTM1 mRNA and protein levels correlated well with BAG3 levels following overexpression and knock-down of BAG3 (Figure 20 C, D). These results showed a strict co-regulation of BAG3 and SQSTM1 and

suggested that macroautophagy stimulation by BAG3 possibly involves the recruitment of the ubiquitin-receptor protein SQSTM1.

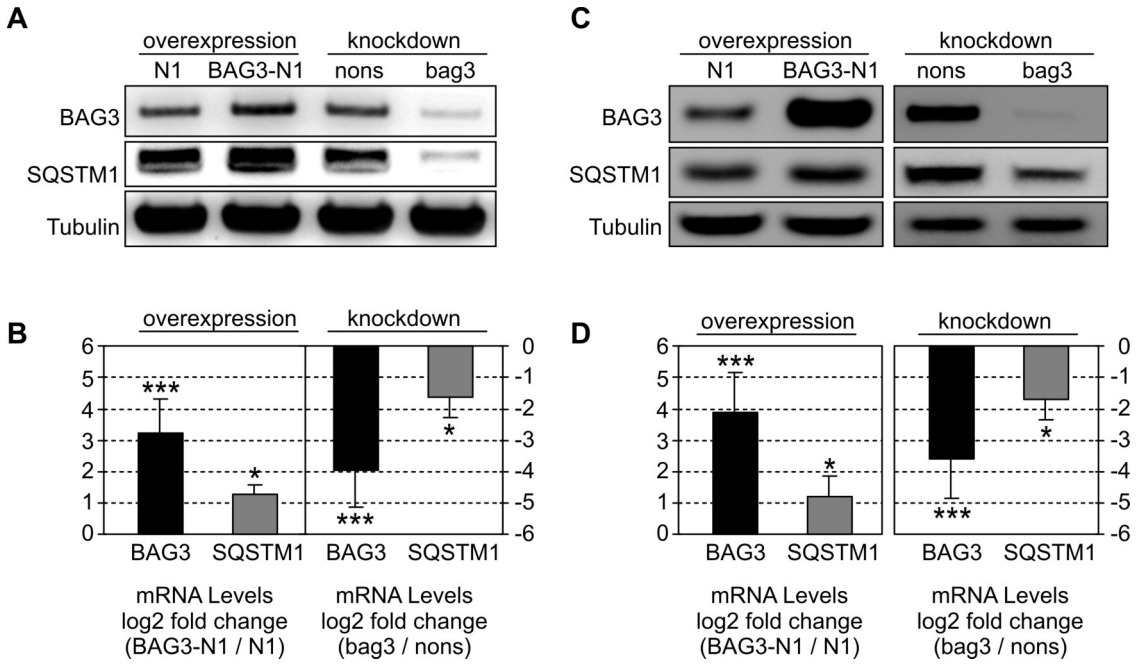

Figure 20: I90 cells were transfected with a BAG3 expression plasmid (BAG3-N1) or vector control (N1) and bag3 or nonsense (nons) siRNA, as indicated. After transfection for 24 h protein and mRNA levels of BAG3 and SQSTM1 were detected by Western-blot (**A**) and real-time PCR analysis (**B**), respectively. Tubulin served as loading control in the Western-blot analysis. Transcript levels are depicted as the mean log2 ±SEM expression ratio of target genes in BAG3-N1 or bag3 siRNA cells relative to N1 or nons siRNA cells, respectively. *P<0.05 and ***P<0.001 versus N1 or nons, n=3. (**C**) and (**D**) Same experiment as in (A) and (B) but 293 cells were used instead of I90 cells.

C.3.2 BAG3 physically interacts with SQSTM1

It has been reported that both, BAG3 and SQSTM1, are up-regulated in response to proteasome inhibition (Wang et al, 2008; Kuusisto et al, 2001). Proteasome inhibition is a well-known trigger for macroautophagy induction (Ding & Yin, 2008). Thus, the co-regulation of these two genes when proteasome function is impaired implies a possible functional relationship of both proteins in macroautophagic processes. To test this possibility, it was examined whether BAG3 physically interacts with SQSTM1 by Co-IP studies. Indeed, SQSTM1 could be pulled-down when BAG3 was immunoprecipitated and *vice versa*, at endogenous BAG3 levels as well as when BAG3 was overexpressed (Figure 21). These experiments also showed that an increased amount of SQSTM1 co-sedimented with BAG3 upon BAG3 overexpression, which was expected in light of the induced SQSTM1 expression. It was also investigated whether BAG1 binds to SQSTM1. Although Hsc/Hsp70 efficiently co-precipitated with BAG1, similar to the BAG3-IP, SQSTM1 could not be detected in BAG1-immunocomplexes (Figure 21). Interestingly, these analyses also showed that less

Hsc/Hsp70 was associated with BAG1 in BAG3-overexpressing cells, suggesting that BAG proteins bind to Hsc/Hsp70 in a competitive manner. Furthermore, SQSTM1 Co-IP studies were performed and the immunocomplexes were analyzed by using the *cBAG* antibody, which detects both, BAG1 and BAG3. However, only BAG3, but not BAG1, could be detected in SQSTM1 immunoprecipitates (Figure 21). These data suggested a specific interaction of BAG3 with SQSTM1, which does not involve Hsc/Hsp70 or the BAG domain.

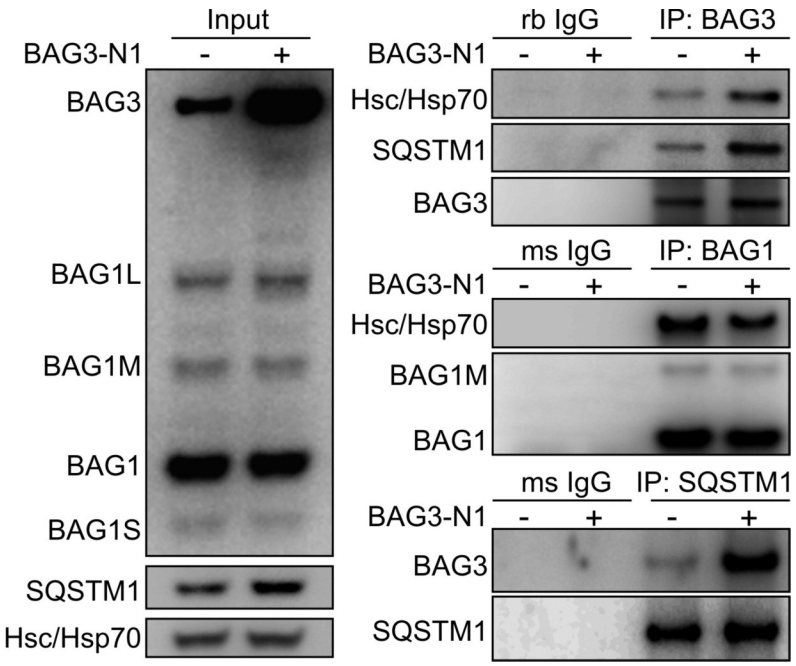

Figure 21: Co-immunoprecipitation (Co-IP) studies testing the interaction of SQSTM1 with BAG3. I90 cells were transfected with BAG3 expression plasmid (BAG3-N1) or vector control. After 24 h, BAG3 (upper panel), BAG1 (middle panel) and SQSTM1 (lower panel) were immunoprecipitated followed by analysis of co-sedimented proteins, as indicated. As negative control purified rabbit (rb) and mouse (ms) IgG was used. Left panel shows relative amounts of proteins in lysates used for Co-IP (Input).

C.3.3 BAG3 might sequester proteins into inclusion bodies in concert with SQSTM1

The co-regulation and the physical interaction of BAG3 and SQSTM1 indicated a functional relationship of both proteins in the macroautophagy pathway. In order to test this possibility, GFP was fused to BAG3 and immunofluorescence based co-localization analyses of BAG3-GFP with SQSTM1 were performed. Staining of SQSTM1 in BAG3-GFP-transfected I90 cells showed punctuated and spheric structures that were also positive for BAG3-GFP (Figure 22). Moreover, in BAG3-GFP-positive cells, SQSTM1 appeared to form larger spheric structures (up to 2 µm in diameter) compared with surrounding non-transfected cells, where only smaller (<1 µm in diameter) SQSTM1-positive punctuated structures were found. These findings could suggest that BAG3 stimulates the sequestering of proteins into inclusion bodies in concert with SQSTM1.

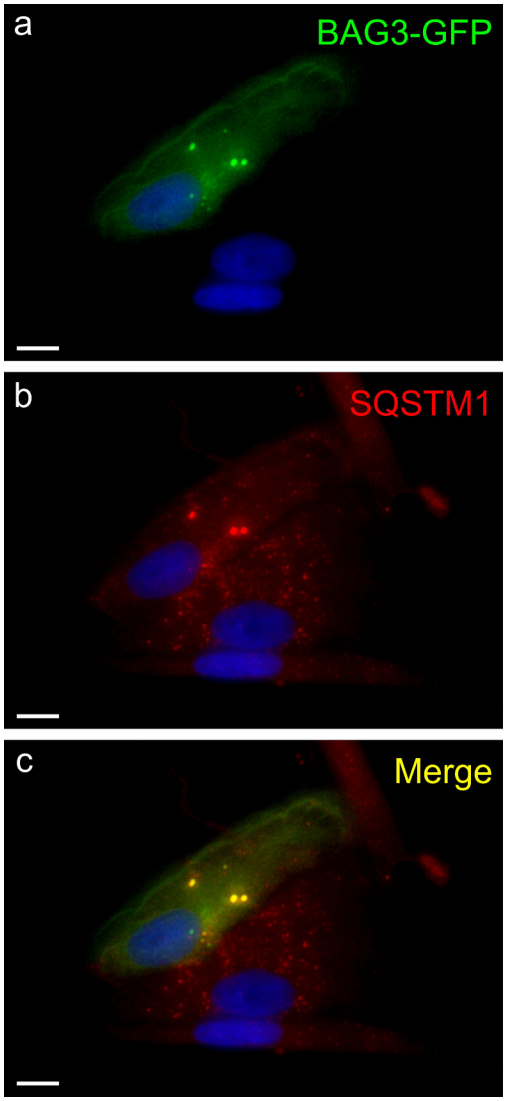

Figure 22: I90 cells were transfected with a BAG3-GFP fusion plasmid for 48 h followed by indirect immunofluorescence staining of endogenous SQSTM1. (a) Direct fluorescence of BAG3-GFP (green), (b) indirect immunofluorescence of SQSTM1 (red) and (c) the stainings of (a) and (b) overlapped. DAPI (blue) was used to stain DNA. Representative pictures are shown. Bar: 10 µm.

C.3.4 BAG3 is not subject to macroautophagic degradation upon starvation

It has been shown that in addition to the quality control substrates that are sequestered by SQSTM1 in inclusion bodies, SQSTM1 itself is also subject to macroautophagic degradation (Ding & Yin, 2008; Pankiv et al, 2007). Therefore, it is possible that also BAG3 is captured in inclusion bodies and degraded by macroautophagy. When macroautophagy was induced by the well-known trigger of amino-acid starvation, the levels of both, BAG3 and SQSTM1 markedly decreased after one hour and BAG3 levels, but not SQSTM1, were rapidly replenished (Figure 23A). Unexpectedly and in contrast to SQSTM1, BAG3 degradation could not be blocked by the lysosomal inhibitor cocktail NH_4Cl/leupeptin (NH_4Cl/Leu). Instead, BAG3 levels, but not SQSTM1, could be rescued by the proteasome inhibitor lactacystin (Figure 23B). These data showed that BAG3 is continuously degraded by proteasomes and that, in contrast to SQSTM1, BAG3 is not degraded by macroautophagy, at least not under conditions when the ubiquitin/proteasome system functions properly.

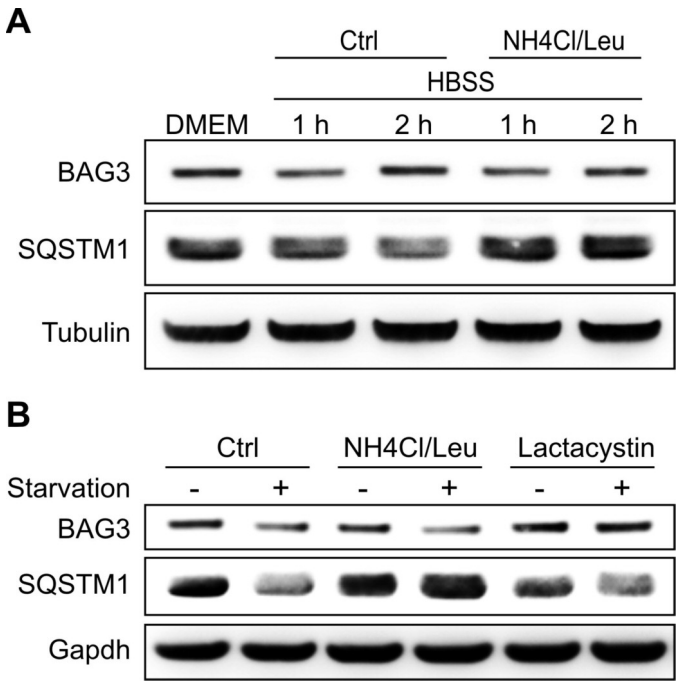

Figure 23: (**A**) I90 cells were cultured in standard medium (DMEM) or amino-acid free medium (HBSS) for 1 h or 2 h in the absence (Ctrl) or the presence of the lysosomal inhibitors NH_4Cl (20 mM) and leupeptin (5 µM) (NH_4Cl/Leu). Thereafter, levels of BAG3 and SQSTM1 were detected by immunoblot analysis. Tubulin was used to ensure equal protein loading. (**B**) I90 cells were cultured in DMEM (-) or starved for 1 h in amino-acid deficient HBSS (+) either in the absence of inhibitors (Ctrl), the presence of the lysosomal inhibitor NH_4Cl/Leu (20 mM/5 µM) or the proteasome inhibitor lactacystin (2 µM). Subsequently, immunoblot analyses of the indicated proteins were performed. Gapdh served as loading control.

C.4 Protein degradation during cellular aging

The present results so far indicated that BAG1 and BAG3 have specific roles in PQC by regulating proteasomal and macroautophagic pathways, respectively. The shift from BAG1 to BAG3 observed during cellular aging (Figure 10) thus suggested possible alterations of proteasomal and macroautophagic activity in aged cells. Hence, in the next step it was investigated whether protein degradation is altered during the cellular aging process.

C.4.1 Overall proteasomal and lysosomal proteolytic capacity in young and old cells

As a first step, total proteasomal and lysosomal proteolytic activities were analyzed in lysates from young and old cells using the fluorescent substrates Suc-LLVY-AMC and Z-FR-AMC, respectively. Suc-LLVY-AMC is processed specifically by the chymotrypsin-like activity of proteasomes, whereas Z-FR-AMC is cleaved by lysosomal proteases of the cathepsin family. Overall proteasomal activity has been reported to decrease during aging in a large number of cell types and tissues from a variety of organisms (Breusing & Grune, 2008). Consistent with these studies, the proteasomal chymotrypsin-like activity in lysates from old I90 cells was significantly reduced compared to young cells (Figure 24). Conversely, the lysosomal proteolytic activity of cathepsins was enhanced (Figure 24). These results may indicate that

PQC during aging involves a shift from the proteasomal to the lysosomal degradation pathway.

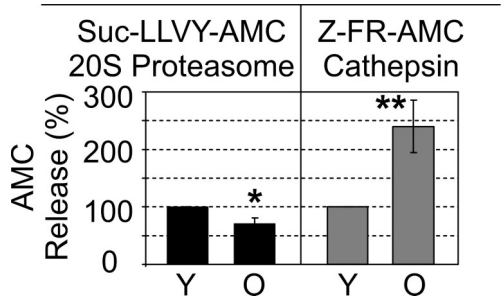

Figure 24: Proteasomal chymotrypsin-like and total cathepsin activity was analyzed in enzymatically active lysates from young (Y) and old (O) I90 cells using the fluorescence probes Suc-LLVY-AMC and Z-FR-AMC, respectively. AMC fluorescence was recorded every 2 min for a total period of 30 min at 37°C in the absence and presence of proteasome (MG132, 20 µM) or lysosomal inhibitors (Pep.A/E64, both 10 µg/ml). Specific activity was determined by subtracting AMC fluorescence (+inhibitor) from AMC fluorescence (-inhibitor). Values expressed are mean ± SEM from three independent experiments. *P<0.05 and **P<0.01 versus activity in young cells, n=3.

C.4.2 The number of autophagosomes is increased in aged cells

In the next step, it was analyzed whether the increased cathepsin activity in old cells is associated with an increased macroautophagy activity. First, the levels of autophagosomes in young and old cells were investigated. Analysis of LC3 expression revealed increased protein and mRNA levels in aged cells (Figure 25A, C). Consistent with these data, indirect immunofluorescence analysis of endogenous LC3 revealed a higher number of LC3-positive autophagosomes in old cells (Figure 25D). To extend these studies, the levels and localization of WD40 repeat protein WIPI1 (WD40 repeat protein interacting with phospho-inositides 1) were compared in young and old cells. WD40 repeat proteins are β-propeller platforms that regulate multi-protein complex assembly. WIPI1 exhibits a 7-bladed propeller structure and a conserved motif for interaction with phospholipids. WIPI1 is involved in autophagosome formation and localizes to early autophagosomes, where WIPI1 is concentrated and can be detected in vesicular structures (Proikas-Cezanne et al, 2007). Similar to LC3, increased mRNA and protein levels of WIPI1 were found in old cells (Figure 25B, C). Moreover, indirect immunofluorescence analysis suggested enhanced formation of autophagosomes during cellular aging as a significantly higher proportion of aged cells showed WIPI1-positive punctuated structures (Figure 25D).

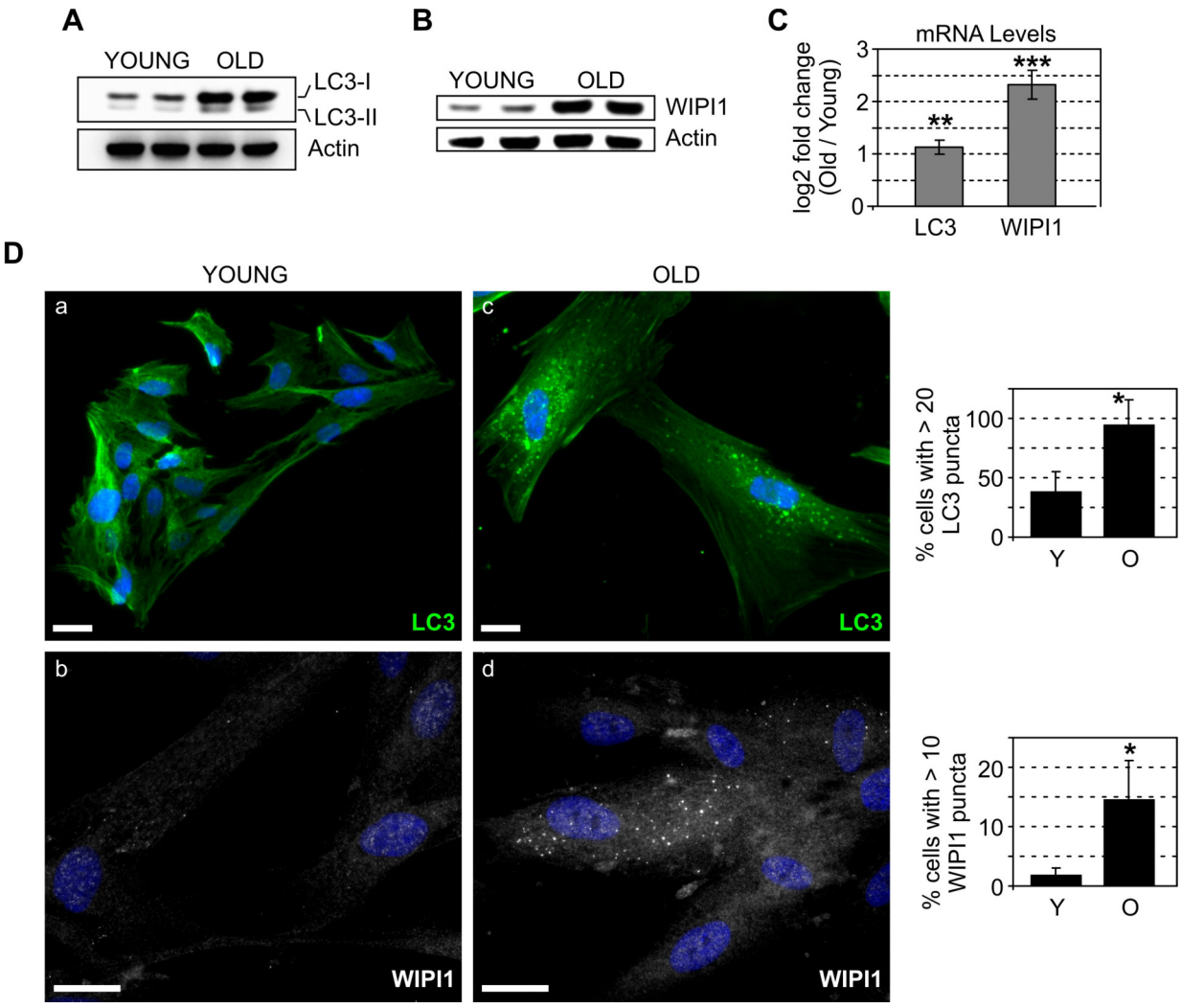

Figure 25: (**A**) and (**B**) Immunoblot analysis of LC3 and WIPI1 levels, respectively, in young and old I90 cells. Actin served as loading control. (**C**) Real-time PCR analysis of LC3 and WIPI1 mRNA levels in young and old I90 cells. Depicted is the mean expression ratio (log2) ± SEM of target genes in old cells relative to young cells. **P<0.01 and ***P<0.001 versus young, n=3. (**D**) Indirect immunofluorescence staining of endogenous LC3 (green, a, c) and WIPI1 (white, b, d) was performed in I90 cells of young and old age. DAPI (blue) was used to stain DNA. Representative pictures are shown. Bar: 20 µm. Diagrams show percentage of cells with indicated characteristics. Values expressed in the diagram are mean ± SEM from three independent experiments (50 cells were counted per group per experiment). *P<0.05 versus young cells, n=3.

C.4.3 The number of inclusion bodies is increased in aged cells

The above presented results showed that the number of autophagosomes is significantly increased in old cells. In the next step the kind of cargo residing within autophagosomes was investigated. It was of particular interest whether autophagosomes in old cells are loaded with PQC substrates. In the first step, the ubiquitin-receptor protein SQSTM1 was analyzed which, as aforementioned, plays a central role in polyUb-protein degradation by macroautophagy (Pankiv et al, 2007). SQSTM1 mRNA levels were slightly increased in old cells, but this effect was not statistically significant (data not shown). Steady-state protein levels of SQSTM1 seemed to be down-regulated, however, a more detailed analysis

revealed increased levels of SDS-resistant high molecular weight SQSTM1 polymers in aged cells (Figure 26A). These polymers might result from inclusion bodies that are formed by SQSTM1during the sequestration process of quality control substrates. Accordingly, a higher number of old cells showed large SQSTM1-positive globular structures up to 2 µm in diameter in the cytoplasm as well as in the nucleus (Figure 26B). In contrast, SQSTM1 staining in young cells was dispersed throughout the cytoplasm and concentrated in few smaller (<1 µm) punctuated structures. These data indicated that old cells may form inclusion bodies composed of SQSTM1 and quality control substrates for subsequent macroautophagic degradation. Accordingly, the SQSTM1 bodies found in old cells co-localized with polyUb signals and LC3 (Figure 27A, B), and numerous LC3-positive autophagosomes were positive for polyubiquitin (Figure 27C). Thus, during aging, the cells obviously recruit the macroautophagy pathway to degrade polyUb-proteins.

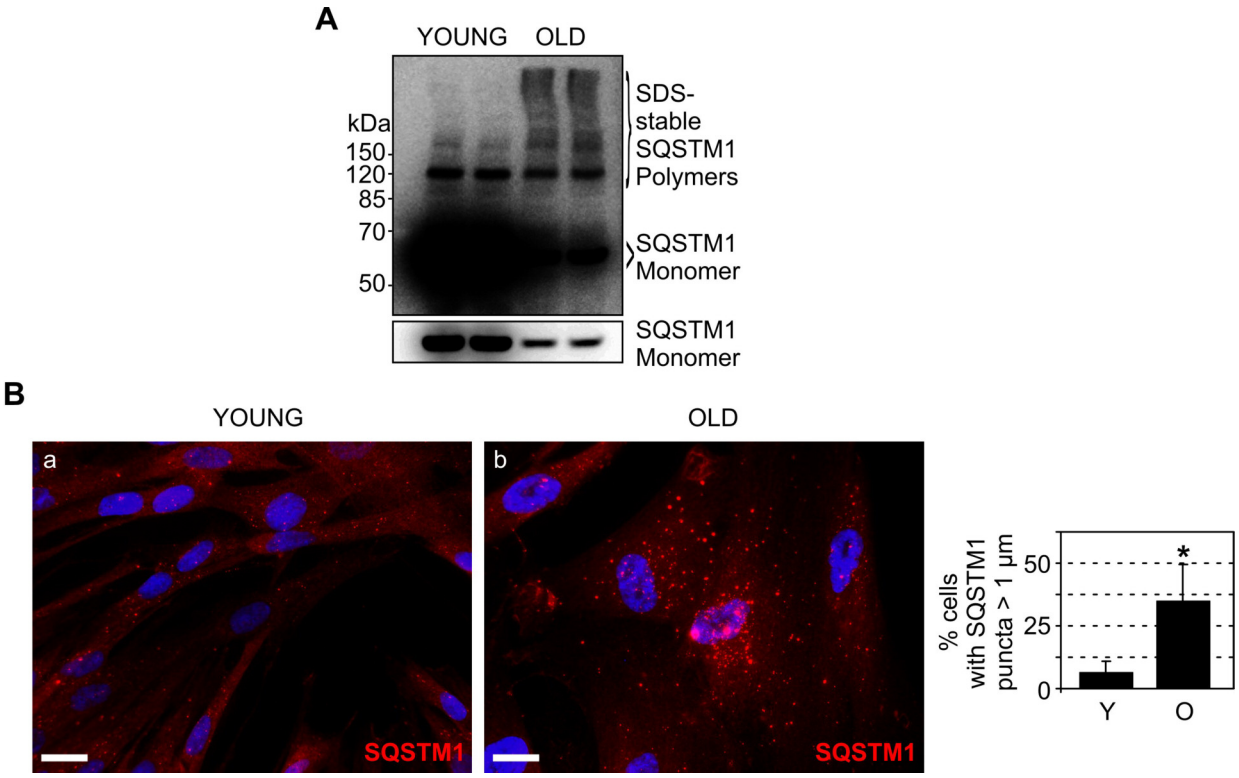

Figure 26: (**A**) Immunoblot analysis of SQSTM1 in young and old I90 cells. Note, old cells showed increased levels of SDS-stable SQSTM1 polymers despite a decrease of SQSTM1 monomer levels. (**B**) Indirect immunofluorescence staining of endogenous SQSTM1 (red) in I90 cells of young (a) and old (b) age. DAPI (blue) was used as a nuclear marker. Representative pictures are shown. Bar: 20 µm. Diagram shows percentage of cells with SQSTM1 puncta > 1 µm in diameter. Values expressed are mean ± SEM from three independent experiments (50 cells were counted per group per experiment). *P<0.05 versus young cells, n=3.

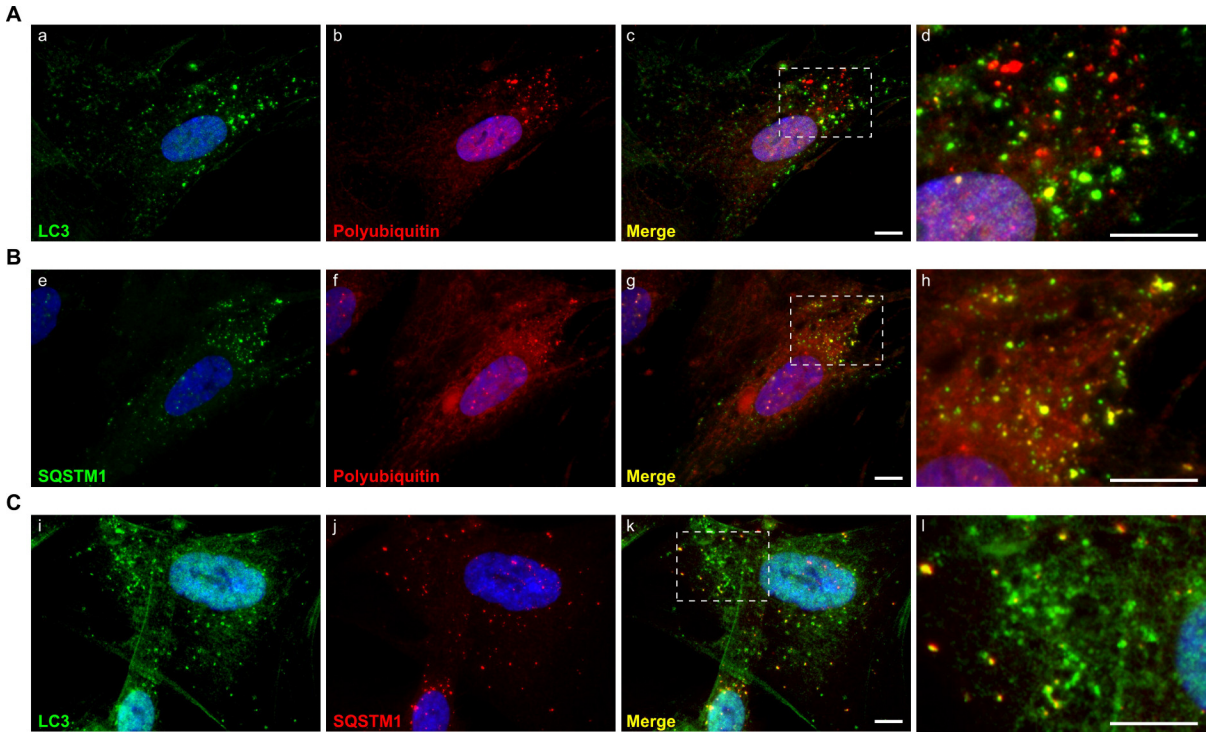

Figure 27: Old I90 cells were analyzed for co-localization of LC3 and polyubiquitin (**A**), SQSTM1 and polyubiquitin (**B**) as well as LC3 and SQSTM1 (**C**) by indirect immunofluorescence stainings. Polyubiquitin indicates polyUb-proteins stained with an antibody specific for polyubiquitin conjugates. (a+b), (e+f) and (i+j) are shown overlapped in (c), (g) and (k), respectively. Magnification of marked areas in (c), (g) and (k) are shown in (d), (h) and (l), respectively. DAPI (blue) was used to stain DNA. Representative pictures are shown. Bar: 20 µm.

C.4.4 The macroautophagic flux is increased in aged cells

The increased number of autophagosomes and inclusion bodies in old cells as shown above could not only reflect an increased formation but also a decreased degradation rate of these structures. Thus, it is very important to compare the kinetic of the phagocytic process by analyzing the current macroautophagic flux in young and old cells. Therefore, cells were treated with the vacuolar H^+-ATPase inhibitor Bafilomycin A1 (BafA1), which inhibits acidification of lysosomes thereby potently inhibiting lysosomal proteases. Strikingly, LC3-II levels increased more prominently in aged cells upon treatment with BafA1 (Figure 28A). Additionally, similar results were obtained when the lysosomal protease inhibitor cocktail Pep.A/E64 was used instead of BafA1 (Figure 28B). These data indicated that the macroautophagic flux is elevated during cellular aging and that the increased number of macroautophagic structures seen in old cells is rather due to enhanced formation than decreased degradation. This view could be further substantiated by monitoring the polyUb-protein flux through the proteasomal and lysosomal systems. In old cells, polyUb-proteins accumulated in the presence of both, the proteasome inhibitor lactacystin as well as the lysosomal inhibitors NH_4Cl/Leu (Figure 28C). Moreover, in the presence of NH_4Cl/Leu the ubiquitin-binding protein SQSTM1 also accumulated, suggesting that old cells might use in

addition to the proteasomal system a SQSTM1-dependent macroautophagy pathway to remove polyUb-proteins. In contrast, young cells did not respond to the lysosomal inhibitors, neither by increased levels of polyUb-proteins nor SQSTM1. Instead, accumulation of polyUb-proteins occurred exclusively upon treatment with lactacystin (Figure 28C), suggesting that young cells used preferentially or exclusively the ubiquitin/proteasome system for polyUb-protein degradation.

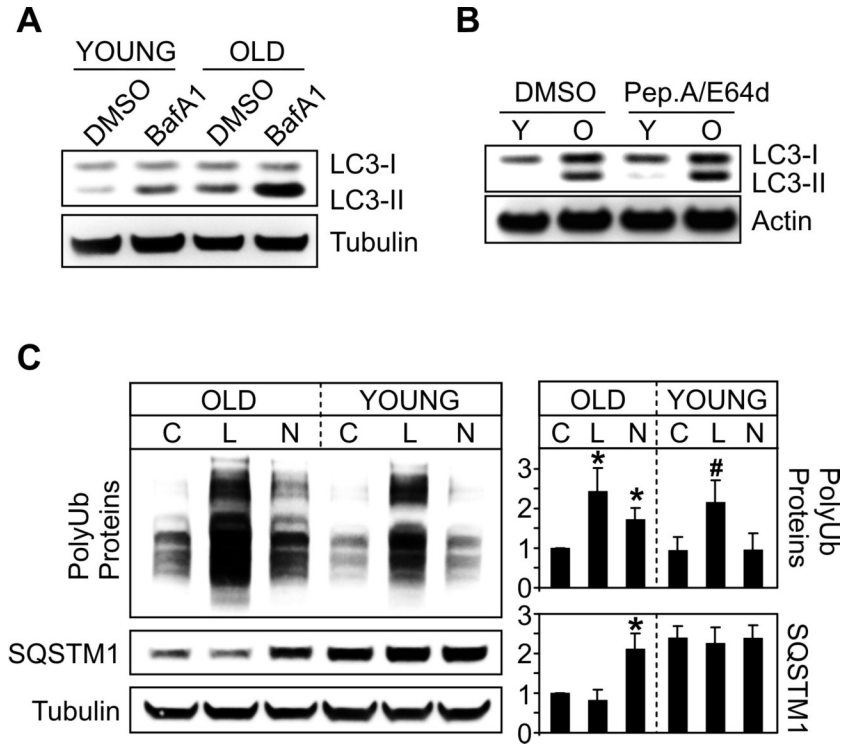

Figure 28: (**A**) Young and old I90 cells were treated for 2 h with bafilomycin A1 (BafA1, 2 µM) to induce lysosomal inhibition or DMSO as control followed by immunoblot analysis of LC3-I and LC3-II levels. Tubulin served as loading control. (**B**) Similar analysis as in (A) but Pepstatin A and E64 (both 10 µg/ml; Pep.A/E64) was used to inhibit lysosomal activity. Y, young cells. O, old cells. (**C**) Old and young I90 cells were treated for 1 h with DMSO as control (C), lactacystin (L, 2 µM) or NH_4Cl (20 mM) plus leupeptin (Leu, 5 µM) (N, NH_4Cl/Leu). Western-blot analyses were performed for detection of indicated proteins. In the diagram (right panel), levels of polyUb-proteins and SQSTM1 are depicted after normalization to corresponding Tubulin levels. Values are expressed as mean ± SEM. *P<0.05 versus old control, $^{\#}$P<0.05 versus young control, n=3.

C.4.5 The basal 26S proteasomal flux is unaltered during cellular aging

It should be noted that, like young cells, aged cells responded strongly to lactacystin treatment (Figure 28C), suggesting that basal proteasomal flux is unaltered, although the *in vitro* analysis (Figure 24) revealed a lower overall proteasomal capacity in old cells. The differences between the proteasomal activity in cell lysates and the polyUb-protein accumulation in response to lactacystin can be explained regarding the different experimental settings. Analysis of proteasomal activity in cell lysates based on fluorescent

substrates measures the overall proteasomal-proteolytic capacity of a cell. This is because fluorescent substrates are in excess and reach proteasomes only by diffusion. In contrast, monitoring polyUb-protein accumulation in response to a specific proteasome inhibitor in living cells measures the activity of the ubiquitin/proteasome system involving the amounts of present quality control substrates, their chaperone recognition, ubiquitination and proteasomal degradation. Thus, the lactacystin assay measures the currently present substrate flux through the 26S proteasomal system. It can be concluded that the overall proteasomal capacity is decreased in aged cells possibly due to decreased proteasomal mass or impaired assembly, as reported previously (Farout & Friguet, 2006). However, the present findings suggested that at the basal level the flux of polyUb-proteins through the 26S proteasomal system is unaltered during aging of cells.

C.4.6 Ultra-structural analysis of macroautophagic structures in young and old cells

The results shown in Figure 25 suggested an increase in the number of macroautophagic structures during aging of cells including early/initial (WIPI1-positive) and late/degradative (LC3-positive) autophagosomes. To substantiate these findings, transmission electron microscopy (TEM) was performed in cooperation with the group of Prof. Dr. U. Wolfrum. At the ultra-structural level autophagosomes can be detected as single, double, or multiple-membrane-bound structures containing clearly identifiable cytoplasmic constituents such as ribosomes, endoplasmic reticulum (ER) membranes and mitochondria. However, cytoplasmic constituents within autophagosomes are clearly visible only in early/initial autophagosomes. The contents of late/degradative autophagosomes upon fusion with lysosomes (also refereed to as autolysosomes) are partially degraded. Thus, autolysosomes appear as membrane-enclosed organelles containing darkly stained, electron-dense fragments of cytoplasmic debris. Old I90 cells showed numerous macroautophagic bodies containing granular or multi-lamellar cytoplasmic material, whereas in young cells, these structures were only sporadically observed (Figure 29). In addition to these early/initial autophagosomes containing clearly identifiable cytoplasmic material, also a higher number of autolysosomes containing electron-dense, partially amorphous material could be detected in old cells. Hence, the TEM studies indicated an increased formation of autophagosomes as well as their lysosomal degradation in old cells compared to young cells. These data strongly corroborated the immunofluorescence analysis as well as the macroautophagic flux measurements shown in Figures 25 and 28. Together these data clearly demonstrated an increased macroautophagic activity that accompanies the cellular aging process.

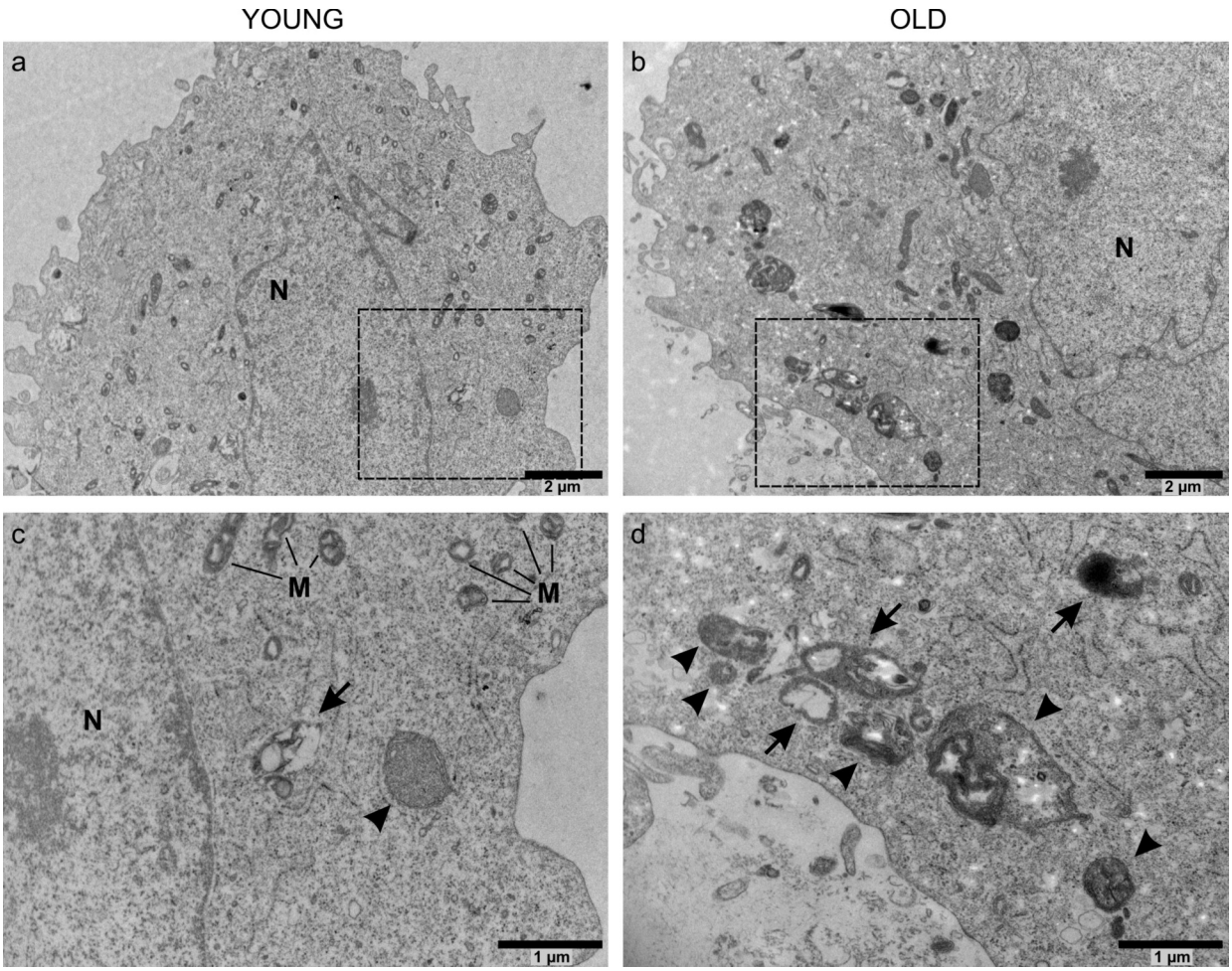

Figure 29: Transmission electron microscopic analysis of young (a) and old (b) I90 cells after counterstaining of the sections with uranyl acetate. Magnifications of marked areas in (a) and (b) are shown in (c) and (d), respectively. An arrow indicates an autolysosome, and arrow heads indicate autophagosomes. M, mitochondrion. N, nucleus.

C.4.7 Aged cells degrade insoluble polyUb-proteins by macroautophagy

A recent study showed the existence of two distinct quality control compartments. Soluble proteins are sequestered near proteasomes, whereas insoluble, terminally aggregated proteins are sequestered in LC3-positive inclusion bodies (Kaganovich et al, 2008). Thus, it was analyzed whether aged cells use the macroautophagy pathway to dispose insoluble polyUb-proteins. Therefore, lysates from old I90 cells were fractionated into TritonX-100 (TX-100)-soluble and -insoluble material following inhibition of macroautophagy activity. Macroautophagy activity was suppressed either by NH_4Cl/Leu treatment for 1 h or, in a genetic approach, by a 4 days-lasting siRNA-mediated knock-down of Atg7, a protein essential for the conjugation of PE to LC3 and thus for the macroautophagy process *per se*. Knock-down of Atg7 in old cells strongly suppressed the macroautophagic flux, as determined by the decreased accumulation of LC3-II upon NH_4Cl/Leu treatment (Figure 30A). Interestingly, in old cells, NH_4Cl/Leu treatment provoked the accumulation of polyUb-

proteins as well as SQSTM1 almost exclusively in the TX-100-insoluble fraction (Figure 30A). Similarly, also Atg7 knock-down resulted in the accumulation of SQSTM1 and polyUb-proteins predominantly in the insoluble fraction. With respect to the Atg7 knock-down effects, it should be noted that equal amounts (15 µg) of protein were loaded in each lane. The Histone H3 levels, which were used for normalization of insoluble proteins, were greatly decreased in Atg7 knock-down cells. This was possibly due to a rise of the total insoluble protein / Histone H3 ratio. Therefore, the accumulation of polyUb-proteins and SQSTM1 could in fact be even stronger than indicated by the immunoblot. In addition, accumulation of polyUb-proteins by NH_4Cl/Leu was suppressed in the Atg7 knock-down background (Figure 30A), confirming that polyUb-protein accumulation provoked by NH_4Cl/Leu was due to a blockade of the macroautophagy pathway. Together these data indicated that aged cells use the macroautophagy pathway to dispose insoluble quality control substrates, possibly by a SQSTM1-dependent mechanism.

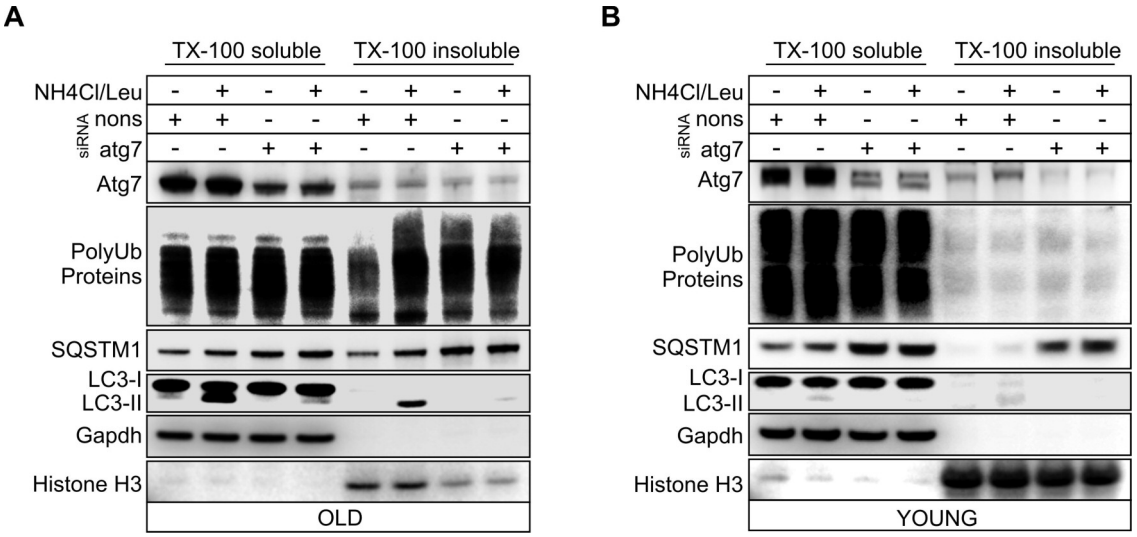

Figure 30: I90 cells of old (**A**) and young (**B**) age were transfected with atg7 or nonsense (nons) siRNA. After transfection for 4 days, the cells were treated with NH_4Cl/Leu or DMSO for 1 h followed by fractioning of cell lysates in TritonX-100 (TX-100)-soluble and -insoluble material. Equal protein amounts of both fractions were directed to immunoblot analysis for detection of indicated protein levels. Gapdh and Histone H3 were used as loading controls of soluble and insoluble fractions, respectively.

As a next step it was analyzed how young cells respond to macroautophagy inhibition. In contrast to old cells, young cells did not accumulate polyUb-proteins in response to NH_4Cl/Leu treatment or Atg7 knock-down, in neither the soluble nor the insoluble fraction (Figure 30B). However, upon Atg7 knock-down SQSTM1 accumulated in both fractions. Short term lysosomal inhibition with NH_4Cl/Leu had little to no effect on SQSTM1 levels. Thus, it seemed that in young cells SQSTM1 exhibits a much slower lysosomal turnover rate

compared with old cells. However, the Atg7 knock-down experiments clearly show a significant macroautophagic breakdown of SQSTM1 also in young cells, but this either does not involve polyUb-proteins degradation (no assembly of polyUb-containing SQSTM1 inclusion bodies) or polyUb-proteins can switch from the macroautophagy pathway, when inhibited, to another proteolytic system such as the ubiquitin/proteasome system. Since SQSTM1 bodies found in young cells were smaller than in old cells (Figure 26B) and since polyUb-positive SQSTM1 bodies could never be observed in young cells (data not shown), the former possibility should be favoured.

C.5 The role of BAG3 in macroautophagy during cellular aging

The findings presented in Figure 30 suggested that during aging, the cell is increasingly stressed by insoluble quality control substrates that have to be degraded by macroautophagy. Accordingly, in old cells a significantly higher proportion of polyUb-proteins was found in the TX-100-insoluble fraction (Figure 31). Interestingly, old cells showed also higher levels of BAG3 in the TX-100-insoluble fraction. These data could indicate that the increased macroautophagic turnover of insoluble polyUb-proteins observed in aged cells is mediated by BAG3. It should be noted that BAG1L as a nuclear protein was also found in the TX-100-insoluble fraction.

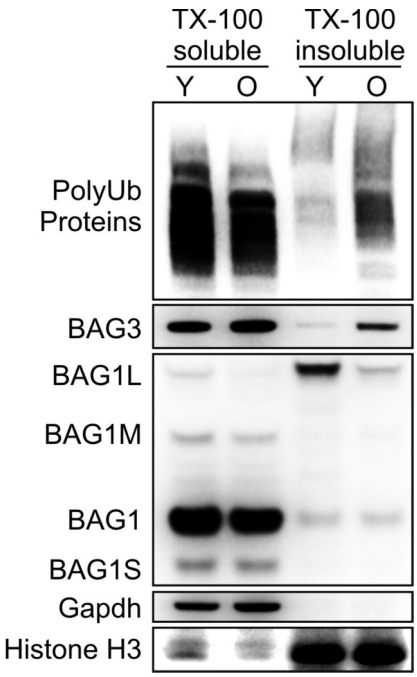

Figure 31: Immunoblot analysis of indicated proteins of young (Y) and old (O) I90 cells upon fractionation of cell lysates in TritonX-100 (TX-100)-soluble and -insoluble material. Equal protein amounts of both fractions were directed to immunoblot analysis. Gapdh and Histone H3 were used as loading controls of soluble and insoluble fractions, respectively.

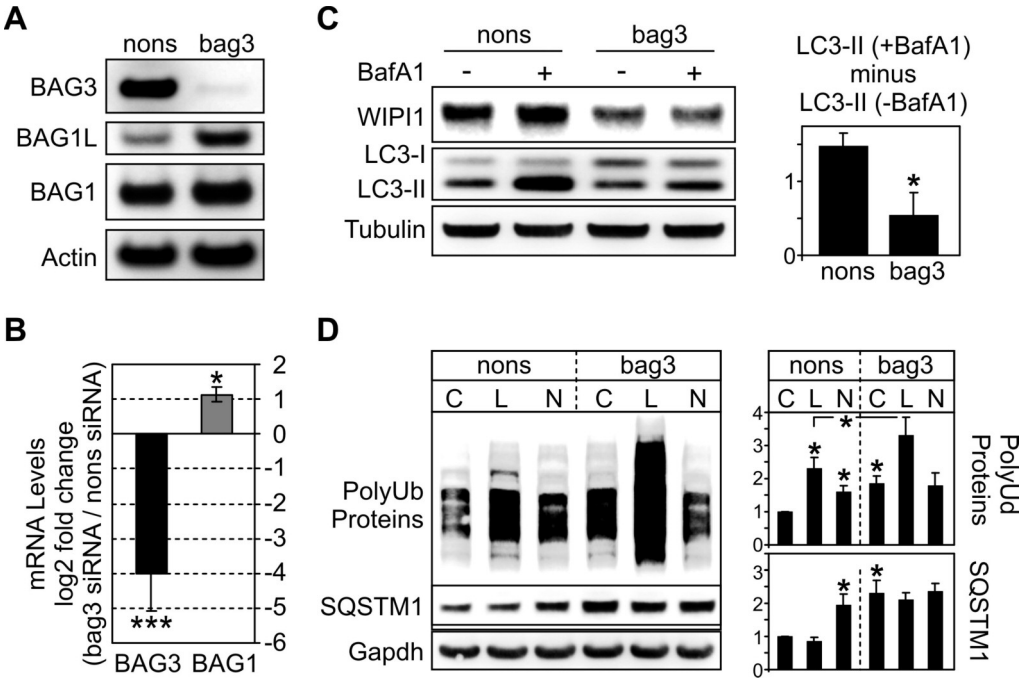

Figure 32: (**A**) and (**B**) After transfection for 96 h of old I90 cells with bag3 or nonsense (nons) siRNA, BAG1 and BAG3 protein and mRNA levels were analyzed by immunoblot (**A**) and real-time PCR (**B**) analysis, respectively. Actin was used for normalization. Transcript levels in bag3 siRNA cells are depicted as the mean log2 expression ratio ±SEM relative to nons siRNA cells. *P<0.05 and ***P<0.001 versus nons, n=3. (**C**) Old I90 cells transfected as in (A) were treated for 2 h with bafilomycin A1 (BafA1, 2 µM). Thereafter, immunoblot analysis of LC3 and WIPI1 levels was performed. The macroautophagic flux is depicted in the diagram (right panel). Therefore, normalized LC3-II levels in the absence of inhibitors were subtracted from corresponding levels obtained in the presence of BafA1. Values are expressed as mean ± SEM. *P<0.05 versus nons, n=3. (**D**) Same analysis as in Figure 28C but old I90 cells transfected as in (A) were used. C, control; L, lactacystin, N, NH_4Cl/Leu. In the diagram (right panel) levels of indicated proteins were normalized to corresponding Gapdh levels. Values are expressed as mean ±SEM from three independent experiments. *P<0.05 versus nons control, or as indicated, n=3.

C.5.1 BAG3 depletion decreases the macroautophagic flux in old cells

To investigate a potential role of BAG3 in the macroautophagic degradation of polyUb-proteins observed during cellular aging, siRNA-mediated BAG3 knock-down was performed in old I90 cells. BAG3 protein levels were efficiently depleted by siRNA (Figure 32A). Consistent with the data obtained with 293 cells, knock-down of BAG3 in old I90 cells was accompanied by the induction of BAG1 at the protein (Figure 32A) as well as transcriptional level (Figure 32B). In the next step, macroautophagic flux measurements were performed on the basis of LC3-II accumulation in the presence of the lysosomal inhibitor BafA1. BAG3-depletion significantly reduced the accumulation of LC3-II in the presence of BafA1 (Figure 32C). Moreover, BAG3 depletion was also accompanied by reduced levels of WIPI1. These findings indicated that the macroautophagic flux in old cells depends on BAG3. Accordingly, the accumulation of SQSTM1 and polyUb-proteins in the presence of NH_4Cl/Leu was completely suppressed in the BAG3 knock-down background (Figure 32D). Moreover, in

BAG3-depleted cells, basal polyUb-protein levels were elevated, suggesting that impairment of macroautophagy by BAG3 knock-down led to the failure of PQC. Interestingly, accumulation of polyUb-proteins in the presence of the proteasome inhibitor lactacystin was enhanced (Figure 32D), suggesting that the knock-down of BAG3 forced old cells to use the ubiquitin/proteasome system more extensively, possibly by the concomitant induction of BAG1.

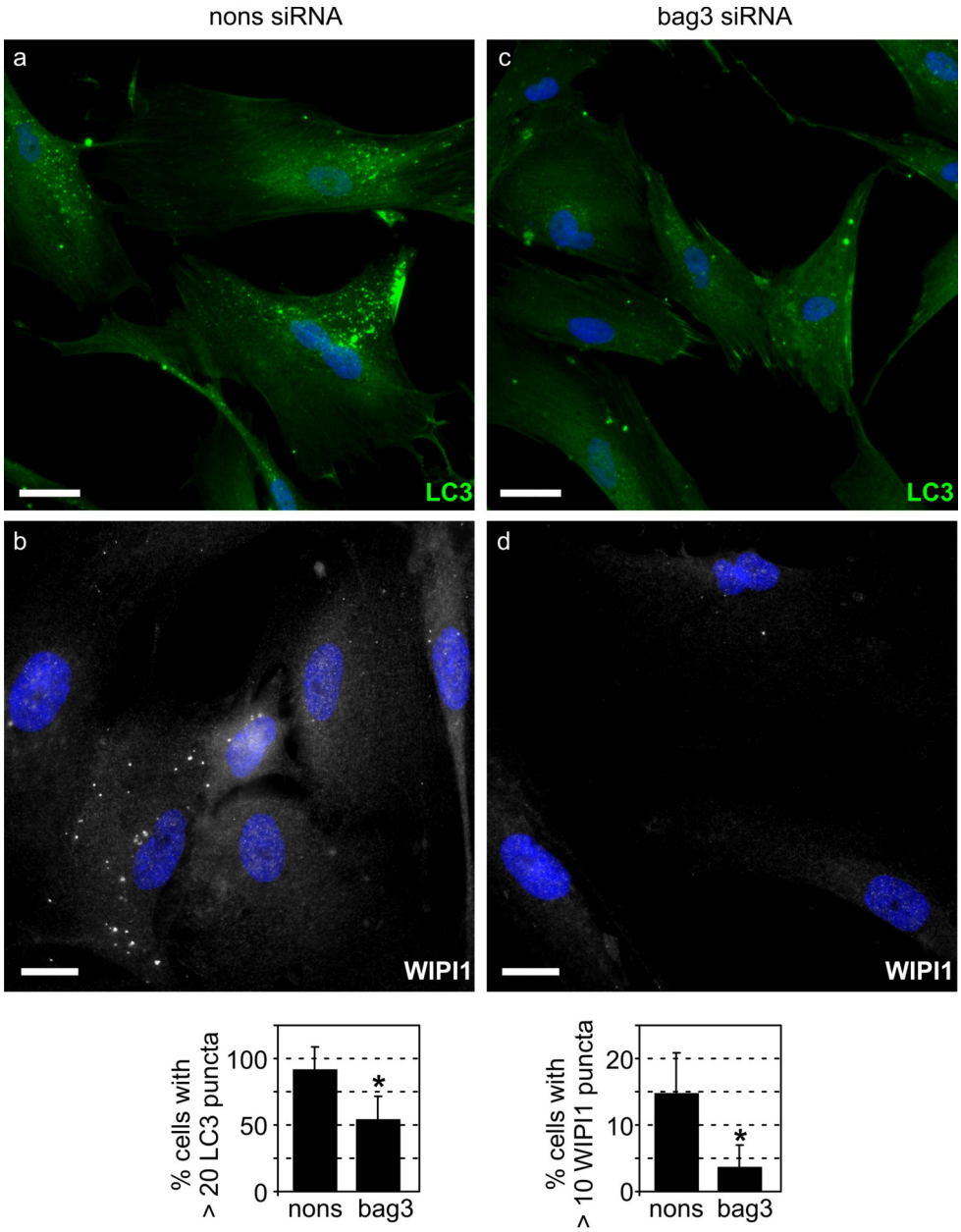

Figure 33: Indirect immunofluorescence analysis of endogenous LC3 (green, a, c) and WIPI1 (white, b, d) in old I90 cells transfected with nons (a, b) and bag3 siRNA (c, d) for 96 h. DAPI (blue) was used as a nuclear marker. Representative pictures are shown. Bar: 20 µm. Diagrams show percentage of cells with indicate characteristics. Values expressed in the diagram are mean ± SEM from three independent experiments (50 cells were counted per group per experiment). *P<0.05 versus young cells, n=3.

C.5.2 The number autophagosomes decreases in aged cells upon BAG3 knock-down

The results shown in Figure 32 suggested that BAG3 depletion in old cells leads to a decreased macroautophagic activity. Accordingly, indirect immunofluorescence analysis of endogenous LC3 revealed less LC3-positive autophagosomes in old cells that were depleted of BAG3 (Figure 33). Moreover, also the number of WIPI1-positive autophagosomes was significantly decreased in BAG3 knock-down cells (Figure 33). Together, these data strongly suggested that autophagosome formation and macroautophagic polyUb-protein degradation in old cells depend on BAG3.

C.5.3 BAG3 overexpression in young cells enhances lysosomal polyUb-protein degradation

In the next step, it was investigated whether BAG3 overexpression in young cells activates the macroautophagy pathway for the removal of polyUb-proteins. And indeed, BAG3 overexpression in young cells led to an increased lysosomal flux of LC3-II (Figure 34A), indicating an activation of the macroautophagy pathway. Strikingly, in BAG3-transfected young cells, polyUb-proteins and SQSTM1 accumulated in the presence of NH_4Cl/Leu (Figure 34B). These results suggested that BAG3 can recruit a SQSTM1-dependent lysosomal pathway in young cells to dispose polyUb-proteins as seen above in old cells.

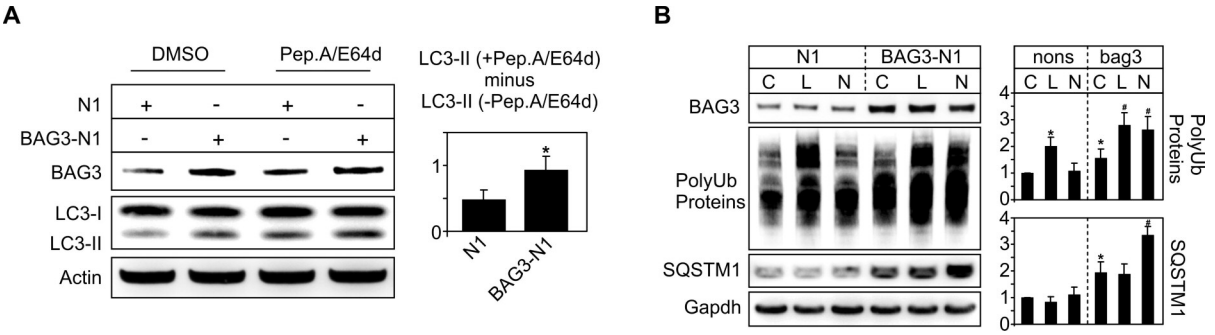

Figure 34: (**A**) Young I90 cells were transfected either with a BAG3 expression plasmid (BAG3-N1) or vector control (N1). After transfection for 48 h cells were treated with Pepstatin A and E64 (both 10 µg/ml; Pep.A/E64) or DMSO as control for 2 h. Thereafter, immunoblot analysis of indicated proteins was performed. Values expressed in the diagram (right panel) are mean ±SEM. *P<0.05 versus N1, n=3. (**B**) Same analysis as in Figure 28C but young I90 cells transfected as in (A) were used. *P<0.05 versus N1 control, #P<0.05 versus BAG3-N1 control, n=3.

C.5.4 BAG3 overexpression recruits the macroautophagy pathway in young cells

The results shown in Figure 34 indicated that BAG3 overexpression can activate macroautophagy and a lysosomal pathway for polyUb-protein degradation in young cells. To analyze whether polyUb-proteins were degraded by macroautophagy, BAG3 overexpression

experiments were performed in a macroautophagy-suppressed background. For this purpose, Atg7 was depleted by siRNA-mediated knock-down. Reduced Atg7 expression resulted in a strong suppression of macroautophagy as determined by the decreased accumulation of LC3-II in the presence of NH_4Cl/Leu (Figure 35). In Atg7- and thus macroautophagy-deficient cells, overexpression of BAG3 did no longer promote the accumulation of polyUb-proteins after lysosomal inhibition with NH_4Cl/Leu. Hence, lysosomal polyUb-protein degradation caused by BAG3 was no longer measurable in the macroautophagy-suppressed background. These findings supported the hypothesis that BAG3 stimulates the macroautophagic degradation of polyUb-proteins.

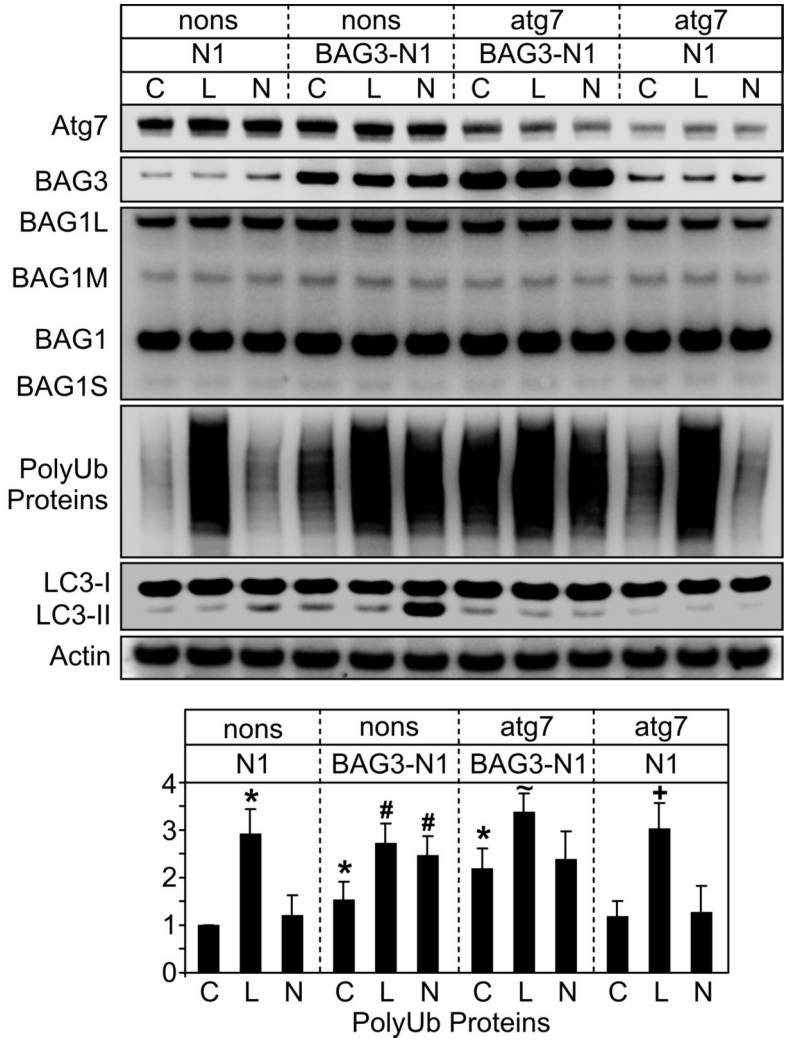

Figure 35: Young I90 cells were transfected with a BAG3 expression plasmid (BAG3-N1) or vector control (N1) and additionally with atg7 or nonsense (nons) siRNA, as indicated. After transfection for 48 h, cells were treated either with DMSO (C, control), lactacystin (L) or NH_4Cl/Leu (N), as performed in Figure 28C. Thereafter, Western-blot analyses were performed for detection of indicated proteins. In the diagram levels of polyUb-proteins are depicted after normalization to corresponding Actin levels. Values are expressed as mean ± SEM. *, $^{\#}$, $^{\sim}$ and $^{+}$, $P<0.05$ versus C N1, C BAG3-N1, C BAG3-N1 atg7 and C N1 atg7, respectively, n=3.

C.5.5 Macroautophagic polyUb-protein degradation depends on SQSTM1

The present findings so far suggested a direct functional relationship between BAG3 and SQSTM1 in macroautophagic processes. Therefore, it was of interest to examine whether the BAG3-mediated recruitment of the macroautophagy pathway into the PQC system of young cells depends on SQSTM1. Hence, the effects of BAG3 overexpression on polyUb-proteins as monitored in Figure 35 were analyzed additionally in a SQSTM1 knock-down background. SQSTM1 expression could be efficiently suppressed by specific siRNA (Figure 36). Strikingly, polyUb-protein levels, which increased in BAG3-transfected cells upon NH_4Cl/Leu treatment, did no longer accumulate in SQSTM1-depleted cells despite overexpressing BAG3 (Figure 36). Thus, the BAG3 effects on polyUb-proteins were efficiently suppressed by knock-down of SQSTM1. These data strongly indicated that BAG3 acts in concert with SQSTM1 to stimulate macroautophagic polyUb-protein degradation.

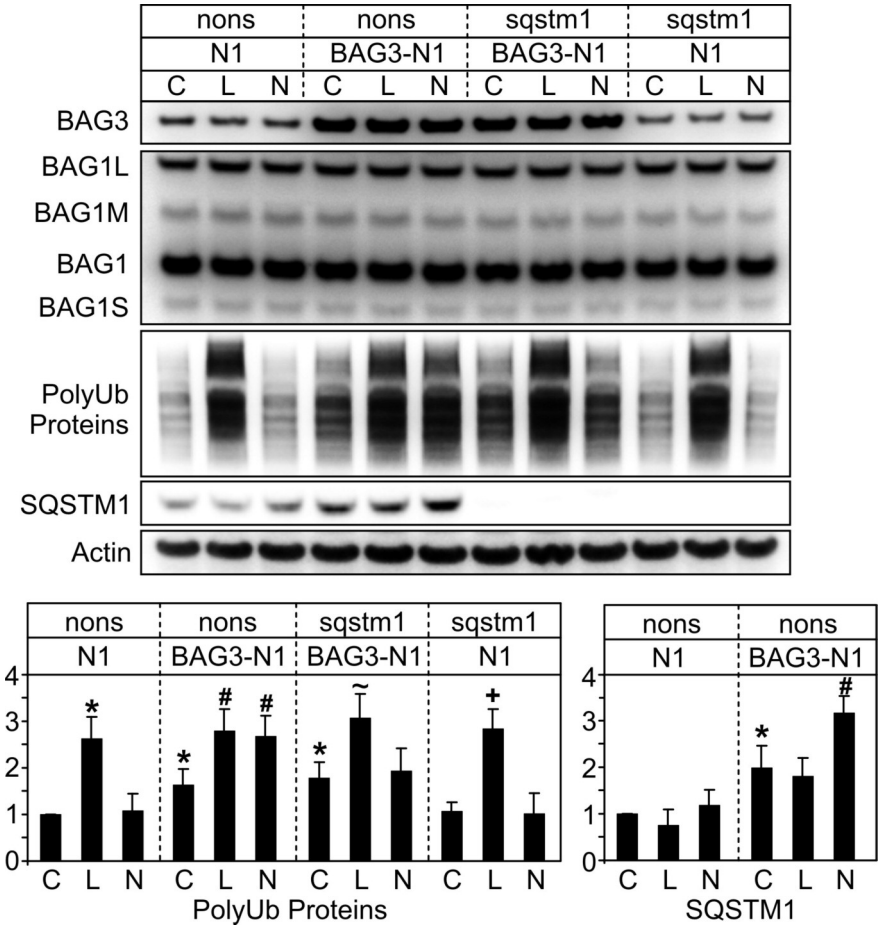

Figure 36: Young I90 cells were transfected with a BAG3 expression plasmid (BAG3-N1) or vector control (N1) and additionally with sqstm1 or nonsense (nons) siRNA, as indicated. After transfection for 48 h, cells were treated either with DMSO (C, control), lactacystin (L) or NH_4Cl/Leu (N), as performed in Figure 26 C. Thereafter, levels of indicated proteins were detected by immunoblot analysis. In the diagram levels of polyUb-proteins and SQSTM1 are depicted after normalization to corresponding Actin levels. Values are expressed as mean ± SEM. *, $^{\#}$, $^{\sim}$ and $^{+}$, $P<0.05$ versus C N1/nons, C BAG3-N1, C BAG3-N1 sqstm1 and C N1 sqstm1, respectively, n=3.

C.5.6 BAG3 overexpression impairs proteostasis in young cells

It should be noted that in BAG3-overexpressing young cells, the basal levels of polyUb-proteins were increased (Figures 34B, 35, 36), indicating that BAG3 interfered with the PQC system of young cells. Young and old cells showed a different ratio of soluble/insoluble polyUb-proteins (Figure 31). As mentioned before, a recent study showed the existence of two distinct quality control compartments: soluble proteins are sequestered near proteasomes, whereas insoluble, terminally aggregated proteins are sequestered in LC3-positive inclusion bodies (Kaganovich et al, 2008). Accordingly, the present study showed that aged cells dispose predominantly insoluble polyUb-proteins by macroautophagy (Figure 30A). Moreover, the present data suggested that in contrast to old cells, young cells show almost exclusively soluble quality control substrates, and thus proteasomal substrates (Figure 31). BAG1 and BAG3 bind to the same domain of Hsc/Hsp70 very likely in a competitive manner since less amounts of BAG1 could be co-immunoprecipitated with Hsc/Hsp70 upon BAG3 overexpression (Figure 21). As a consequence, the coupling of Hsc/Hsp70 with proteasomes, which is mediated by BAG1 (Lüders et al, 2000a), is suggested to decline in BAG3 overexpressing young cells. Thus, BAG3 overexpression shifts the PQC system in young cells from the ubiquitin/proteasome system towards macroautophagy. This could explain the accumulation of polyUb-proteins in BAG3-overexpressing young cells, since the activated degradation pathway does not match the present pool of quality control substrates. Thus, it can be concluded that a proper ratio of BAG1/BAG3, adjusted to the ratio of soluble to insoluble (aggregated) quality control substrates, might be more important to maintain proteostasis than the abundance of BAG3.

C.6 BAG3 to BAG1 ratio and macroautophagy in the aging rodent brain

Many age-related neurodegenerative diseases including Alzheimer's disease, Parkinson's disease, Huntington's disease and ALS are associated with the aberrant accumulation of protein aggregates in neuronal tissues (Figure 37). The main protein components of disease-associated aggregates are diverse. For example, Alzheimer's disease is characterized by extracellular aggregates called "senile plaques" that mainly consist of amyloid-β, a cleavage fragment of the amyloid-precusor protein (APP) (Goedert & Crowther, 2003. Alzheimer's disease is also associated with the aberrant formation of intracellular aggregates known as "neurofibrillary tangles". These tangles are mainly composed of the microtubule-associated protein tau which exhibits a conformational change and a hyperphosphorylated state. In Parkinson's disease α-synuclein constitutes the main component of the characteristic protein aggregates called "Lewy bodies" (Ono et al, 2008). In ALS intracellular ubiquitinated protein inclusions are found primarily composed of the TAR DNA binding protein 43 (TDP-43) or, in

genetic forms, of mutant SOD1 (Mackenzie et al, 2007). Although the protein components of disease-associated aggregates are diverse in the different pathologies, all the aggregate-prone proteins form fibrils with a characteristic cross-β sheet quaternary structure known as amyloid (Figure 37) (Chiti & Dobson, 2006). Interestingly, a further common feature of amyloidogenic aggregates found in age-related disorders is the presence SQSTM1, suggesting that these aggregates are actually subject for macroautophagic degradation (Komatsu et al, 2007; Pankiv et al, 2007; Zatloukal et al, 2002). However, the aberrant accumulation of SQSTM1-positive aggregates in disease-affected brain areas implies an impairment of the macroautophagy pathway during disease pathology. Since these neurodegenerative pathologies are associated with aging, it was of interest to investigate whether the age-related adaptation of PQC pathways observed in the cellular models could be confirmed in models of *in vivo* brain aging. Therefore, potential alterations of BAG expression and BAG-controlled PQC pathways, in particular the recruitment of the macroautophagy pathway, were investigated in the aging rodent brain.

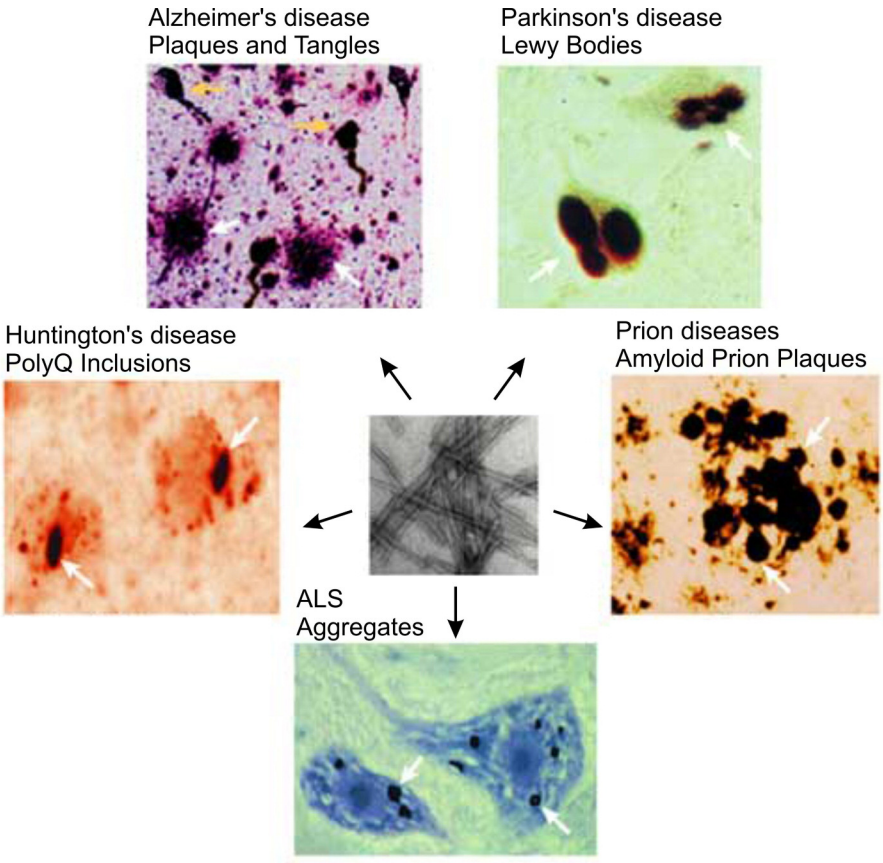

Figure 37: Aberrant protein aggregates characteristic of human neurodegenerative disorders. Although the main protein components of protein aggregates accumulating in neurodegenerative disorders are diverse, the aggregates show a common structural feature: amyloid fibrils with a characteristic cross-β sheet quaternary structure (center). Moreover, these aggregates are often positive for ubiquitin and SQSTM1, suggesting that they are actually subject to macroautophagic degradation. Figure adapted from (Soto, 2003).

C.6.1 The BAG3 to BAG1 ratio is increased during brain aging

To investigate a potential shift from BAG1 to BAG3 during aging of the rodent brain, brain homogenates from young (3 months) and old (24 months) mice were analyzed by Western-blot analysis. Various brain regions including the cerebellum, the hippocampus and the cortex showed increased BAG3 and decreased BAG1L levels in advanced age (Figure 38A, B, C). In the aged midbrain BAG3 was also up-regulated, but BAG1L levels were unaltered.

The cerebellum showed significantly higher expression of BAG3 compared to other brain areas (Figure 38D) and the reciprocal regulation of BAG1 and BAG3 during aging was most significant in this brain region. Therefore, the regulation of BAG1 and BAG3 in this area was also analyzed at the transcriptional level. BAG3 transcript levels were significantly elevated during aging (Figure 38E). BAG1 mRNA levels were slightly decreased, but this effect was not statistically significant. In addition, similar to the cellular aging models, also decreased levels of BAG2 mRNA levels were found.

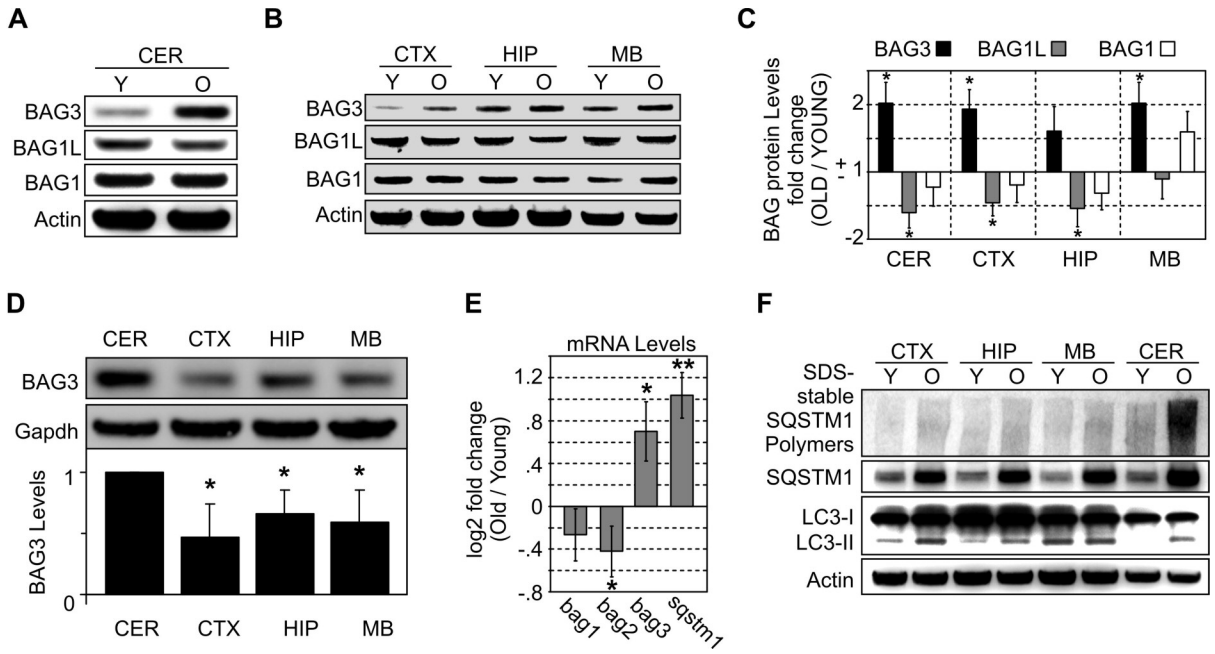

Figure 38: (**A**) Protein extracts from cerebellum (CER) of young (Y, 3 months) and old (O, 24 months) mice were analyzed for BAG1 and BAG3 expression by immunoblot analysis. Actin served as loading control. (**B**) Immunoblot analysis as in (A) but in cortex (CTX), hippocampus (HIP) and mid-brain (MB) from young and old mice. (**C**) Densitometric quantification of BAG protein levels in the cerebellum, cortex, hippocampus and midbrain of young and old mice detected by immunoblot analysis as performed in (A) and (B). Values are expressed as mean ±SEM from three independent experiments. *P<0.05 versus levels of young mice, n=3. (**D**) Comparison of BAG3 protein levels in indicated brain regions of old mice, as indicated. Gapdh served as loading control. In the diagram normalized BAG3 levels are depicted as mean ±SEM from three independent experiments. *P<0.05 versus levels found in CER, n=3. (**E**) Real-time PCR analysis of indicated mRNA levels in cerebellum of young and old mice. Depicted is the log2 expression ratio of target genes in old mice relative to young mice. Values are expressed as mean ±SEM. *P<0.05 and **P<0.01 versus young, n=3. (**F**) Western-blot analysis of macroautophagy markers LC3 and SQSTM1 in indicated brain regions of young and old mice. Note the increase of SDS-stable high-molecular weight SQSTM1 polymers in aged brain tissues. Actin served as loading control.

C.6.2 Levels of SQSTM1 and LC3-II are increased during brain aging

The BAG shift observed during brain aging suggested a potential increase of macroautophagy activity. To investigate this aspect, the levels of the macroautophagy markers SQSTM1 and LC3-II were analyzed in brains of young and old mice. Immunoblot analysis revealed an age-associated increase of SQSTM1 steady-state levels in all brain regions analyzed (Figure 38F). This was most likely due to an increased gene expression as SQSTM1 mRNA levels were significantly up-regulated in the cerebellum of aged mice (Figure 38E). Interestingly, similar to the *in vitro* aging models, elevated levels of SDS-stable SQSTM1 polymers were found (Figure 38F). The highest levels of SQSTM1 polymers were found in the aged cerebellum correlating well with the highest BAG3 levels detected in this area. LC3-II levels were increased in the aged cerebellum, cortex and hippocampus, but not in the midbrain. These data indicated an age-associated increased formation of SQSTM1-positive inclusion bodies and a possible increase of macroautophagy that could be potentially mediated by the increased BAG3 to BAG1 ratio.

C.6.3 Lysosomal cathepsin activity is increased during brain aging

To date, a reliable protocol for the measurement of the *in vivo* macroautophagic flux in the brain does not exist. Nevertheless, to further investigate whether the increased levels of BAG3, SQSTM1 and LC3-II in the aged brain was associated with an increased macroautophagy activity the lysosomal cathepsin activity was compared in hippocampal and cerebellar homogenates from young and old mice. Total cathepsin activity, determined with the fluorescent substrate Z-FR-AMC, was significantly increased in both brain regions of old mice (Figure 39). The specific cathepsin B activity, which was examined with the cathepsin B-specific substrate Z-RR-AMC, was also elevated in aged brain samples (Figure 39). These data support a potential increase of macroautophagy activity during brain aging.

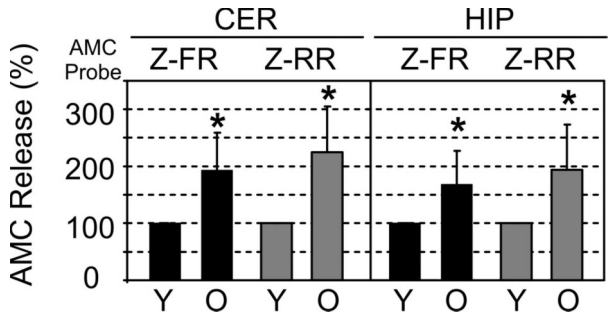

Figure 39: Total cathepsin and specific cathepsin B activity in cerebellum (CER) and hippocampus (HIP) from young and old mice was determined using fluorescence probes Z-FR-AMC (Z-FR) and Z-RR-AMC (Z-RR), respectively, as performed in Figure 24. Values are expressed as mean ±SEM. *P<0.05 versus young, n=3.

C.6.4 The BAG3 to BAG1 ratio is increased specifically in neurons during aging

To identify the cell population in the brain responsible for the altered BAG levels during brain aging, *ex vivo* cultured hippocampal neurons as well as astrocytes from young (2 months) and old (24 months) rats were employed. The purity of astrocytic and neuronal cell cultures was examined by immunoblot analysis by detection of GLT1 and NeuN, respectively. The glutamate transporter GLT1 is specifically expressed in astrocytes whereas NeuN constitutes a specific neuronal nuclear marker protein (Rothstein et al, 1994; Mullen et al, 1992). GLT1 was detected exclusively in the astrocytic cultures (Figure 40), suggesting high purity of the neuronal cultures. NeuN was found predominantly in neuronal cultures but also astrocytic cultures showed weak signals. These signals could be attributed to the presence of resting nuclei of dead neurons, which were observed under the microscope. Analysis of BAG expression revealed strongly elevated levels of BAG3 in neurons isolated from old animals compared with their young counterparts (Figure 40). Furthermore, the levels of BAG1L and BAG1 were down-regulated. In contrast, astrocytes showed no age-associated alterations of BAG levels (Figure 40). These results suggested that in the aged rodent brain, an increase of the BAG3 to BAG1 ratio occurs specifically in neuronal cell populations and that a potential BAG3-associated increase of macroautophagy activity during brain aging is also neuron-specific. Accordingly, analysis the autophagosome marker LC3-II revealed a slight increase in neurons from old animals whereas LC3-II levels in astrocytes were unchanged.

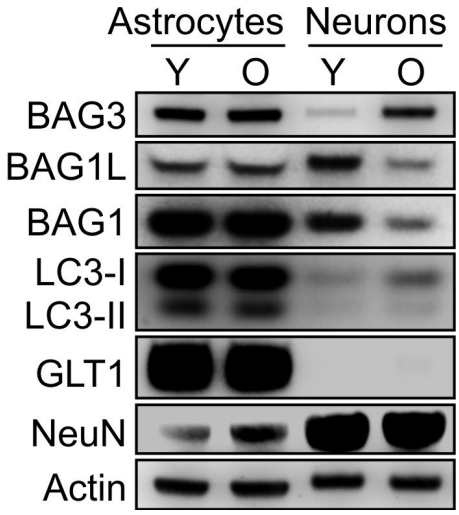

Figure 40: Expression analysis of indicated proteins in primary hippocampal astrocytic and neuronal cell cultures from young (2 months) and old (24 months) rats. Detection of GLT1 and NeuN served as astrocyte and neuron markers, respectively. Note the NeuN signals in astrocytic cultures. These signals were attributed to the presence of resting nuclei of dead neurons, which could be observed under the microscope. Actin was used as loading control.

D DISCUSSION

A main characteristic of several age-associated human neurodegenerative diseases is the accumulation of aberrant protein aggregates. In these protein conformational disorders, also referred to as proteinopathies, protein aggregates are found that contain polyUb-proteins and, thus, proteins that are very likely destined for degradation. Hence, the emergence of such protein conglomerates indicates a dramatic change of the PQC system during aging and/or disease pathology. In the present study, BAG-controlled quality control pathways and their alterations during the aging process were investigated. Here, the focus was on the widely expressed BAG isoforms, BAG1 and BAG3, and their specific roles in protein degradation. The present study identifies BAG1 and BAG3 as key modulators of the proteasomal and macroautophagic pathways, respectively, for the degradation of polyUb-proteins. Moreover, this study shows that BAG1 and BAG3 are reciprocally regulated during aging leading to an increased BAG3 to BAG1 ratio in aged cells. Triggered by increased BAG3 expression, protein homeostasis in aged cells is maintained by recruitment of the macroautophagy pathway involving the polyubiquitin- and LC3-binding protein SQSTM1. These findings and possible implications for age-related proteinopathies of the nervous system are discussed in the following paragraphs.

D.1 Regulation of protein degradation pathways by BAG1 and BAG3

The present findings suggest that BAG1 and BAG3 control a molecular switch between proteasomal and macroautophagic degradation pathways. This raises the question how exactly BAG1 and BAG3 exert the function in differentially regulating the ubiquitin/proteasome system and macroautophagy, respectively.

D.1.1 Regulation of the ubiquitin/proteasome system by BAG1

The results of the present study suggest that BAG1 is essential for effective proteasomal degradation of polyUb-proteins. With respect to the basic role of BAG1 in the ubiquitin/proteasome system, Höhfeld and colleagues have reported convincing mechanistic insights (Lüders et al, 2000a). Their study demonstrates that BAG1 can bind to the proteasome via the ubiquitin-like domain (UBL) found at the N-terminus of BAG1. Furthermore, by simultaneous binding to Hsc/Hsp70 via the BAG domain, BAG1 couples the chaperone to proteasomes. Considering the function of BAG1 as a nucleotide exchange factor of Hsc/Hsp70 (Sondermann et al, 2001; Höhfeld & Jentsch, 1997), it is likely that BAG1 mediates chaperone substrate transfer to proteasomes. The present findings showing

that BAG1 is essential for effective proteasomal degradation of polyUb-proteins strongly supports this hypothesis.

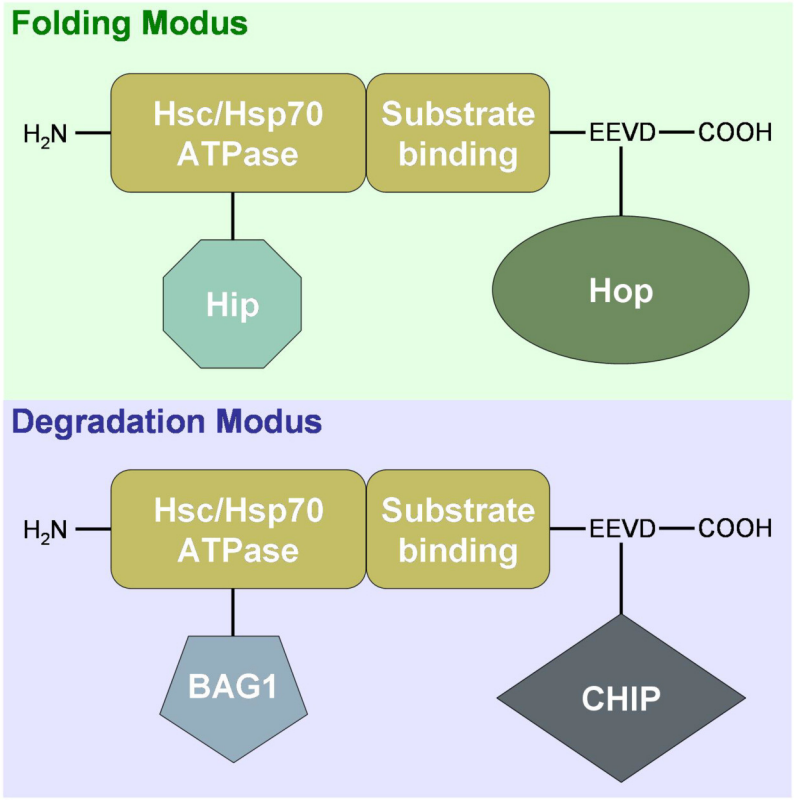

Figure 41 Hsc/Hsp70 folding and degradation activity depends on co-factor binding. The folding activity of Hsc/Hsp70 is promoted by co-factors like Hip and Hop. In contrast, a ternary complex of Hsc/hsp70 together with BAG1 and CHIP constitutes a degradation machine which stimulates ubiquitination and proteasomal degradation of chaperone-hold substrates.

A previous study showed that BAG1 itself is polyubiquitinated by the E3 ubiquitin ligase CHIP in a non-canonical manner (Alberti et al, 2002). The polyubiquitin chain attached to BAG1 is linked preferentially via lysine 27 and, interestingly, does not serve as a degradation signal. Instead, BAG1 polyubiquitination confers binding of the co-chaperone to the proteasome in addition to the integrated ubiquitin-like domain. The cooperative action of CHIP and BAG1 in proteasomal degradation has been further substantiated by analysis of glucocorticoid hormone receptor (GR) degradation (Demand et al, 2001). This analysis showed that overexpression of BAG1 alone is insufficient to increase the degradation rate of the receptor. However, BAG1 stimulates GR degradation when overexpressed together with CHIP. In this context, it has been shown that BAG1 accepts Hsc/Hsp70 substrates and presents them to the CHIP ubiquitin conjugation machinery. CHIP possesses three major domains: a three tandem tetratricopeptide repeat (TPR) domain at the N-terminus, a charged central domain, and a U-box domain at the C-terminus (McDonough & Patterson, 2003). The U-box domain

involves a modified ring finger motif typically present in ubiquitin ligases. Through the TPR domain CHIP interacts with the EEVD sequence located at the C-terminus of Hsc70/Hsp70. As BAG1 binds to the N-terminal ATPase domain of Hsc/Hsp70, CHIP and BAG1 can simultaneously bind to Hsc/Hsp70. Thus, a ternary complex of Hsc/Hsp70 together with CHIP and BAG1 is thought to function as a degrading machine of the ubiquitin/proteasome system. This process involves substrate sequestration by Hsc/Hsp70, substrate ubiquitination by CHIP and substrate transfer to proteasomes by BAG1. Hence, BAG1 and CHIP are thought to direct Hsc/Hsp70-dependent protein triage decision from folding to degradation, whereas binding of Hip and Hop is suggested to promote the folding activity of the chaperone (Figure 41) (Höhfeld et al, 2001).

On the other hand, BAG1 has been shown to inhibit proteasomal degradation of the protein tau. Tau has been linked to several neurodegenerative conditions like Alzheimer's disease and forms of frontotemporal dementia (Elliott et al, 2007). As the tau protein can be degraded by the 26S proteasome following polyubiquitination by CHIP (Hatakeyama et al, 2004), BAG1 should rather stimulate tau degradation as reported for the GR. However, a recent study showed that tau is a substrate for the ubiquitin-independent working 20S proteasome system because it has little secondary structure (Carrettiero et al, 2009). In this study, the 20S proteasome pathway has been shown to be the main route for tau degradation. Interestingly, tau degradation by the 20S proteasome is mediated by Hsc/Hsp70 in cooperation with BAG2. Thus, the observed decrease of tau degradation upon BAG1 overexpression could be due to a competitive inhibition of the BAG2-Hsc/Hsp70 interaction and the resulting decrease of 20S proteasomal tau degradation. These results show the high complexity of the BAG-controlled chaperone-associated proteasomal degradation pathways and the need of proper ratio of BAG1 and BAG2 that is adjusted to the amounts of different quality control substrates. Interestingly, a recent study showed that tau degradation declines with age (Dickey et al, 2009). Considering the down-regulation of BAG2 in the analyzed aging models, it is possible that the slowed tau turnover during aging is due to the diminished capacity of the BAG2-Hsc/Hsp70-mediated 20S proteasome pathway. Future studies will have to investigate this interesting correlation in more detail.

D.1.2 Regulation of the macroautophagy pathway by BAG3

In contrast to BAG1, BAG3 regulates the degradation of polyUb-proteins by macroautophagy. BAG3 binds to the same domain of Hsc/Hsp70 as BAG1, presumably in a competitive manner. One might therefore speculate that a ternary complex composed of Hsc/Hsp70, CHIP and BAG3 handles substrates for macroautophagic degradation. In line

with this view, it has been shown that CHIP can enhance proteasomal as well as lysosomal protein degradation pathways (Shin et al, 2005). Interestingly, CHIP-mediated degradation via the proteasome seems to depend on the TPR domain and thus on chaperone binding. In contrast, the CHIP-stimulated lysosomal pathway depends on the U-box domain implying the requirement of polyubiquitination reactions. Thus, CHIP is able to target substrates for different degradation pathways via different mechanisms and it is possible that the different functions of CHIP are regulated by BAG1 and BAG3. However, a role of CHIP or Hsc/Hsp70 in BAG3-mediated macroautophagy processes remains to be elucidated.

Consistent with the present results, a previous study showed the stimulation of macroautophagy activity by BAG3 (Carra et al, 2008a). This group found that a complex formed by BAG3 together with a small heat-shock protein termed HspB8 is critical for this effect. These authors also showed that the proline-rich domain (PXXP) of BAG3 is required for macroautophagy stimulation, whereas the BAG domain, which binds to Hsc/Hsp70, is dispensable (Carra et al, 2008b). These findings suggested an Hsc/Hsp70-independent function of BAG3 in activating the macroautophagy pathway. Moreover, these authors proposed that BAG3 clears polyQ-huntingtin aggregates in a PXXP-dependent manner by macroautophagy, suggesting that this effect is also Hsc/Hsp70 independent (Carra et al, 2008b). However, in a follow-up study these authors showed that macroautophagy stimulation by BAG3 is linked to the eukaryotic translation initiation factor 2α (eIF2α) pathway (Carra et al, 2009). According to this study, BAG3 overexpression leads to phosphorylation of eIF2α in a PXXP-dependent fashion and this effect was required for macroautophagy induction. In this context, BAG3 has been shown to induce also a general shut-down of protein biosynthesis via eIF2α phosphorylation. This is an important aspect since the aggregation propensity of mutant proteins like polyQ-huntingtin directly correlate with their expression levels. Experimental settings employing overexpression of mutant aggregate-prone proteins are susceptible for misinterpretation as a subtle decrease of the expression of an aggregate-prone protein could lead to false interpretations with respect to protein disaggregation or degradation activity of investigated agents or proteins (Wyttenbach et al, 2008). Hence, it is likely that the reduction of polyQ-aggregates by BAG3 in the studies of Carra and colleagues (Carra et al, 2008) is solely due to translational arrest and not to enhanced macroautophagic degradation. Therefore, these studies are incomplete regarding the potential direct function of BAG3 in the macroautophagic degradation process of quality control substrates and the involvement of Hsc/Hsp70 therein. Besides macroautophagy stimulation, which seems to be independent from Hsc/Hsp70 (Carra et al, 2008), the findings of the present study further suggest a direct role of BAG3 in the sequestration of quality control substrates along with SQSTM1 for macroautophagic degradation. The involvement of

Hsc/Hsp70 herein remains to be elucidated. However, owing to its ability to connect the chaperone system via the BAG domain, BAG3 has a key capability to function in PQC: physical (indirect) interaction with misfolded, defective proteins. Therefore, it is very likely that BAG3 acts as a molecular bridge between the chaperone system and the macroautophagy machinery.

D.1.3 Cooperation of BAG3 and SQSTM1 in the macroautophagy pathway

For long time macroautophagy has been merely described as an unspecific bulk degradation process where cytoplasmic constituents are randomly engulfed by a membrane and then degraded by lysosomal degradative enzymes (Mizushima, 2007). However, in recent years it became increasingly clear that proteins and organelles can be eliminated by macroautophagy also in a highly specific manner. A major role herein plays SQSTM1 (Kim et al, 2008; Pankiv et al, 2007). Based on its ability to bind both, ubiquitin and LC3, SQSTM1 combines two features important for selective degradation of cytoplasmic substrates by macroautophagy: substrate sequestration and recruitment of the autophagosome membrane.

D.1.3.1 Function of SQSTM1 in macroautophagy

SQSTM1 is up-regulated under stressful conditions that lead to an accumulation of misfolded proteins like heat stress, oxidative stress and proteasome inhibition (Kuusisto et al, 2001). SQSTM1 confers cellular protection against oxidative stress as well as the toxicity of mutant aggregate-prone proteins (Heo et al, 2009; Bjørkøy et al, 2005). SQSTM1 is an ubiquitin-binding protein and associates with diverse protein aggregates found in a wide range of proteinopathies among them Parkinson's disease, Huntington's disease and ALS (Zatloukal et al, 2002). It has been proposed that SQSTM1 facilitates macroautophagic degradation of aggregate-prone proteins by directly binding to them and recruiting the autophagosome membrane via binding to LC3-II (Pankiv et al, 2007). SQSTM1 has a strong self-polymerizing activity which is suggested to increase upon binding of ubiquitinated proteins (Bjørkøy et al, 2005). Thus, it seems that SQSTM1 sequestrates ubiquitinated quality control substrates by forming inclusion bodies. These SQSTM1-positive aggregates are then specifically engulfed by the autophagosome membrane via recruitment of LC3-II. Support for this hypothesis comes from elegant *in vivo* studies of macroautophagy-deficient mice in which the Atg5 or Atg7 gene was deleted. These mice showed a severe degenerative phenotype in the liver and CNS which was associated with the accumulation of ubiquitinated protein aggregates (Hara et al, 2006; Komatsu et al, 2006; Komatsu et al, 2005). SQSTM1 gene ablation in these mice prevented the formation of ubiquitin-positive inclusion bodies, corroborating a

critical role of SQSTM1 in macroautophagic substrate sequestration in form of inclusions bodies (Komatsu et al, 2007). Interestingly, the degenerative phenotype could be rescued by SQSTM1 knock-out in the liver but not in the CNS. These findings implicate SQSTM1-positive protein aggregates as the toxic species in the liver but not in neurons of macroautophagy-deficient mice. SQSTM1 knock-out in Atg wildtype mice produces an age-dependent neurodegenerative phenotype which is associated with the accumulation of intracellular aggregates composed of hyperphosphorylated tau (Ramesh Babu et al, 2008). It is not clear whether this phenotype is directly linked to macroautophagy impairment as these mice also suffer from severe obesity in late age. Together these findings suggest a possible key role of SQSTM1 in regulating selective protein turnover by macroautophagy, a process that is gaining importance during disease pathology of proteinopathies as well as during the aging process.

As recently reported, SQSTM1 is not only important for selective protein breakdown but also for the selective turnover of whole organelles by macroautophagy (Kim et al, 2008). It was demonstrated that the macroautophagic turnover of peroxisomes can be stimulated by introducing an ubiquitin moiety into a peroxisome-located integral membrane protein. The degradation process of such ubiquitinated peroxisomes required the ubiquitin tag on the cytoplasmic surface of peroxisomes as well as the presence of SQSTM1. Furthermore, SQSTM1 knock-down led to an increase of the peroxisomal mass supporting the physiological relevance of the observed ubiquitin/SQSTM1-dependent organelle turnover pathway. These findings suggest that in addition to protein turnover ubiquitin signals are also used to facilitate selective turnover of cytoplasmic organelles by macroautophagy. It would be interesting to know whether defective mitochondria are selectively degraded by a similar mechanism. It is generally accepted that mitochondria are eliminated by macroautophagy (Kundu & Thompson, 2005). However, it is unknown how damaged mitochondria are recognized and degraded selectively. Uncovering the exact molecular mitochondria quality control mechanism would be a breakthrough in the field of aging research since the continuous production of reactive oxygen species by damaged mitochondria has been causally associated with the aging process and a wide variety of age-related degenerative disorders. Future studies addressing mitochondrial turnover mechanisms should investigate the potential role of ubiquitin signalling, SQSTM1 as well as BAG3 therein.

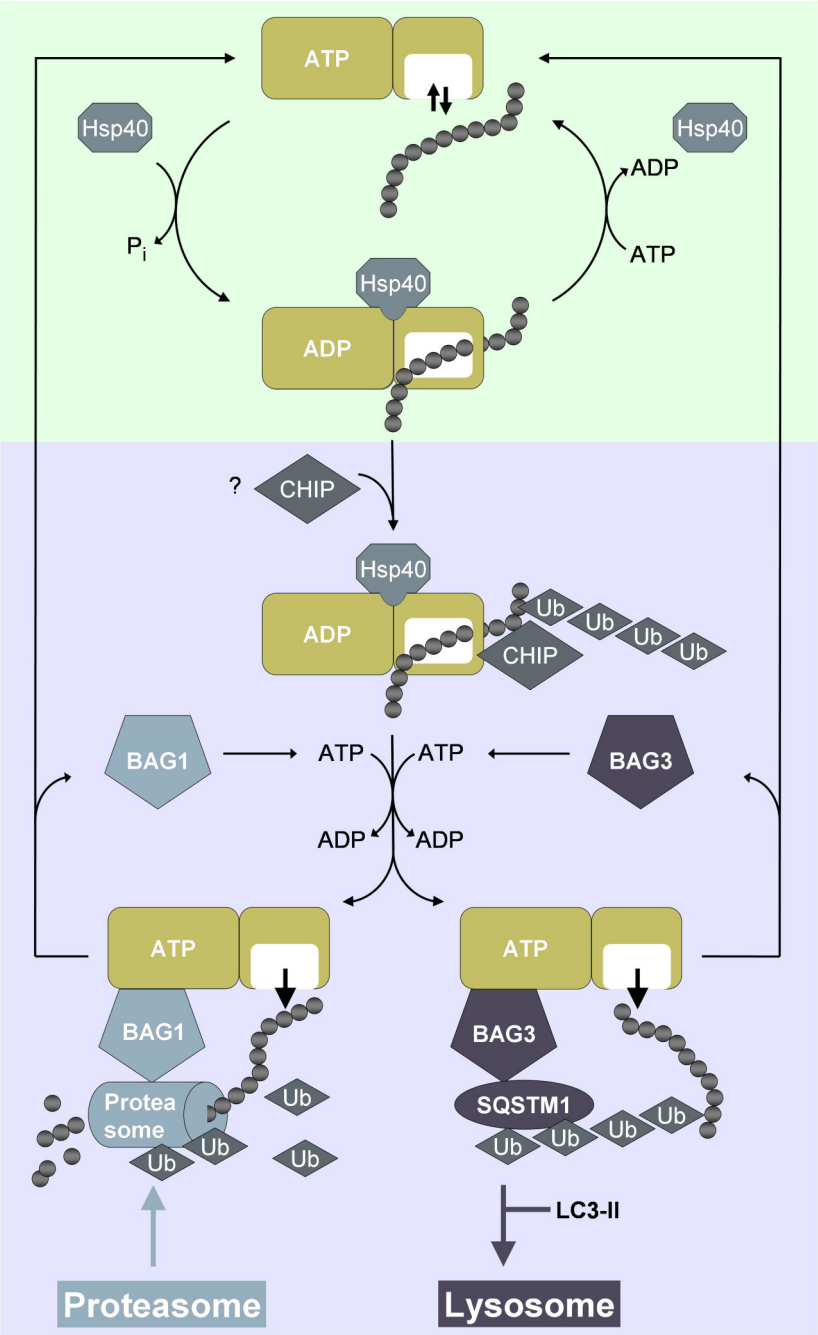

Figure 42: Hypothetical model how BAG1 and BAG3 determine turnover routes of Hsc/Hsp70-bound quality control substrates. The folding cycle (highlighted in green) of Hsc/Hsp70 (khaki) in eukaryotes involves the action of Hsp40 which stimulates ATP to ADP hydrolysis on Hsc/Hsp70 resulting in an Hsc/Hsp70 conformation with high substrate affinity. Spontaneous ADP to ATP exchange triggers dissociation of the Hsc/Hsp70-substrate complex and the release of the substrate. The substrate then may fold or undergo further Hsc/Hsp70 reaction cycles until folding is complete. However, when substrate folding fails Hsc/Hsp70 switches into the degradation modus (highlighted in blue) by binding of CHIP which polyubiquitinates the chaperone-bound substrate. The substrate's turnover route is determined by BAG proteins. BAG1 couples Hsc/Hsp70 to the proteasome and stimulates nucleotide exchange on Hsc/Hsp70, thereby transferring the substrate from the chaperone to the proteasome where the substrate is degraded. In contrast, BAG3 induces substrate transfer from Hsc/Hsp70 to the macroautophagy machinery by loading the substrate onto SQSTM1. SQSTM1 then recruits the autophagosome membrane via binding of LC3-II and upon fusion of the mature autophagosome with lysosomes the substrate is degraded by lysosomal hydrolases.

D.1.3.2 The role of BAG3 in SQSTM1-mediated substrate sequestration

Recently, it was demonstrated that an ubiquitin-red fluorescent protein (RFP) fusion protein, which was originally designed as a UFD-specific proteasome reporter, is degraded in COS-7 cells also by macroautophagy in a SQSTM1-dependent manner (Kim et al, 2008). These findings suggest that a quality control substrate, which is destined for degradation by ubiquitination, can take at least two different turnover routes. This raises the question how the cell controls the degradation of a protein substrate by the proteasomal and lysosomal systems when the same degradation signal is used. The current findings suggest that BAG1 and BAG3 might determine a substrate's fate to be degraded either by the proteasome or by macroautophagy. As discussed above, BAG1 couples Hsc/Hsp70 to the proteasome and stimulates nucleotide exchange on Hsc/Hsp70. This is thought to result in substrate transfer from the chaperone to the proteasome. Thus, BAG1 promotes the proteasomal degradation route of a chaperone substrate. In contrast, BAG3 could be the molecular link between the chaperone system and the macroautophagy machinery. The present study shows that BAG3 binds to SQSTM1 and Hsc/Hsp70. Therefore, it is likely that BAG3 couples Hsc/Hsp70 to SQSTM1. By stimulating nucleotide exchange on SQSTM1-targeted Hsc/Hsp70 molecules, BAG3 could induce substrate transfer from the chaperone to SQSTM1. Since SQSTM1 has a strong polymerizing activity (Bjørkøy et al, 2009), successive substrate transfer from Hsc/Hsp70 to SQSTM1 would result in inclusion bodies containing quality control substrates. Accordingly, the immunofluorescence studies show that BAG3 can induce the formation of large SQSTM1-positive inclusions. Considering the co-localization of BAG3-GFP with these large SQSTM1-positive aggregates, it is very likely that BAG3 has a direct function in the sequestration process of chaperone substrates and the formation of inclusion bodies along with SQSTM1. Taken together, by targeting chaperones to the proteasomal and macroautophagic systems, respectively, and inducing on site the release of the chaperone-hold substrate, BAG1 and BAG3 might determine the turnover route of a polyubiquitinated chaperone-bound quality control substrate (see hypothetical model in Figure 42).

Upon fusion of autophagosomes with lysosomes the content and the inner autophagosome membrane are degraded by lysosomal hydrolases (see Figure 4; Ding & Yin, 2008). Accordingly, LC3-II molecules that associate with the inner autophagosome membrane as well as SQSTM1, which is packed together with the cargo within autophagosomes, are degraded as well. Thus, these proteins are degraded while fulfilling a specific function in the macroautophagic process. Therefore, it was of interest to investigate whether BAG3, which is potentially involved in substrate sequestration along with SQSTM1, is also subject to macroautophagic degradation. However, unlike SQSTM1, BAG3 is not degraded by macroautophagy induced by amino-acid starvation. Thus, BAG3 is either not captured within

inclusion bodies and autophagosomes or is resistant to lysosomal hydrolysis. Considering the mechanistic model of how BAG3 could influence the sequestration process, the former possibility should be favoured. By stimulating nucleotide exchange on Hsc/Hsp70-substrate complexes, BAG3 induces the release of the substrate from the chaperone in close vicinity to SQSTM1. In the polyubiquitinated state the substrate is bound directly by SQSTM1 via the ubiquitin-associated (UBA) domain. The binding of several polyubiquitin chains by SQSTM1 is thought to result in the cross-linking of SQSTM1 monomers and quality control substrates (Bjørkøy et al, 2005). Thus, binding of polyUb-proteins strongly increases the polymerizing activity of SQSTM1 and this is the prerequisite for capturing of substrates in inclusion bodies. In this mechanistic model, it is likely that BAG3 and Hsc/Hsp70 can escape from the forming inclusion body since they are not marked by ubiquitination and thus not bound by the UBA domain of SQSTM1. Similarly, also BAG1 and Hsc/Hsp70 are not degraded by the proteasome although the mechanistic model predicts coupling of both proteins to the degradation complex.

D.1.4 Decrease of the BAG3 to BAG1 ratio upon acute amino-acid depletion

The current data further suggest that BAG3 is subject to proteasomal degradation upon amino-acid starvation. It is well known that cells induce macroautophagy upon amino-acid depletion for nutrient supply (Komatsu et al, 2005). This raises the question why BAG3, as a stimulator of macroautophagy, is rapidly degraded by the proteasome when cells are starved. One simple explanation is that BAG3 as a co-chaperone could act as a stimulator of macroautophagy only for PQC reasons when misfolded proteins accumulate but has no role in the activation of macroautophagy for nutrient supply. The underlying mechanism for macroautophagy induction by amino-acid depletion is the deactivation of the mTOR kinase (Pattingre et al, 2008). The mTOR kinase stimulates protein translation, cell growth and suppresses macroautophagy. Under normal nutrient conditions the mTOR kinase is hold in an active state by the essential amino-acid L-leucine, whose cell import depends on the presence and efflux of L-glutamine by a bidirectional transporter (Nicklin et al, 2009). Amino-acid depletion and thus mTOR inhibition result in the activation of a complex cascade finally leading to macroautophagy induction. eIF2α, which is supposed to play a role in BAG3-mediated macroautophagy induction (Carra et al, 2009), seems not to be a down-stream effector of the mTOR signalling pathway (Bolster et al, 2003). Rather eiF2α acts upstream of mTOR by regulating PI3K signalling which leads to macroautophagy induction via the Akt/mTOR pathway (Kazemi et al, 2007). However, since under starvation direct mTOR signals to the macroautophagy machinery are described that do not depend on the eIF2α pathway (Wouters & Koritzinsky, 2008; Jung et al, 2009a), it is very likely that mTOR

signalling does not rely on BAG3 or the eIF2α pathway for macroautophagy stimulation under nutrient restriction. But why is BAG3 degraded by the proteasome and rapidly depleted upon amino-acid deprivation? One explanation could be the fact that in addition to the macroautophagy pathway also the proteasome plays a crucial role in supplying amino-acids under starvation conditions. Macroautophagy is relative to the ubiquitin/proteasome system a rather time-consuming and slow-reacting catabolic process as it requires the formation and maturation of autophagosomes and their transport to and fusion with lysosomes (Kuma et al, 2004). Therefore, macroautophagy might be insufficient to supply the cell with required nutrients under acute amino-acid restriction. Accordingly, a previous study demonstrated that in early stages of starvation, amino-acids for *de novo* protein synthesis are supplied by proteasomal degradation of pre-existing proteins (Vabulas & Hartl, 2005). Thus, for maintaining protein biosynthesis in early stages of starvation, the cell might stimulate the proteasomal degradation system. BAG3 and BAG1 likely compete for binding to Hsc/Hsp70. Starvation-induced degradation of BAG3 results in a decreased BAG3 to BAG1 ratio and, consequently, very likely in an enhanced interaction of Hsc/Hsp70 with BAG1. As BAG1 couples Hsc/Hsp70 to the proteasome, an increased proteasomal degradation of chaperone substrates is suggested. Hence, focussing on BAG1 during early stages of starvation is a reasonable mechanism to supply amino-acids for biosynthesis.

D.2 The switch from proteasomal to macroautophagic degradation…

D.2.1 …under acute stress conditions

The present findings suggest that BAG1 and BAG3 control a molecular switch between proteasomal and macroautophagic degradation pathways. Several reports indicate a cross-talk between the two degradation systems, since macroautophagy is activated upon proteasome inhibition (Ding & Yin, 2008). Macroautophagy is generally induced under protein denaturating conditions like ER stress and oxidative stress (Høyer-Hansen & Jäättelä, 2007; Scherz-Shouval et al, 2007; Pattingre et al, 2008). Thus, it seems that macroautophagy induction is an adaptive response under conditions that increase the amount of misfolded proteins. In line with a role of BAG3 in this adaptive process, BAG3 expression has been shown to be induced upon proteasome inhibition (Wang et al, 2008). Moreover, as previously shown, BAG3 gene expression is controlled by heat-shock-factor-1 (HSF1), a transcription factor that also controls expression of heat-shock-proteins (Franceschelli et al, 2008). Consistent with this finding, several studies demonstrated increased BAG3 expression along with heat-shock-proteins under protein denaturating conditions (Pagliuca et al, 2003). It is interesting to note, that like BAG3 also SQSTM1 is up-regulated under protein denaturing stress conditions (Kuusisto et al, 2001). It can be

concluded that under physiological conditions, PQC is mainly achieved by BAG1-dependent 26S proteasomal degradation. However, under acute stress conditions, when misfolded proteins accumulate and the aggregation potential increases, the ubiquitin/proteasome system might be insufficient for complete clearance of defective proteins. Due to the barrel-shaped architecture with the 13 Å narrow entrance channel proteasomes can only degrade unfolded proteins (Nandi et al, 2006). Thus, nondissociable protein aggregates cannot be degraded by the ubiquitin/proteasome system and even an inhibitory effect of such aggregates on proteasomes has been described (Bence et al, 2001; Ding & Yin, 2008). The inhibitory effects of non-processed aggregates on proteasome activity can be explained by blocking of substrate binding sites on proteasomes. These inhibitory effects can result in a vicious cycle since proteasome inhibition leads to accumulation of protein aggregates which in turn inhibit the proteasome. In contrast to the proteasomal system, protein aggregates can be effectively degraded in the macroautophagy pathway (Rubinsztein, 2006). Thus, under protein denaturating stress conditions the cell has to increasingly rely on the macroautophagic degradation system to maintain proteostasis. Hence, it can be concluded that the transient switch from proteasomal to macroautophagic degradation under acute stress conditions, which is at least in part mediated by the up-regulation of BAG3 and SQSTM1, is an important adaptation not only for efficient clearance of protein aggregates but also for protection of the proteasomal system (see Figure 43).

The results of the present study also show that BAG3 is continuously degraded by proteasomes and that, in contrast to SQSTM1, BAG3 is not degraded by macroautophagy, at least not under basal conditions when the ubiquitin/proteasome system functions properly. The finding that BAG3 is subject to proteasomal degradation is in accord with a previously published study showing that BAG3 levels are restricted by the proteasome (Virador et al, 2009). It is an interesting aspect that cells regulate BAG3 levels by a post-translational mechanism involving the ubiquitin/proteasome system. This mechanism implies that under basal conditions BAG3 levels are kept low in cells. However, under stress conditions when proteasome function is impaired, BAG3 protein levels raise quickly. Thus, cells potentially use BAG3 as an intrinsic proteasome sensor, which accumulate when proteasome function is impaired or overwhelmed. The resulting increase of the BAG3 to BAG1 ratio then could trigger the enhanced use of the macroautophagic system to maintain PQC. Thus, in addition to the described transcriptional regulation of BAG3 expression, direct accumulation of BAG3 protein levels due to proteasome impairment could contribute to the induction of the macroautophagy pathway observed following proteasome inhibition.

D.2.2 …during aging

The present study suggests that during aging a persistent shift from BAG1 to BAG3 determines the constitutive activation of the macroautophagic system for the degradation of quality control substrates. The possible reasons why proteostatic control during aging is achieved by a shift towards macroautophagy is discussed in the following paragraphs.

D.2.2.1 Proteasome function during aging

The occurrence of oxidized proteins is a hallmark of aging in a large number of cell types and tissues from a variety of organisms (Brunk & Terman, 2002; Breusing & Grune, 2008). It is still a matter of debate whether accumulation of oxidatively modified proteins during aging is caused by their increased production or decreased turnover or both (Breusing & Grune, 2008). Undoubtedly, during aging oxidative damage to proteins is faster than their proteolysis. Oxidatively modified proteins tend to form cross-links to other macromolecules and several groups showed that such cross-linked aggregates can inhibit proteasome function (Breusing & Grune, 2008). The presence of such cross-linked proteins in old cells has been associated with the decline of proteasome activity observed during aging (Grune et al, 2004). Consistent with this hypothesis, the present data show decreased proteasomal chymotrypsin-like activity in cell lysates from old I90 cells. It should be noted, however, that proteasome activity is generally measured *in vitro* by using proteasome-specific fluorescent substrates. This activity assay has limitations and measures only the overall proteasomal-proteolytic capacity in cell and tissue homogenates because fluorescent substrates are present in excess and reach proteasomes only by diffusion. Thus, this assay does not provide information about the activity of the ubiquitin/proteasome system with respect to the amounts of present quality control substrates, their chaperone recognition, ubiquitination and proteasomal degradation. Importantly, potential alterations of the proteasomal substrate flux cannot be examined by determining solely the overall proteolytic capacity of present proteasomes.

Therefore, in the present study also the current substrate flux through the ubiquitin/proteasome system was determined in living cells by monitoring accumulation of polyUb-proteins in response to the specific proteasome inhibitor lactacystin. This analysis revealed that at least under basal conditions the general substrate flux through the proteasomal system is not altered with age. In sum, these findings indicate that the overall proteasomal capacity is decreased in aged cells possibly due to increased levels of cross-linked protein species as generally assumed (Grune et al, 2004). This could be also due to a decrease in the proteasomal mass or impaired assembly of proteasome subunits which

accompanies the biological aging process, as reported previously (Farout & Friguet, 2006). The age-related decrease of the overall proteasomal-proteolytic capacity could be critical especially under severe stress conditions which might overwhelm the proteasomal system rather in old than young cells. At the basal level, however, the current data suggest that the proteasomal-proteolytic capacity in old cells is sufficient to assure degradation of present proteasome substrates similar to that of young cells. These results also imply that adequate amounts of BAG1 are expressed in aged cells to maintain degradation of proteasome substrates present under basal conditions. Future studies should aim to compare the activity of the ubiquitin/proteasome system in young and old cells under stress conditions and potential alterations should be regarded in dependence of BAG1 levels.

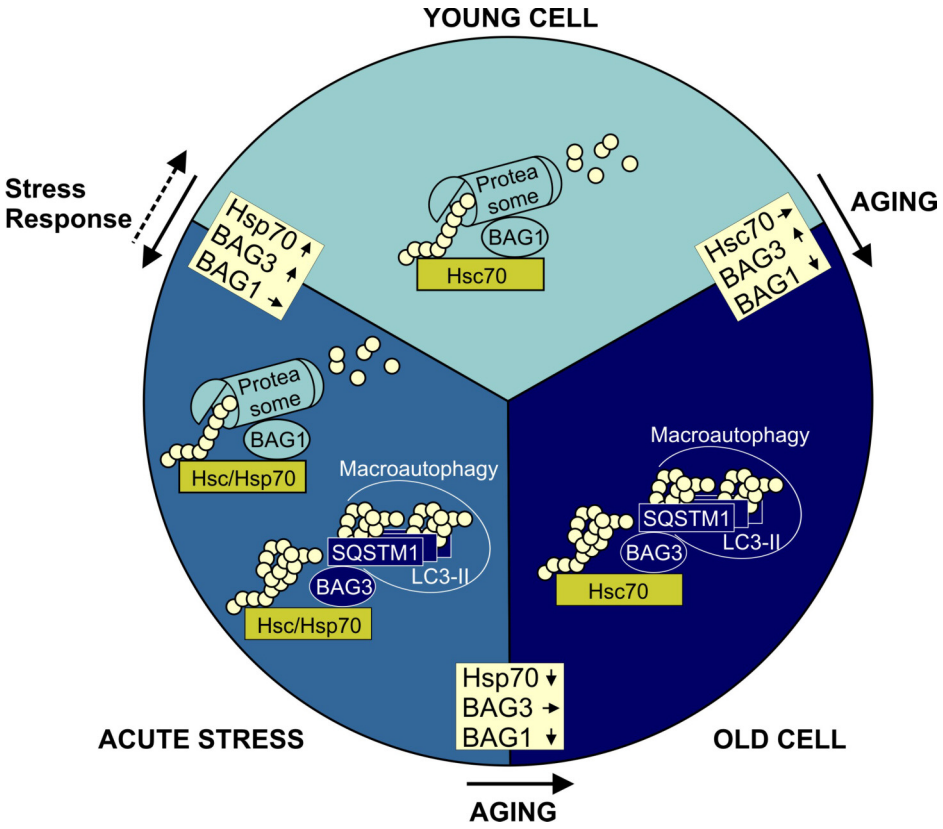

Figure 43: Model of the BAG3-mediated recruitment of the macroautophagy pathway during aging and stress. In young cells Hsc70-associated protein degradation is mainly accomplished through the proteasomal system by BAG1-mediated coupling of Hsc70 to the proteasome. During aging the protein oxidation potential increases leading to insoluble cross-linked protein aggregates that are poor proteasome substrates and thus BAG1 is replaced by BAG3 to enhance the coupling of Hsc70 to SQSTM1. This ensures that in old cells Hsc70-associated protein degradation is mainly conducted by the macroautophagy machinery, which can also handle insoluble protein aggregates. Under acute stress conditions BAG1-mediated coupling of Hsc/Hsp70 to the proteasome persists as Hsp70 and BAG3 are both up-regulated which avoids competition of BAG proteins for Hsc/Hsp70 binding. Up-regulation of BAG3 and Hsp70 alleviates the increased burden of insoluble quality control substrates by induction of macroautophagy. Under these conditions, the BAG1-regulated proteasomal Hsc/Hsp70-associated degradation pathway is protected from protein aggregates and enabled to work properly. When cells are irreversibly damaged, transition to the aging phenotype is conducted by down-regulation of BAG1 and Hsp70 whereas BAG3 levels remain high.

Furthermore, the fact that the proteasomal-proteolytic capacity in aged cells is sufficient to degrade proteasome substrates present under basal conditions, it can be stated that accumulation of oxidatively modified proteins observed during aging is not primary due to an impaired proteasome system. Rather the production of such protein species might increase progressively during aging leading finally to a point where their production rate exceeds their proteolysis rate. This imbalance then ultimately leads to accumulation of cross-linked protein aggregates characteristic of aged cells and tissues. Once these protein species accumulate, their inhibitory effects on the proteasome system might further stimulate their accumulation. In conclusion, it seems likely that the primary cause leading to accumulation of oxidatively modified protein species during aging is rather their increased production than their decreased proteasomal turnover rate, but secondary, a decreased turnover rate could occur due to inhibitory effects of accumulating cross-linked protein aggregates.

D.2.2.3 Autophagy activity during aging

The present study strongly suggests that during cellular aging macroautophagy activity is increased. Assuming an increased production of oxidatively modified proteins during aging, induction of macroautophagy is a plausible adaptation of the cellular PQC system to the changed environmental conditions. As discussed above, oxidatively modified proteins form cross-linked protein aggregates that cannot be degraded by the ubiquitin/proteasome system. Moreover, protein aggregates might even inhibit the proteasomal pathway. Thus, it is reasonable that during aging cells adapt to chronic oxidative stress levels and constitutively recruit the macroautophagy pathway to protect not only the proteome but also the ubiquitin/proteasome system in the aging cellular environment (see Figure 43).

On the other hand, it has been suggested that the autophagic capacity declines with age (Cuervo, 2003). It should be noted, however, that the term autophagy encompasses three different degradation pathways involving lysosomal activity: macroautophagy, microautophagy and chaperone-mediated autophagy (CMA). Microautophagy, a degradative process in which lysosomes directly engulf cytoplasmic material, has so far not been investigated in the context of aging. CMA is a selective autophagy pathway in which protein substrates are translocated from the cytoplasm into the lumen of lysosomes via the lysosomal receptor LAMP2A. It is generally accepted that rates of CMA decrease with age because of a decrease in the levels of the LAMP2A receptor (Massey et al, 2006; Kiffin et al, 2007). Although it is widely assumed that macroautophagy declines with age, original literature addressing this issue is extremely sparse. Only one study describes decreased macroautophagy induction in the liver of aged rats in response to an anti-lipolytic agent which

mimicked starvation conditions (Del Roso et al, 2003). However, this study provides no information about age-related alterations of macroautophagy activity linked to PQC pathways. In contrast to the current view that macroautophagy declines with age, a recent study showed that macroautophagy activity is increased in the liver of old rats following heat stress, strongly arguing for enhanced activation of macroautophagy during aging in response to proteotoxic stress (Oberley et al, 2008). Moreover, increased macroautophagy activity was demonstrated in a mouse model of Hutchinson-Gilford progeria. These mice exhibit an accelerated aging phenotype which was associated with an extensive basal activation of macroautophagy compared to the youthful control mice (Marino et al, 2008). Interestingly, while writing the present doctoral thesis, a study was published documenting the up-regulation of several macroautophagy-related genes and activation of the macroautophagy pathway during cellular senescence, strongly supporting the findings of the present study (Young et al, 2009). But still, regardless of these facts the prevalent dogma in the field is that macroautophagy activity declines with age. This is also extensively concluded in many review articles about aging and autophagy curiously without referring to original experimental data (Cuervo et al, 2005; Martinez-Vicente & Cuervo, 2007; Cuervo, 2008). The perceived decrease in the macroautophagic potential during aging is probably explained by the progressive, age-dependent accumulation of biological "garbage", such as lipofuscin (age pigment), an intralysosomal, polymeric, undegradable material. Apparently, the accumulation of such “waste” material is indicative of a catabolic insufficiency with respect to this material, but not of a general decline in macroautophagy. Rather, it reflects an imbalance between the production of this material and the degradation capacity. This raises the question whether lipofuscin accumulation in aged cells is due to increased formation or decreased lysosomal degradation. Regarding the present findings the former possibility should be favoured. The present studies were performed on aged but pre-senescent cells before the massive accumulation of lipofuscin-like material occurs. At this aging level, cells clearly show an increase of macroautophagy activity for maintaining protein homeostasis. Moreover, these cells show an increased ratio of insoluble to soluble quality control substrates. These findings indicate that aged cells need to adapt their PQC system to an altered environmental condition which promotes the production of insoluble and aggregated proteins. The increased aggregate-prone milieu in aged cells is likely caused by chronically elevated oxidative stress levels. Progressively increasing production of oxidatively modified cross-linked proteins during aging could lead to a point where the lysosomal degradative capacity is overwhelmed which, finally, results in the accumulation of lipofuscin-like material. Accordingly, lipofuscin accumulation can be observed even in young cells upon repeated treatment with oxidative stress-inducing agents (Brunk & Terman, 2002; Jung et al, 2009b). Hence, the findings of the present study contrast the current assumption that lipofuscin

accumulation during aging is due to a general decline of macroautophagy activity. Rather, macroautophagy is induced during aging in an attempt to counteract the increased generation of insoluble quality control substrates.

In conclusion, the integration of the macroautophagy pathway into the cellular PQC system seems to be an important adaptation to the heightened pro-oxidant and aggregate-prone milieu developing during aging. This view is supported by the observed life-span extensions of model organisms by promoting either anti-oxidant defense systems or macroautophagy (Meléndez et al, 2003; Wickens, 2001). In this context it is interesting to note that promoting basal levels of macroautophagy enhances not only longevity but also resistance to oxidative stressors in the adult (Simonsen et al, 2008). This fact strongly indicates that the impact of macroautophagy on aging and longevity is directly linked to oxidative stress alleviation.

D.2.3...during brain aging

Human disorders of the adult affect frequently the nervous system, among them many devastating neurodegenerative disorders like Alzheimer's disease, Parkinson's disease and ALS. The current hypothesis states that these disorders are caused by a failure of the protein homeostasis network since aberrant protein aggregates are found in all of these pathologies (Paulson, 1999; Rubinsztein, 2006). This fact indicates that the PQC system fails to adapt to the aging cellular environment particularly in neuronal cells. But what could be the reason that during aging proteotoxic stress conditions occur primarily in the nervous system?

The findings of the present study show that the BAG3 to BAG1 ratio increases during aging of the rodent brain. The shift from BAG1 to BAG3 is very likely accompanied by an increased macroautophagy activity as lysosomal cathepsin activity as well as SQSTM1 and LC3-II levels were increased in the aged brain as well. Thus, these findings suggest that PQC in the aging brain involves the recruitment of the macroautophagy pathway by BAG3. A closer look revealed that during brain aging the shift from BAG1 to BAG3 occurs specifically in neurons whereas in astrocytes BAG levels remain unchanged. Hence, it seems that, in particular, neurons need to adapt their PQC system to an aging cellular environment. Neurons are substantially different from other non-neuronal cell types in the brain in that they are mostly post-mitotic, whereas astrocytes continue to divide throughout the lifespan of an organism (Cicero & Herrup, 2005). Thus, the non-neuronal tissue in the brain maintains its regeneration capacity by elimination and replacement of sick cells. In contrast, neurons need to survive and function properly throughout the whole life-span of an organism. This fact indicates that in particular neurons underlie a progressive aging process to which the

proteostasis network needs to adapt. Thus, the age-associated and BAG3-mediated recruitment of the macroautophagy pathway could be a highly important process specifically for neurons.

The BAG3-mediated macroautophagic degradation pathway is considerably more potent than the BAG1-regulated ubiquitin/proteasome system with respect to protein aggregates (Bence et al, 2001). Hence, the up-regulation of this pathway in aging neurons is plausible to combat the age-associated increase of oxidative stress and the accompanied accumulation of cross-linked proteins. Moreover, considering that the concentration of such potentially toxic protein species raises more prominently in post-mitotic cells which cannot dilute their cytoplasm by cell division, the recruitment of the macroautophagy pathway becomes in particular important for neurons of the aging brain. Thus, the dysfunction of the BAG1 to BAG3 switch and the failure of the macroautophagy pathway to cope with the increased load of damaged proteins as neurons age could be the reason for the malfunction of the protein homeostasis network and the accumulation of protein aggregates characteristic of human neurodegenerative disorders, as discussed in the following sections.

D.3 Protein quality control in age-related proteinopathies

Many late-onset neurodegenerative diseases of sporadic and hereditary form are associated with the formation of aberrant protein aggregates. This observation indicates the failure of PQC during aging or disease pathology. Inherited forms of proteinopathies often go along with mutations in proteins conferring protein instability and aberrant protein conformation that lead to a gain of toxic function (Forman et al, 2004). These proteins should normally be recognized by the chaperone system and subjected to degradation. Proteasomal and macroautophagic turnover routes are both described for most of the proteinopathy-causing mutant proteins among them SOD1 (Kabuta et al, 2006), α-synuclein (Shin et al, 2005), polyQ-huntingtin (Jana et al, 2005; Yamamoto et al, 2006) and tau (Olzmann & Chin, 2008; Carrettiero et al, 2009). But how can these mutant proteins escape the cellular quality control mechanisms in particular during aging? One explanation could be that the mutant proteins themselves compromise quality control pathways, as discussed below.

D.3.1 Potential impairment of the ubiquitin/proteasome system

Many groups showed the impairment of the ubiquitin/proteasome system in models of proteinopathies. For example, mutant polyQ-huntingtin and mutant α-synuclein proteins exhibit inhibitory effects on the proteasome system in cellular disease models and on purified

proteasomes (Emmanouilidou et al, 2008 Seo et al, 2004; Waelter et al, 2001; Zhang et al, 2008). Similarly, ALS-causing mutant SOD1 variants have been shown to impair proteasome function upon overexpression in cells and mouse models (Urushitani et al, 2002; Cheroni et al, 2009). However, it is not clear whether these alterations are a cause or late effect of disease. In some polyQ disease models at early symptomatic stages, neuronal dysfunction is observed in the absence of proteasome impairment (Bowman et al, 2005), strongly arguing against a causal role of proteasome inhibition in these disorders. Moreover, it cannot be ruled out that the observed decrease of proteasome function in disease models could reflect an apoptotic feature as proteasomes are target of activated caspases (Adrain et al, 2004; Jang et al, 2007). Moreover, impairment of the ubiquitin/proteasome pathway seems to be a general feature of disease models in which overexpression of mutant proteins results in massive production of intracellular aggregates that can block proteasome binding sites (Bence et al, 2001). Thus, the observed proteasome impairment effects could be an overexpression artefact as it seems rather unlikely that physiological expression of a single mutant protein, in some dominant inherited proteinopathies from only one mutant allele, can induce the collapse of the main cellular protein turnover system simply by blocking substrate binding sites. The proteasome is competent to degrade almost the entirety of damaged proteins produced in a cell and is confronted continuously with protein aggregation also in the absence of mutant protein expression. Thus, to a certain extent the cell should be capable of protecting the ubiquitin/proteasome system from protein aggregates, for example by recruitment of the macroautophagy pathway.

On the other hand, it is possible that mutant proteins act further upstream and specifically disturb proteasome function for example by sequestering factors essential for proteasome subunit expression or proteasome assembly. However, such effects have not been described yet in proteinopathies. Furthermore, regarding the essential role of the ubiquitin/proteasome system in development and cell survival, one can speculate that mutations leading to a failure of this pathway would be embryonic lethal or result rather in juvenile than late-onset forms of proteinopathies. Considering all these facts, it is questionable whether proteasome impairment by mutant aggregate-prone proteins is the primary cause leading to at least age-related proteinopathies. But what could then be the final trigger leading to failure of the proteostasis network in age-related proteinopathies?

D.3.2 Aging and potential impairment of the macroautophagy pathway

Many genetic forms of proteinopathies are late-onset diseases although aggregate-prone proteins linked causally to pathogenesis are expressed from begin of life. Therefore, an

additional age-related trigger seems to be involved contributing to disease pathology. Independent whether protein aggregates or their precursors are the toxic species, the accumulation of toxic mutant proteins in cells is undoubtedly critical for disease pathology (Taylor et al, 2002). Aging could be the final trigger that allows aggregate-prone proteins to reach a toxic level either simply by age-determined up-regulation of gene expression or by a decreased degradation rate. Up-regulation of gene expression during aging is documented for SOD1 (de Haan et al, 1992; Oh-Ishi et al, 1995; Scarpa et al, 1987). This superoxide scavenging enzyme is thought to be up-regulated in response to elevated oxidative stress levels that accompanies the aging process. This age-depended effect could potentially be the ultimate trigger elevating mutant SOD1 levels to a toxic threshold in SOD1-linked ALS cases. However, for other proteinopathy-linked proteins such an age-related up-regulation of gene expression is not documented. In contrast, gene expression of several aggregate-prone proteins seems to be down-regulated during aging. For example, tau transcript levels are reported to decrease during brain aging (Lu et al, 2004). This does not avoid, however, that mutant, but also wild-type, tau protein accumulates during aging in tau-pathology affected brain areas, for example, in patients with FTDP-17 or Alzheimer's disease (Berger et al, 2007). In these pathologies, also referred to as tauopathies, the tau turnover rate seems to decline with age. Accordingly, a recent study identified aging as a factor that slows tau degradation in a tauopathy mouse model (Dickey et al, 2009). Similarly, protein levels of α-synuclein are increased during brain aging despite a decrease of gene expression, strongly indicating that also α-synuclein turnover declines with age (Chu & Kordower, 2007; Li et al, 2004; Malatynska et al, 2006). These findings raise the question in which way biological aging can affect protein turnover of aggregate-prone proteins. The present study shows that aging is associated with a change of protein turnover routes and that aged cells increasingly rely on the macroautophagy pathway to sustain proteostasis. However, the recruitment of the macroautophagy pathway during aging for PQC reasons would rather suggest an improved elimination capacity particularly for aggregated proteins. Thus, it is unlikely that the switch towards macroautophagy *per se* results in a decreased degradation rate of aggregate-prone proteins. However, it is also conceivable that aggregate-prone proteins unfold their toxicity in aged cells by inhibiting the macroautophagy pathway and thereby their own degradation. The fact that lysosomal degradation pathways can be targeted by aggregate-prone proteins is documented for some Parkinson-linked mutant forms of α-synuclein which inhibit the CMA pathway, thereby slowing their own degradation (Cuervo et al, 2004). Moreover, it has been shown that also the macroautophagy pathway is a target of aggregate-prone proteins. Mutant polyQ-huntingtin proteins seem to inhibit this pathway by sequestering beclin-1, a key kinase involved in autophagosome formation (Shibata et al, 2006). For other aggregate-prone proteins potential macroautophagy impairment effects are not investigated yet. Thus,

to date it is only speculative to consider such effects as a common feature of proteinopathy-causing proteins. However, impairment of the macroautophagy pathway as a causal event in late-onset proteinopathies would be plausible and explain some of the main characteristics of these pathologies. It would explain the accumulation of mutant proteins in form of ubiquitin- and SQSTM1-positive inclusion bodies due to their impaired degradation. Moreover, it explains why many inherited forms of proteinopathies are strictly associated with age because the mutant proteins would then unfold their toxicity predominantly in aged cells but keep largely silent in young cells that rely less on macroautophagy to maintain proteostasis. Furthermore, it would be a plausible explanation for secondary developing proteasome impairment effects observed in these pathologies as the cell is compromised in protecting the ubiquitin/proteasome system from cross-linked protein species that are increasingly produced in the aging cellular environment. Finally, macroautophagy inhibition in aged cells could also be the underlying pathological event for sporadic late-onset proteinopathies, where no mutant aggregate-prone protein is present. In these cases unknown crucial factors that lead to impairment of this important PQC adaptation process would contribute to a strict age-dependent failure of the proteostasis network and the characteristic aberrant accumulation of ubiquitin-positive protein aggregates. Future studies will have to show whether an impairment of this adaptation process is indeed the pathological trigger leading to age-related proteinopathies.

D.3.3 Macroautophagy inducers as potential therapeutics in proteinopathies

While the underlying toxicity of proteinopathy-linked proteins is unknown, preventing the accumulation of toxic protein levels is the best strategy to alleviate these pathologies. Mutant aggregate-prone proteins can be degraded by both, the ubiquitin/proteasome pathway and macroautophagy (Rubinsztein, 2006). Thus, elevating the proteolytic capacity of a cell by promoting these pathways could be a promising therapeutic target. However, in addition to PQC substrates the proteasome system also eliminates many short-lived signalling and regulatory proteins controlling for example cell cycle and apoptosis (Adams, 2001). Consequently, general promotion of the proteasome system would presumably result in dysregulation of many cellular pathways and thus have severe side effects. In contrast, in the macroautophagy pathway predominantly long-lived protein substrates are degraded, suggesting that macroautophagy has a minor regulatory role for cellular processes. Thus, promoting macroautophagy activity by small molecule enhancers could be a promising therapeutic approach to combat proteinopathies (Finkbeiner et al, 2006). Accordingly, several studies showed beneficial effects of macroautophagy enhancers like rapamycin, trehalose and lithium in cell models of Parkinson’s disease and Huntington’s disease

(Rubinsztein et al, 2005; Ravikumar et al, 2002; Sarkar et al, 2007; Sarkar et al, 2009). These molecules not only suppressed protein aggregation but also cell death in a macroautophagy-dependent manner. However, although macroautophagy can specifically eliminate misfolded and aggregated proteins, it is nonetheless a bulk degradation process as well. Hence, the general induction of this pathway by rapamycin or lithium would also result in unwanted degradation of native long-lived proteins and, even more critically, of healthy organelles like mitochondria and peroxisomes. Moreover, overstimulation of macroautophagy has been linked to apoptosis and other forms of cell death (Shimizu et al, 2004). Therefore, future studies should delineate the macroautophagy pathway in more detail and focus on the selective quality control pathway which specifically eliminates aggregate-prone proteins and damaged organelles by macroautophagy. The current findings indicate that the BAG3-regulated macroautophagy pathway could be selective for damaged proteins since BAG3 as a co-chaperone is potentially capable to direct specifically chaperone-bound substrates to the macroautophagic degradation machinery by transferring them to SQSTM1. The detailed examination of how BAG3 and SQSTM1 are regulated as well as an in depth analysis of their function in macroautophagy could provide a basis for a better understanding of the selective macroautophagy protein turnover pathway. Furthermore, future analyses should also focus on the investigation of ubiquitin and the potential macroautophagy-specific K63-linked polyubiquitin degradation signal (Tan et al, 2008; Olzmann & Chin, 2008) as well as the recently identified new candidate ubiquitin-receptor proteins NBR1 (neighbor of BRCA1 gene 1) and UBQLN1 (Ubiquilin 1) (Kirkin et al, 2009; Kim et al, 2009; N'Diaye et al, 2009) and their role in the selective macroautophagy pathway. Knowing the molecular basis of this pathway could show great promise for the development of therapeutic agents which afford the specific elimination of aggregate-prone proteins and damaged organelles without inducing the macroautophagy process as a whole. This would afford not only to lower mutant toxic protein levels in inherited proteinopathies but also to alleviate the increased burden of insoluble quality control substrates during aging and thus reduce the risk of sporadic age-related protein conformational disorders.

E MATERIAL AND METHODS

E.1 Media and buffers

Luria-Bertani (LB) medium:	10 g/l Bacto-tryptone, 5 g/l Bacto-yeast extract, 10 g/l NaCl
LB agar plates:	10 g/l Bacto-tryptone, 5 g/l Bacto-yeast extract, 10 g/l NaCl, 15 g/l agar and antibiotics (ampicillin: 100 µg/ml, kanamycin: 50 µg/ml)
TAE buffer:	44.5 mM Tris-HCl (pH 7.5), 45.5 mM boric acid, 1 mM EDTA
SDS protein lysis buffer:	62.5 mM Tris-HCl (pH 7.5), 1 mM EDTA, 2% SDS and 10% sucrose
NP40 buffer:	50 mM Tris-HCl (pH 8), 150 mM NaCl, 1% (v/v) NP40
Protein loading buffer:	10% SDS, 20% glycerine, 125 mm Tris-HCl (pH 6.8), 1 mM EDTA, 0.02% bromphenol blue, 10% β-mercaptoethanol
Stacking gel buffer:	0.6 M Tris-HCl (pH 6.8), 0.4% (w/v) SDS
Resolving gel buffer:	1.5 M Tris-HCl (pH 8.8), 0.4% (w/v) SDS
SDS running buffer:	25 mM Tris-HCl (pH 8.3), 192 mM glycine, 0.1% (w/v) SDS
Protein transfer buffer:	25 mM Tris-HCl (pH 8.3), 192 mM glycine
Ponceau S solution:	0.1% (w/v) Ponceau S, 3% (v/v) acetic acid
Electroporation buffer:	135 mM KCl, 0.2 mM $CaCl_2$, 2 mM $MgCl_2$, 5 mM EGTA, 10 mM HEPES (pH 7.5) and 25% heat-inactivated FBS, (sterile-filtered 0.2 µm)
Co-IP buffer	50 mM Tris-HCl pH 7.5, 150 mM NaCl, 2 mM EDTA, 1 mM EGTA, 0.5% NP40, (sterile-filtered 0.2 µm)
10x PBS:	1.3 M NaCl, 27 mM KCl, 15 mM NH_2PO_4, adjust to pH 7.4
PBS-T:	PBS, 0.05% Tween20
Hypotonic buffer:	10 mM HEPES pH 7.6, 10 mM K-acetate, 1.5 mM Mg-acetate, 2 mM DTT (added before use)
Protease assay buffer:	15 mM HEPES pH 7.6, 130 mM K-acetate, 1.5 mM Mg-acetate, 1.5 mM $CaCl_2$, 1.6 mM DTT (add before use), 8 mM ATP (add before use)

E.2 Culturing of cell lines and determination of cellular age

Human embryonic kidney cells 293 (HEK, 293) were purchased from the American Type Culture Collection. Primary human fibroblasts IMR90 (I90) and WI38 cells were purchased from Coriell Institute for Medical Research. Cells were cultured in Dulbecco's modified Eagle medium (Gibco) supplemented with 1 mM sodium pyruvate (Gibco), 10% (v/v) fetal bovine

serum (FBS; PAA Laboratories), 1x nonessential amino-acids (Gibco), 100 U/ml penicillin and 100 U/ml streptomycin (both from Gibco) at 37°C in a 5% CO_2-humidified atmosphere. Medium was refreshed every 3 days during cultivation and every 24 h in an experimental setting. Cumulative population doubling (PD) levels of I90 and WI38 cells were determined by summation of PDs calculated with the formula: (log cell number harvested – log cell number seeded) / log 2. Cell number was determined using a Neubauer chamber. I90 and WI38 cells became senescent at PD 60 and PD 54, respectively. Thus, I90 cells with PD 52-58 and WI39 cells with PD 46-52 were considered as old whereas cells with PD below 30 (for both cell lines) were considered as young. When I90 cells were employed for experiments without analyzing age effects, cells were used at mid-age (PD 35-47).

E.3 Ex vivo cell culture

Mixed primary hippocampal cultures from young (2 months) and aged (24 months) animals were prepared essentially as described previously (Brewer, 1997). In detail, Sprague Dawley rats were anesthetised with halothane and decapitated by guillotine. The hippocampi were rapidly dissected from the brain in 3 ml Hibernate A (Life technologies) and the menniges and excess white matter were removed under the stereomicroscope. Hippocampi were placed on a sterile prewet filter paper and cut into 0.5 mm slices perpendicular to the long axes of the hippocampi using a tissue chopper. Slices were transferred to 5 ml Hibernate A supplemented with B27 (Hibernate A/B27). After shaking 8 min at 30°C, slices were transferred to 5 ml Hibernate A/B27 containing 12 mg papain and incubated for 30 min in a 30°C water bath with a rotating platform. Digested slices were transferred to 2 ml Hibernate A/B27 and triturated 10 times with a 1-ml blue polypropylene pipet tip with a 0.9 mm opening. Supernatants were collected and subjected to subcellular fractionation using 1:1 solution of optiprep/Hibernate A. Neuron enriched fractions were resuspended in Neurobasal medium (Invitrogen) supplemented with B27 and 5 ng/ml basal fibroblast growth factor (Sigma). Neurons were cultured in a humidified atmosphere with 5% CO_2 at 37°C. Protein samples were prepared after 7 days in vitro (7DIV). In a parallel set of experiment, pure astrocytic cultures were obtained by treatment with 100 µM NMDA for 24 h to specifically eliminate neurons.

E.4 Molecular cloning and expression plasmids

Plasmids were cloned by polymerase chain reaction (PCR) methods followed by the In-Fusion recombination reaction (Clontech). Coding sequences were PCR amplified using the

proof-reading DNA polymerase based Phusion High-Fidelty PCR Kit (Finnzymes), according to manufacturers' protocol. The standard PCR protocol is listed in Table 1.

Reaction mixture	**PCR reaction**
10 µl 5x Phusion HF buffer	initial denaturation 98°C 30 s
1 µl template DNA (~100 ng)	25-32x
0.5 µl For Primer (100 pmol/µl)	denaturation 98°C 20 s
0.5 µl Rev Primer (100 pmol/µl)	annealing 55-60°C 30 s
1 µl dNTPs (10 mM)	elongation 72°C 30 s/kb
1.5 µl DMSO	
0.5 µl Phusion DNA Polymerase (2 U/µl)	final extension 72°C 10 min
34.5 µl ddH_20	hold 4°C

Table 1: Standard protocol for polymerase chain reaction (PCR)

For purification of PCR products, reaction mixtures were subjected to electrophoresis using 1% agarose gels in *TAE buffer* supplemented with ~0.5 µg/ml ethidium bromide (AppliChem). After electrophoresis desired PCR products were extracted from agarose slices using the DNA extraction kit NucleoSpin Extract II (Macherey-Nagel) following the manufacturers' instructions. The same purification protocol was used for target vectors following digestion with desired restriction endonucleases. Generally, vector restriction (~4 µg) was carried out at 37°C over night in a 100 µl volume containing 5 µl of each restriction enzyme, 10 µl of the appropriate 10x restriction buffer (New England Biolabs) and 1 µl BSA (100x, New England Biolabs) using low-retention tubes (Kisker). Target vector and inserts were mixed in a 2:1 molar ratio in a final volume of 10 µl for subsequent recombination by the In-Fusion reaction according to manufacturers' protocol (Clontech). Following recombination the reaction mixture was diluted with 20 µl ddH_20 and 5 µl thereof was used for transformation of chemical competent cells of *E. coli* strain DH5α. For transformation DH5α cells were incubated for 30 min with DNA on ice followed by a heat-shock for 90 sec at 42°C. Thereafter, cells were incubated 2 min on ice and resuspended in *LB medium*. After incubation for 1 hour at 37°C, DH5α cells were plated on *LB agar plates* containing appropriate antibiotics for selection of transformants. Plates were incubated over night at 37°C and single-grown colonies were isolated and propagated in 10 ml *LB medium* cultures supplemented with antibiotics. Plasmid DNA was isolated from bacteria using the NucleoSpin Plasmid Kit (Macherey-Nagel) according to manufacturers' instructions. Afterwards, purified plasmid DNA was checked by restriction analysis and DNA sequencing (Genterprise).

To obtain expression plasmids for human BAG3 (pBAG3-N1) and human BAG3 fused to EGFP (pBAG3.EGFP-N1) partial human BAG3 cDNA containing the full coding sequence was cloned into pEGFP-N1 (Clontech). Human BAG3 coding sequence was amplified by PCR using I90 cDNA as template. Primer sequences used to clone BAG3 plasmids are listed

in Table 2. To construct pBAG3-N1 the target vector pEGFP-N1 was digested with BamHI and NotI to remove the EGFP gene. To clone pBAG3.EGFP-N1 target vector was linearized with BamHI. PCR products were inserted using the In-Fusion reaction (Clontech).

pBAG3.EGFP-N1 Rev	5'-GGCGACCGGTGGATCCGGTGCTGCTGGGTTACCAG-3'
pBAG3-N1 Rev	5'-TCTAGAGTCGCGGCCCTACGGTGCTGCTGGGTTACCAG-3'
Common For	5'-CGCGGGCCCGGGATCATGAGCGCCGCCACCCAC-3'

Table 2: Primers used to clone human BAG3 expression plasmids pBAG3.EGFP-N1 and pBAG3-N1.

To obtain p103QHtt.EGFP-N1 and p25QHtt.EGFP-N1, sequences coding for huntingtin exon 1 fused to EGFP with N-terminal 103 glutamines and 25 glutamines were PCR amplified using p426-103Q-GPD and p426-25Q-GPD, respectively (Addgene plasmids 1184 and 1181, respectively; Krobitsch and Lindquist, 2000) as template. Primer sequences used to clone p103QHtt.EGFP-N1 and p25QHtt.EGFP-N1 are listed in Table 3. PCR products were cloned by using the In-Fusion reaction (Clontech) into BamHI- and NotI-restricted pEGFP-N1 which results in the excision of the EGFP gene.

p25/103QHtt.EGFP-N1 For	5'-CGCGGGCCCGGGATCATGGCGACCCTGGAAAAGC-3'
p25/103QHtt.EGFP-N1 Rev	5'-TCTAGAGTCGCGGCCTTACTTGTACAGCTCGTCC-3'

Table 3: Primers used to clone p25QHtt.EGFP-N1 and p103QHtt.EGFP-N1

Blunt-ending and recircularization
5 µl DNA (~200 ng)
1 µl dNTPs (660 µM each)
2 µl T4-Ligase buffer (10x)
0.5 µl DNA Polymerase I (large Klenow fragment)
11.5 µl H2O
15 min at 25°C
20 min at 75°C
1 µl ATP (20mM)
1 µl T4 Ligase
over night at 16°C

Table 4: Standard protocol for vector blunt ending and recircularization

To construct the control vector p-N1, basis vector pEGFP-N1 was digested with BamHI and NotI followed by DNA polymerase I (large Klenow fragment; New England Biolabs) mediated blunt-ending and vector recircularization using T4-Ligase (New England Biolabs) as

described in Table 4. Expression plasmids for GFP-LC3 (Jackson et al, 2005), d2GFP (Matsuda & Cepko, 2007), Ub-R-GFP and Ub-G76V-GFP (Dantuma et al, 2000) were provided by Addgene. Construction of human BAG1L and BAG1S expression plasmid is described elsewhere (Froesch et al, 1998; Schmidt et al, 2003).

E.5 Cell transfection

Cells were transfected by electroporation using the Amaxa Nucleofector I (program U-24) and standard electroporation cuvettes with a gap-width of 0.4 cm (Sigma). Generally, pelletted cells (maximum $5x10^6$ cells) were resuspended in 400 µl electroporation buffer, premixed with appropriate amounts of DNA or siRNA, transferred air bubble-free into the cuvette and immediately electroporated. After electroporation, cells were allowed to recover for 10 min in the cuvette at room temperature before seeding on culture dishes. To achieve 293 cells stably expressing d2GFP (d2HEK cells), cells were seeded after transfection in 96-well plates with one cell per well. After 2 weeks, cell clones with weak green fluorescence were isolated and analysed for d2GFP expression.

E.6 Small interfering RNA (siRNA)-mediated knock-down

siRNAs were purchased from Eurofins MWG Operon as 19-mer duplexes with 3'-dTdT overhangs. siRNA were solved in 1x Universal siMAX buffer (Eurofins MWG Operon) to a concentration of 1 µg/ml and stored at -80°C. To verify specificity of BAG1 and BAG3 knock-down effects, two independent sets of siRNA duplexes were used for each target gene. Sequences of used siRNAs are listed in Table 5. Generally, cells were transfected with 20 µg of siRNA. In all knock-down experiments, same amounts of siRNA targeting a nonsense sequence were transfected as control.

bag1 -1	5'-GCACGACCUUCAUGUUACC-3'
bag1 -2	5'-ACACCGUUGUCAGCACUUG-3'
bag3 -1	5'-AAUGUGCCAGGAGCCAUAG-3'
bag3 -2	5'-GAGUGUGGCUACAGAAGAG-3'
sqstm1	5'-ACAGAUGGAGUCGGAUAAC-3'
atg7	5'-GCACUAGAGUGUGCAUAUG-3'
nonsense	5'-AUUCUCCGAACGUGUCACG-3'

Table 5: Small interfering RNA sequences

E.7 Western-blot analysis

To obtain protein lysates from different brain regions of young and old mice, whole brains of C57BL/6 mice (3 and 24 months) were rapidly removed, transferred into ice-cold Ca^{2+}-, Mg^{2+}-free Hanks' balanced salt solution, dissected and immediately cryo-freezed in liquid N_2. For preparation of protein lysates, brain samples were resuspended in *NP40 buffer*, sonicated and incubated for 10 min on ice. After centrifugation (10 min, 10 000 g, 4°C), supernatants were collected, brought to 2% SDS with 3x *protein lysis buffer* supplemented with 1% (v/v) protease inhibitor mix and 1% (v/v) phosphatase inhibitor mix (Sigma) and boiled for 5 min at 99°C. For preparation of protein lysates from cells, adherent cell monolayers were washed two times with ice-cold *PBS* and lysed in 1x *protein lysis buffer* supplemented with 1% (v/v) protease inhibitor mix and 1% (v/v) phosphatase inhibitor mix (Sigma). Samples were briefly sonicated and boiled for 3 min at 99°C. Protein concentration was determined by the bicinchoninic acid (BCA) method (Pierce, Rockford, IL, USA) according to manufacturers' protocol and using bovine serum albumin (BSA) as a standard. Generally, 15 µg of total protein were subjected to SDS-PAGE. Prior to electrophoresis *protein loading buffer* was added to samples and protein samples were cooked again for 3 min at 99°C with constant shaking. Thereafter, protein samples were subjected to SDS–PAGE using precast NuPAGE 4-12% Bis-Tris gels with MES running buffer (Invitrogen) or hand-cast gels together with *SDS-running buffer*-driven Mini Protean III system (Bio-Rad). Following gel electrophoresis proteins were transferred to nitrocellulose membranes in *protein transfer buffer* containing 20% (v/v) methanol for 2 hours at constant 46 V using the wet blot-based Mini Trans-Blot Electrophoretic Transfer Cell system (Bio-Rad). Thereafter, protein transfer was checked by reversible staining of proteins on membranes with *Ponceau S solution*. Blocking of non-specific binding-sites on the nitrocellulose membrane was carried out in *PBS-T* containing 5% (w/v) non-fat dry milk powder for 30 min at room temperature. For immunodetection, blots were incubated with primary antibody in *PBS-T* overnight at 4°C (for polyclonal antibodies with high background *PBS-T* was supplemented with 2.5% (w/v) non-fat dry milk powder). Subsequently, membranes were washed twice with PBS-T and incubated with HRP-conjugated secondary antibodies (Jackson Immunoresearch) in PBS-T for 1.5 hours. After three final washes with PBS-T, membrane-bound secondary antibodies (1:5000) were detected by chemiluminescence using either SuperSignal (Pierce) or, for weak signals, Immobilon (Millipore) substrates and visualized with the Fuji LAS-3000 intelligent dark box (Fujifilm). Antibodies used throughout this study are listed in Table 6. The *cBAG* antibody, a kind gift from Prof. Dr. F. Ulrich Hartl, was raised in rabbits against the human BAG domain in BAG1M (aa 151–263).

monoclonal anti-BAG1	sc33704; Santa Cruz
polyclonal anti-BAG3	ab47124; abcam
polyclonal anti-LC3B	L7543; Sigma
monoclonal anti-GFP	MMS-118P; Covance
polyclonal anti-WIPI1	HPA007493; Sigma
polyclonal anti-Ubiquitin	Z0458; Dako
monoclonal anti-SQSTM1	sc28359; Santa Cruz
monoclonal anti-Hsc/Hsp70	SPA820; Stressgen
monoclonal anti-Hsp90	SPA830; Stressgen
monoclonal anti-Tubulin	T9026; Sigma
anti-Polyubiquitin (FK1)	PW8805; biomol
monoclonal anti-Gapdh	ab9482; abcam
polyclonal anti-Actin	A5060; Sigma
polyclonal anti-BAG domain (*cBAG*)	Dr F. Ulrich Hartl

Table 6: Antibodies used throughout this study

E.8 Immunocytochemistry

For immunocytochemical staining, I90 cells were grown on sterile glass cover slips in 6-well plates. Cells were washed three times with ice-cold PBS on ice and then fixed with 3.5% (w/v) paraformaldehyde in PBS for 5 min at 4°C and 10 min at room temperature. After two washes with ice-cold PBS a second methanol fixation step was carried out for 6 min at -20°C. After two additional washes with PBS, unspecific antibody binding sites were blocked with PBS containing 3% (v/v) FBS for 1 hour at room temperature. After incubation of cells with primary antibodies (1:200) over night at 4°C, cells were washed three times with PBS containing 1% (v/v) FBS and then incubated in the dark with Cyanine- (Cy2-, Cy3- or Cy5-) conjugated secondary antibodies (Jackson Immunoresearch) 1:250 in PBS for 1.5 hours at room temperature. After three washes with PBS containing 1% (v/v) FBS, cells were mounted onto glass slides with the DAPI containing Prolong Gold antifade reagent (Invitrogen) and the edges of coverslips were sealed with nail polish. Microscopic analysis was performed with an inverted Axiovert 200 microscope (Zeiss) equipped with a SPOT RT CCD-camera from Diagnostic Instruments (Visitron).

E.9 Co-immunoprecipitation (Co-IP)

Cells were washed twice with ice-cold PBS and lysed on ice in *Co-IP buffer* supplemented with 1% (v/v) protease inhibitor mix and 1% (v/v) phosphatase inhibitor mix (both from Sigma). Lysis was carried out on ice for 20 min in the cell dish after scraping adherent cells off the plate. Thereafter, cell lysates were collected carefully and transferred to low-retention tubes (Kisker). After centrifugation (30 min, 15 000 g, 4°C), supernatants were collected and normalized to the protein content. Co-IP was carried out in 500 µl tubes and generally 2 µg of

antibody were added to an input volume of 300 µl with 1.5-2 µg/µl protein. As control IPs were done with same amounts of purified rabbit or mouse IgG (Sigma). After samples were incubated for 1 hour at 4°C with gentle rotation, ~20 µl protein G sepharose beads (GE Healthcare) were added and the samples incubated for one additional hour at 4°C with constant rotation. Immunocomplexes were pelletted and washed three times with Co-IP Buffer. For immunoblot analysis of precipitated proteins, immunocomplexes were dissociated by adding 25 µl of 4x *protein loading buffer* to samples and heating them for 10 min at 99°C.

E.10 Quantitative real-time reverse transcription–PCR analysis

Total RNA from brain samples and cultured cells was extracted using the NucleoSpin RNA II Kit according to the manufacturers' instructions (Macherey-Nagel). Reverse transcription was performed on 500-1000 ng total RNA in a final reaction volume of 20 µL containing 2 µL reverse transcriptase buffer (Qiagen), 2 µL dNTPs (5 mM; Qiagen), 2 µL oligo(dT)23 primer (10 µm; Sigma), 10 U RNasin (Promega) and 4 U Omniscript Reverse Transcriptase (Qiagen). Synthesis of cDNA was carried out for 60 min at 37°C. Real-time PCR was performed in a 25 µL reaction volume containing 1 µL cDNA, 0.5 µL sense and antisense primers (100 pmol/µl, Eurofins MWG Operon) and 12.5 µL of 2x Absolute SYBR Green Fluorescein Mix (Thermo Scientific) using the iCycler real-time thermocycler (Bio-Rad). Thirty-five cycles of amplification were carried out following 15 min denaturation at 95°C. PCR cycle conditions were denaturation at 95°C for 15 s, primer annealing at 60°C for 15 s and elongation at 72°C for 20 s. The PCR cycle number that generated the first fluorescence signal above threshold (CT) was determined. The generation of specific PCR products was confirmed by melting curve analysis. Quantitative real-time PCR data were applied to REST (Pfaffl et al, 2002) for calculation and to test for significance by a randomisation test. Statistical significance was accepted at a level of $P<0.05$. Actin was used as a reference gene in the I90 aging cell model, in all other experiments the ribosomal protein gene L19. Primer sequences are listed in Table 7.

human BAG1 For	5'-TCACCCACAGCAATGAGAAG-3'
human BAG1 Rev	5'-ATTAACATGACCCGGCAACC-3'
human BAG2 For	5'-GCTCAGGCGAAGATCAACG-3'
human BAG2 Rev	5'-GCCTCATGTCCTGGCTATTTT-3'
human BAG3 For	5'-CTCCATTCCGGTGATACACGA-3'
human BAG3 Rev	5'-TGGTGGGTCTGGTACTCCC-3'
human BAG4 For	5'-AGGAGGCGATGGCTACTATCC-3'
human BAG4 Rev	5'-TTGGACCATACGCTCCATTTG-3'
human BAG5 For	5'-AGTTATCGGCTTCAGTGGTCT-3'
human BAG5 Rev	5'-CTGCCCGCTTCCTAGCTTG-3'
human BAG6 For	5'-AGTGTCCACGCATCCGTAG-3'

human BAG6 Rev	5'-CCCAAACAGTGAGTTTCTGAGG-3'
human LC3B For	5'-AAGGCGCTTACAGCTCAATG-3'
human LC3B Rev	5'-CTGGGAGGCATAGACCATGT-3'
human Hsc70 For	5'-CCATGGTGCTGACCAAGATGAAG-3'
human Hsc70 Rev	5'-TCGTCGATCGTCAGGATGGACAC-3'
human Hsp90 For	5'-TGGTGTGGTTGACTCTGAGGA-3'
human Hsp90 Rev	5'-GGAGGTATGATAGCGCAGCA-3'
human WIPI1 For	5'-GGACTGCACATCCCTAGCAAT-3'
human WIPI1 Rev	5'-TTGTGTGACTGACTACCACCA-3'
human SQSTM1 For	5'-AAGCCGGGTGGGAATGTTG-3'
human SQSTM1 Rev	5'-GCTTGGCCCTTCGGATTCT-3'
mouse BAG1 For	5'-GCAGCAGGGAGTTGACTAGAA-3'
mouse BAG1 Rev	5'-TTACTTCCTCGGTTTGGGTCG-3'
mouse BAG2 For	5'-AGACGCAGCTACTGCTGTTG-3'
mouse BAG2 Rev	5'-CGGATCGTTTCCACCGAGAC-3'
mouse BAG3 For	5'-CTGGGAGATCAAAATCGACCC-3'
mouse BAG3 Rev	5'-GCTGAAGATGCAGTGTCCTTAG-3'
mouse SQSTM1 For	5'-CGATGACTGGACACATTTGTCT-3'
mouse SQSTM1 Rev	5'-GTCCTTCCTGTGAGGGGTCT-3'
human/mouse L19 For	5'-GAAATCGCCAATGCCAACTC-3'
human/mouse L19 Rev	5'-TTCCTTGGTCTTAGACCTGCG-3'
human/mouse Actin For	5'-CTACAATGAGCTGCGTGTGGC-3'
human/mouse Actin Rev	5'-CAGGTCCAGACGCAGGATGGC-3'

Table 7: Primer sequences used in quantitative real-time PCR analyses.

E.11 Measurement of proteasome and cathepsin activity

For preparation of enzymatically active cell extracts, young and old IMR90 cells were washed twice with ice-cold *PBS* and collected by trypsinization. Cells were resuspended and incubated for 10 min in *hypotonic buffer* at 4°C and then passed 10 times through a 25-gauge needle. The homogenate was spun for 5 min at 640 g at 4°C, and then, after the supernatant was brought to 90 mM K-acetate, centrifuged again at 10 000 g for 20 min at 4°C. Supernatants were collected, normalized to protein content and cryo-freezed in liquid nitrogen. Enzymatic reaction was started by mixing active cell extracts (6–8 µg protein in 25 µl) from young and old I90 cells with 25 µl of *protease assay buffer*, supplemented either with 70 µM Suc-LLVY-AMC (Sigma; for proteasome activity) or 70 µM Z-FR-AMC (Calbiochem; for total cathepsin activity), both 1:100 from 7 mM stocks made in DMSO. AMC fluorescence was recorded in a black 96-well plate (Greiner) at 37°C in 2 min intervals for a total time period of 30 min using the Victor3V Multilabel counter (Perkin Elmer). Specific proteasomal and cathepsin L activity was determined by subtracting unspecific AMC fluorescence obtained in the presence of proteasome inhibitor MG132 (20 µM) and lysosomal inhibitors E64 and pepstatin A (both 10 µg/ml), respectively.

For measurement of proteasome and cathepsin activity in brains of young and old mice, hippocampal and cerebellar brain samples dissected as described in E.7 were resuspended

in *hypotonic buffer*, sonicated on ice and then passed 20 times through a 25-gauge needle followed by the same purification and measurement procedure as described for I90 cells. Specific cathepsin B activity was measured with the cathepsin B-specific fluorescent substrate Z-RR-AMC (Biomol).

E.12 Transmission electron microscopy

Transmission electron microscopy (TEM) was performed in co-operation with Dr U. Wolfrum. as described previously (Mersseman et al, 2008). In brief, cells were prefixed in 2.5% glutaraldehyde, 0.1 M sucrose, 0.1 M cacodylate buffer (pH 7.3) for 1 h at room temperature. After three washes for 10 min in 0.1 M cacodylate buffer, cells were post-fixed for 1 h in 1 ml 2% OsO4, 0.1 M sucrose and 0.1 M cacodylate buffer, dehydrated and embedded in araldite resin. Ultrathin sections were cut with a Leica Ultracut S microtome and were counterstained with 2% aqueous uranyl acetate. Sections were analysed in a FEI Tecnai 12 BioTwin transmission electron microscope and imaged with an SCCD SIS MegaView III camera.

E.13 Statistical methods

Statistical significance was determined by Student's t-test using SIGMA STAT software (SPSS Science). Statistical significance was accepted at a level of $P<0.05$. The results are expressed as mean plus ±SEM.

F REFERENCES

Adams J (2001) Proteasome inhibition in cancer: development of PS-341. *Semin. Oncol.* **28:** 613–619

Adrain C, Creagh EM, Cullen SP & Martin SJ (2004) Caspase-dependent inactivation of proteasome function during programmed cell death in Drosophila and man. *J. Biol. Chem.* **279:** 36923–36930

Alberti S, Demand J, Esser C, Emmerich N, Schild H & Hohfeld J (2002) Ubiquitylation of BAG-1 suggests a novel regulatory mechanism during the sorting of chaperone substrates to the proteasome. *J. Biol. Chem.* **277:** 45920–45927

Anfinsen CB (1973) Principles that govern the folding of protein chains. *Science* **181:** 223–230

Arndt V, Rogon C & Höhfeld J (2007) To be, or not to be--molecular chaperones in protein degradation. *Cell. Mol. Life Sci.* **64:** 2525–2541

Arndt V, Daniel C, Nastainczyk W, Alberti S & Höhfeld J (2005) BAG-2 acts as an inhibitor of the chaperone-associated ubiquitin ligase CHIP. *Mol. Biol. Cell* **16:** 5891–5900

Balch WE, Morimoto RI, Dillin A & Kelly JW (2008) Adapting proteostasis for disease intervention. *Science* **319:** 916–919

Berger Z, Roder H, Hanna A, Carlson A, Rangachari V, Yue M, Wszolek Z, Ashe K, Knight J, Dickson D, Andorfer C, Rosenberry TL, Lewis J, Hutton M & Janus C (2007) Accumulation of pathological tau species and memory loss in a conditional model of tauopathy. *J. Neurosci.* **27:** 3650–3662

Baumeister W, Walz J, Zühl F & Seemüller E (1998) The proteasome: paradigm of a self-compartmentalizing protease. *Cell* **92:** 367–380

Bence NF, Sampat RM & Kopito RR (2001) Impairment of the ubiquitin-proteasome system by protein aggregation. *Science* **292:** 1552–1555

Bimston D, Song J, Winchester D, Takayama S, Reed JC & Morimoto RI (1998) BAG-1, a negative regulator of Hsp70 chaperone activity, uncouples nucleotide hydrolysis from substrate release. *EMBO J.* **17:** 6871–6878

Bjørkøy G, Lamark T, Brech A, Outzen H, Perander M, Overvatn A, Stenmark H & Johansen T (2005) p62/SQSTM1 forms protein aggregates degraded by autophagy and has a protective effect on huntingtin-induced cell death. *J. Cell Biol.* **171:** 603–614

Bjørkøy G, Lamark T, Pankiv S, Øvervatn A, Brech A & Johansen T (2009) Monitoring autophagic degradation of p62/SQSTM1. *Meth. Enzymol.* **452:** 181–197

Bolster DR, Kubica N, Crozier SJ, Williamson DL, Farrell PA, Kimball SR & Jefferson LS (2003) Immediate response of mammalian target of rapamycin (mTOR)-mediated signalling following acute resistance exercise in rat skeletal muscle. *J. Physiol. (Lond.)* **553:** 213–220

Bowman AB, Yoo S, Dantuma NP & Zoghbi HY (2005) Neuronal dysfunction in a polyglutamine disease model occurs in the absence of ubiquitin-proteasome system impairment and inversely correlates with the degree of nuclear inclusion formation. *Hum. Mol. Genet.* **14:** 679–691

Breusing N & Grune T (2008) Regulation of proteasome-mediated protein degradation during oxidative stress and aging. *Biol. Chem.* **389:** 203–209

Brewer GJ (1997) Isolation and culture of adult rat hippocampal neurons. *J. Neurosci. Methods* 71: 143–155

Brunk UT & Terman A (2002) Lipofuscin: mechanisms of age-related accumulation and influence on cell function. *Free Radic. Biol. Med.* **33:** 611–619

Bukau B & Horwich AL (1998) The Hsp70 and Hsp60 chaperone machines. *Cell* **92:** 351–366

Carra S, Brunsting JF, Lambert H, Landry J & Kampinga HH (2009) HspB8 Participates in Protein Quality Control by a Non-chaperone-like Mechanism That Requires eIF2{alpha} Phosphorylation. *J. Biol. Chem.* **284:** 5523–5532

Carra S, Seguin SJ, Lambert H & Landry J (2008a) HspB8 chaperone activity toward poly(Q)-containing proteins depends on its association with Bag3, a stimulator of macroautophagy. *J. Biol. Chem.* **283:** 1437–1444

Carra S, Seguin SJ & Landry J (2008b) HspB8 and Bag3: a new chaperone complex targeting misfolded proteins to macroautophagy. *Autophagy* **4:** 237–239

Carrettiero DC, Hernandez I, Neveu P, Papagiannakopoulos T & Kosik KS (2009) The cochaperone BAG2 sweeps paired helical filament- insoluble tau from the microtubule. *J. Neurosci.* **29:** 2151–2161

Chang H, Tang Y, Hayer-Hartl M & Hartl FU (2007) SnapShot: molecular chaperones, Part I. *Cell* **128:** 212

Chen S & Smith DF (1998) Hop as an adaptor in the heat shock protein 70 (Hsp70) and hsp90 chaperone machinery. *J. Biol. Chem.* **273:** 35194–35200

Cheroni C, Marino M, Tortarolo M, Veglianese P, Biasi S de, Fontana E, Zuccarello LV, Maynard CJ, Dantuma NP & Bendotti C (2009) Functional alterations of the ubiquitin-proteasome system in motor neurons of a mouse model of familial amyotrophic lateral sclerosis. *Hum. Mol. Genet.* **18:** 82–96

Chiti F & Dobson CM (2006) Protein misfolding, functional amyloid, and human disease. *Annu. Rev. Biochem.* **75:** 333–366

Chu Y & Kordower JH (2007) Age-associated increases of alpha-synuclein in monkeys and humans are associated with nigrostriatal dopamine depletion: Is this the target for Parkinson's disease? *Neurobiol. Dis.* **25:** 134–149

Cicero S & Herrup K (2005) Cyclin-dependent kinase 5 is essential for neuronal cell cycle arrest and differentiation. *J. Neurosci.* **25:** 9658–9668

Connell P, Ballinger CA, Jiang J, Wu Y, Thompson LJ, Höhfeld J & Patterson C (2001) The co-chaperone CHIP regulates protein triage decisions mediated by heat-shock proteins. *Nat. Cell Biol.* **3:** 93–96

Cuervo AM (2003) Autophagy and aging--when "all you can eat" is yourself. *Science of aging knowledge environment : SAGE KE* **2003:** pe25

Cuervo AM (2008) Autophagy and aging: keeping that old broom working. *Trends Genet.* **24:** 604–612

Cuervo AM, Bergamini E, Brunk UT, Dröge W, Ffrench M & Terman A (2005) Autophagy and aging: the importance of maintaining "clean" cells. *Autophagy* **1:** 131–140

Cuervo AM, Stefanis L, Fredenburg R, Lansbury PT & Sulzer D (2004) Impaired degradation of mutant alpha-synuclein by chaperone-mediated autophagy. *Science* **305:** 1292–1295

Dai Q, Qian S, Li H, McDonough H, Borchers C, Huang D, Takayama S, Younger JM, Ren HY, Cyr DM & Patterson C (2005) Regulation of the cytoplasmic quality control protein degradation pathway by BAG2. *J. Biol. Chem.* **280:** 38673–38681

Dantuma NP, Lindsten K, Glas R, Jellne M & Masucci MG (2000) Short-lived green fluorescent proteins for quantifying ubiquitin/proteasome-dependent proteolysis in living cells. *Nat. Biotechnol.* **18:** 538–543

Del Roso A, Vittorini S, Cavallini G, Donati A, Gori Z, Masini M, Pollera M & Bergamini E (2003) Ageing-related changes in the in vivo function of rat liver macroautophagy and proteolysis. *Exp. Gerontol.* **38:** 519–527

Demand J, Alberti S, Patterson C & Höhfeld J (2001) Cooperation of a ubiquitin domain protein and an E3 ubiquitin ligase during chaperone/proteasome coupling. *Curr. Biol.* **11:** 1569–1577

Desmots F, Russell HR, Michel D & McKinnon PJ (2008) Scythe regulates apoptosis-inducing factor stability during endoplasmic reticulum stress-induced apoptosis. *J. Biol. Chem.* **283:** 3264–3271

Dickey C, Kraft C, Jinwal U, Koren J, Johnson A, Anderson L, Lebson L, Lee D, Dickson D, Silva R de, Binder LI, Morgan D & Lewis J (2009) Aging analysis reveals slowed tau turnover and enhanced stress response in a mouse model of tauopathy. *Am. J. Pathol.* **174:** 228–238

Dill KA, Ozkan SB, Shell MS & Weikl TR (2008) The protein folding problem. *Annual review of biophysics* **37:** 289–316

Ding W & Yin X (2008) Sorting, recognition and activation of the misfolded protein degradation pathways through macroautophagy and the proteasome. *Autophagy* **4:** 141–150

Dobson CM & Karplus M (1999) The fundamentals of protein folding: bringing together theory and experiment. *Curr. Opin. Struct. Biol.* **9:** 92–101

Doong H, Rizzo K, Fang S, Kulpa V, Weissman AM & Kohn EC (2003) CAIR-1/BAG-3 abrogates heat shock protein-70 chaperone complex-mediated protein degradation: accumulation of poly-ubiquitinated Hsp90 client proteins. *J. Biol. Chem.* **278:** 28490–28500

Dragovic Z, Broadley SA, Shomura Y, Bracher A & Hartl FU (2006) Molecular chaperones of the Hsp110 family act as nucleotide exchange factors of Hsp70s. *EMBO J.* **25:** 2519–2528

Dumont P, Burton M, Chen QM, Gonos ES, Frippiat C, Mazarati JB, Eliaers F, Remacle J & Toussaint O (2000) Induction of replicative senescence biomarkers by sublethal oxidative stresses in normal human fibroblast. *Free Radic. Biol. Med.* **28:** 361–373

Duyao M, Ambrose C, Myers R, Novelletto A, Persichetti F, Frontali M, Folstein S, Ross C, Franz M & Abbott M (1993) Trinucleotide repeat length instability and age of onset in Huntington's disease. *Nat. Genet.* **4:** 387–392

Elliott E, Tsvetkov P & Ginzburg I (2007) BAG-1 associates with Hsc70.Tau complex and regulates the proteasomal degradation of Tau protein. *J. Biol. Chem.* **282:** 37276–37284

Elsasser S & Finley D (2005) Delivery of ubiquitinated substrates to protein-unfolding machines. *Nat. Cell Biol.* **7:** 742–749

Emmanouilidou E, Stefanis L & Vekrellis K (2008) Cell-produced alpha-synuclein oligomers are targeted to, and impair, the 26S proteasome. *Neurobiol. Aging*

Farout L & Friguet B (2006) Proteasome function in aging and oxidative stress: implications in protein maintenance failure. *Antioxid. Redox Signal.* **8:** 205–216

Ferreira ST, Felice FG de & Chapeaurouge A (2006) Metastable, partially folded states in the productive folding and in the misfolding and amyloid aggregation of proteins. *Cell Biochem. Biophys.* **44:** 539–548

Finkbeiner S, Cuervo AM, Morimoto RI & Muchowski PJ (2006) Disease-modifying pathways in neurodegeneration. *J. Neurosci.* **26:** 10349–10357

Finn PF & Dice JF (2006) Proteolytic and lipolytic responses to starvation. *Nutrition (Burbank, Los Angeles County, Calif.)* **22:** 830–844

Forman MS, Trojanowski JQ & Lee VM (2004) Neurodegenerative diseases: a decade of discoveries paves the way for therapeutic breakthroughs. *Nat. Med.* **10:** 1055–1063

Franceschelli S, Rosati A, Lerose R, Nicola S de, Turco MC & Pascale M (2008) Bag3 gene expression is regulated by heat shock factor 1. *J. Cell. Physiol.* **215:** 575–577

Froesch BA, Takayama S & Reed JC (1998) BAG-1L protein enhances androgen receptor function. *J. Biol. Chem.* 273: 11660–11666

Frydman J (2001) Folding of newly translated proteins in vivo: the role of molecular chaperones. *Annu. Rev. Biochem.* **70:** 603–647

Fujita N, Hayashi-Nishino M, Fukumoto H, Omori H, Yamamoto A, Noda T & Yoshimori T (2008) An Atg4B mutant hampers the lipidation of LC3 paralogues and causes defects in autophagosome closure. *Mol. Biol. Cell* **19:** 4651–4659

Gassler CS, Wiederkehr T, Brehmer D, Bukau B & Mayer MP (2001) Bag-1M accelerates nucleotide release for human Hsc70 and Hsp70 and can act concentration-dependent as positive and negative cofactor. *J. Biol. Chem.* **276:** 32538–32544

Georgakis GV & Younes A (2005) Heat-shock protein 90 inhibitors in cancer therapy: 17AAG and beyond. *Future oncology (London, England)* **1:** 273–281

Goedert M & Crowther RA (2003) Amyloid plaques, neurofibrillary tangles and their relevance for the study of Alzheimer's disease. *Neurobiol. Aging* **10:** 405-6; discussion 412-4

Götz R, Wiese S, Takayama S, Camarero GC, Rossoll W, Schweizer U, Troppmair J, Jablonka S, Holtmann B, Reed JC, Rapp UR & Sendtner M (2005) Bag1 is essential for differentiation and survival of hematopoietic and neuronal cells. *Nat. Neurosci.* **8:** 1169–1178

Grune T, Jung T, Merker K & Davies KJA (2004) Decreased proteolysis caused by protein aggregates, inclusion bodies, plaques, lipofuscin, ceroid, and 'aggresomes' during oxidative stress, aging, and disease. *Int. J. Biochem. Cell Biol.* **36:** 2519–2530

Haan JB de, Newman JD & Kola I (1992) Cu/Zn superoxide dismutase mRNA and enzyme activity, and susceptibility to lipid peroxidation, increases with aging in murine brains. *Brain Res. Mol. Brain Res.* **13:** 179–187

Hara T, Nakamura K, Matsui M, Yamamoto A, Nakahara Y, Suzuki-Migishima R, Yokoyama M, Mishima K, Saito I, Okano H & Mizushima N (2006) Suppression of basal autophagy in neural cells causes neurodegenerative disease in mice. *Nature* **441:** 885–889

Harman D (1956) Aging: a theory based on free radical and radiation chemistry. *Journal of gerontology* **11:** 298–300

Hartl FU & Hayer-Hartl M (2002) Molecular chaperones in the cytosol: from nascent chain to folded protein. *Science* **295:** 1852–1858

Hatakeyama S, Matsumoto M, Kamura T, Murayama M, Chui D, Planel E, Takahashi R, Nakayama KI & Takashima A (2004) U-box protein carboxyl terminus of Hsc70-interacting protein (CHIP) mediates poly-ubiquitylation preferentially on four-repeat Tau and is involved in neurodegeneration of tauopathy. *J. Neurochem.* **91:** 299–307

Hayflick L (2000) The future of ageing. *Nature* **408:** 267–269

Hebert LE, Beckett LA, Scherr PA & Evans DA Annual incidence of Alzheimer disease in the United States projected to the years 2000 through 2050. *Alzheimer disease and associated disorders* **15:** 169–173

Heo SR, Han AM, Kwon YK & Joung I (2009) p62 protects SH-SY5Y neuroblastoma cells against H2O2-induced injury through the PDK1/Akt pathway. *Neurosci. Lett.* **450:** 45–50

Höhfeld J, Cyr DM & Patterson C (2001) From the cradle to the grave: molecular chaperones that may choose between folding and degradation. *EMBO Rep.* **2:** 885–890

Höhfeld J & Jentsch S (1997) GrpE-like regulation of the hsc70 chaperone by the anti-apoptotic protein BAG-1. *EMBO J.* **16:** 6209–6216

Homma S, Iwasaki M, Shelton GD, Engvall E, Reed JC & Takayama S (2006) BAG3 deficiency results in fulminant myopathy and early lethality. *Am. J. Pathol.* **169:** 761–773

Hosokawa N, Hara Y & Mizushima N (2006) Generation of cell lines with tetracycline-regulated autophagy and a role for autophagy in controlling cell size. *FEBS Lett.* **580:** 2623–2629

Høyer-Hansen M & Jäättelä M (2007) Connecting endoplasmic reticulum stress to autophagy by unfolded protein response and calcium. *Cell Death Differ.* **14:** 1576–1582

Jackson WT, Giddings TH, Taylor MP, Mulinyawe S, Rabinovitch M, Kopito RR & Kirkegaard K (2005) Subversion of cellular autophagosomal machinery by RNA viruses. *PLoS Biol.* **3:** e156

Jana NR, Dikshit P, Goswami A, Kotliarova S, Murata S, Tanaka K & Nukina N (2005) Co-chaperone CHIP associates with expanded polyglutamine protein and promotes their degradation by proteasomes. *J. Biol. Chem.* **280:** 11635–11640

Jang M, Park BC, Lee AY, Na KS, Kang S, Bae K, Myung PK, Chung BC, Cho S, Lee DH & Park SG (2007) Caspase-7 mediated cleavage of proteasome subunits during apoptosis. *Biochem. Biophys. Res. Commun.* **363:** 388–394

Jiang Y, Woronicz JD, Liu W & Goeddel DV (1999) Prevention of constitutive TNF receptor 1 signaling by silencer of death domains. *Science* **283:** 543–546

Johnson BD, Schumacher RJ, Ross ED & Toft DO (1998) Hop modulates Hsp70/Hsp90 interactions in protein folding. *J. Biol. Chem.* **273:** 3679–3686

Jung CH, Jun CB, Ro S, Kim Y, Otto NM, Cao J, Kundu M & Kim D (2009a) ULK-Atg13-FIP200 Complexes Mediate mTOR Signaling to the Autophagy Machinery. *Mol. Biol. Cell*

Jung T, Höhn A, Catalgol B & Grune T (2009b) Age-related differences in oxidative protein-damage in young and senescent fibroblasts. *Arch. Biochem. Biophys.* **483:** 127–135

Kabbage M & Dickman MB (2008) The BAG proteins: a ubiquitous family of chaperone regulators. *Cell. Mol. Life Sci.* **65:** 1390–1402

Kabuta T, Suzuki Y & Wada K (2006) Degradation of amyotrophic lateral sclerosis-linked mutant Cu,Zn-superoxide dismutase proteins by macroautophagy and the proteasome. *J. Biol. Chem.* **281:** 30524–30533

Kaganovich D, Kopito R & Frydman J (2008) Misfolded proteins partition between two distinct quality control compartments. *Nature* **454:** 1088–1095

Kalia SK, Lee S, Smith PD, Liu L, Crocker SJ, Thorarinsdottir TE, Glover JR, Fon EA, Park DS & Lozano AM (2004) BAG5 inhibits parkin and enhances dopaminergic neuron degeneration. *Neuron* **44:** 931–945

Kazemi S, Mounir Z, Baltzis D, Raven JF, Wang S, Krishnamoorthy J, Pluquet O, Pelletier J & Koromilas AE (2007) A novel function of eIF2alpha kinases as inducers of the phosphoinositide-3 kinase signaling pathway. *Mol. Biol. Cell* **18:** 3635–3644

Kermer P, Digicaylioglu MH, Kaul M, Zapata JM, Krajewska M, Stenner-Liewen F, Takayama S, Krajewski S, Lipton SA & Reed JC (2003) BAG1 over-expression in brain protects against stroke. *Brain Pathol.* **13:** 495–506

Kiffin R, Christian C, Knecht E & Cuervo AM (2004) Activation of chaperone-mediated autophagy during oxidative stress. *Mol. Biol. Cell* **15:** 4829–4840

Kiffin R, Kaushik S, Zeng M, Bandyopadhyay U, Zhang C, Massey AC, Martinez-Vicente M & Cuervo AM (2007) Altered dynamics of the lysosomal receptor for chaperone-mediated autophagy with age. *J. Cell. Sci.* **120:** 782–791

Kim PK, Hailey DW, Mullen RT & Lippincott-Schwartz J (2008) Ubiquitin signals autophagic degradation of cytosolic proteins and peroxisomes. *Proc. Natl. Acad. Sci. U.S.A.* **105:** 20567–20574

Kim SH, Shi Y, Hanson KA, Williams LM, Sakasai R, Bowler MJ & Tibbetts RS (2009) Potentiation of Amyotrophic Lateral Sclerosis (ALS)-associated TDP-43 Aggregation by the Proteasome-targeting Factor, Ubiquilin 1. *J. Biol. Chem.* **284:** 8083–8092

Kirkin V, Lamark T, Sou Y, Bjørkøy G, Nunn JL, Bruun J, Shvets E, McEwan DG, Clausen TH, Wild P, Bilusic I, Theurillat J, Øvervatn A, Ishii T, Elazar Z, Komatsu M, Dikic I & Johansen T (2009) A role for NBR1 in autophagosomal degradation of ubiquitinated substrates. *Mol. Cell* **33:** 505–516

Komatsu M, Waguri S, Chiba T, Murata S, Iwata J, Tanida I, Ueno T, Koike M, Uchiyama Y, Kominami E & Tanaka K (2006) Loss of autophagy in the central nervous system causes neurodegeneration in mice. *Nature* **441:** 880–884

Komatsu M, Waguri S, Koike M, Sou Y, Ueno T, Hara T, Mizushima N, Iwata J, Ezaki J, Murata S, Hamazaki J, Nishito Y, Iemura S, Natsume T, Yanagawa T, Uwayama J, Warabi E, Yoshida H, Ishii T & Kobayashi A et al (2007) Homeostatic levels of p62 control cytoplasmic inclusion body formation in autophagy-deficient mice. *Cell* **131:** 1149–1163

Komatsu M, Waguri S, Ueno T, Iwata J, Murata S, Tanida I, Ezaki J, Mizushima N, Ohsumi Y, Uchiyama Y, Kominami E, Tanaka K & Chiba T (2005) Impairment of starvation-induced and constitutive autophagy in Atg7-deficient mice. *J. Cell Biol.* **169:** 425–434

Krobitsch S & Lindquist S (2000) Aggregation of huntingtin in yeast varies with the length of the polyglutamine expansion and the expression of chaperone proteins. *Proc. Natl. Acad. Sci. U.S.A.* **97:** 1589–1594

Kuma A, Hatano M, Matsui M, Yamamoto A, Nakaya H, Yoshimori T, Ohsumi Y, Tokuhisa T & Mizushima N (2004) The role of autophagy during the early neonatal starvation period. *Nature* **432:** 1032–1036

Kundu M & Thompson CB (2005) Macroautophagy versus mitochondrial autophagy: a question of fate? *Cell Death Differ.* **12 Suppl 2:** 1484–1489

Kurz T, Terman A, Gustafsson B & Brunk UT (2008) Lysosomes and oxidative stress in aging and apoptosis. *Biochim. Biophys. Acta* **1780:** 1291–1303

Kuusisto E, Suuronen T & Salminen A (2001) Ubiquitin-binding protein p62 expression is induced during apoptosis and proteasomal inhibition in neuronal cells. *Biochem. Biophys. Res. Commun.* **280:** 223–228

Leroux MR & Hartl FU (2000) Protein folding: versatility of the cytosolic chaperonin TRiC/CCT. *Curr. Biol.* **10:** R260-4

Lints FA (1989) The rate of living theory revisited. *Gerontology* **35:** 36–57

Liu C, Li X, Thompson D, Wooding K, Chang T, Tang Z, Yu H, Thomas PJ & DeMartino GN (2006) ATP binding and ATP hydrolysis play distinct roles in the function of 26S proteasome. *Mol. Cell* **24:** 39–50

Linge A, Weinhold K, Bläsche R, Kasper M & Barth K (2007) Downregulation of caveolin-1 affects bleomycin-induced growth arrest and cellular senescence in A549 cells. *Int. J. Biochem. Cell Biol.* **39:** 1964–1974

Li W, Lesuisse C, Xu Y, Troncoso JC, Price DL & Lee MK (2004) Stabilization of alpha-synuclein protein with aging and familial parkinson's disease-linked A53T mutation. *J. Neurosci.* **24:** 7400–7409

Lüders J, Demand J & Höhfeld J (2000a) The ubiquitin-related BAG-1 provides a link between the molecular chaperones Hsc70/Hsp70 and the proteasome. *J. Biol. Chem.* **275:** 4613–4617

Lüders J, Demand J, Papp O & Höhfeld J (2000b) Distinct isoforms of the cofactor BAG-1 differentially affect Hsc70 chaperone function. *J. Biol. Chem.* **275:** 14817–14823

Lu T, Pan Y, Kao S, Li C, Kohane I, Chan J & Yankner BA (2004) Gene regulation and DNA damage in the ageing human brain. *Nature* **429:** 883–891

Lutz W, Sanderson W & Scherbov S (2008) The coming acceleration of global population ageing. *Nature* **451:** 716–719

Mackenzie IRA, Bigio EH, Ince PG, Geser F, Neumann M, Cairns NJ, Kwong LK, Forman MS, Ravits J, Stewart H, Eisen A, McClusky L, Kretzschmar HA, Monoranu CM, Highley JR, Kirby J, Siddique T, Shaw PJ, Lee VM & Trojanowski JQ (2007) Pathological TDP-43 distinguishes sporadic amyotrophic lateral sclerosis from amyotrophic lateral sclerosis with SOD1 mutations. *Ann. Neurol.* **61:** 427–434

Majeski AE & Dice JF (2004) Mechanisms of chaperone-mediated autophagy. *Int. J. Biochem. Cell Biol.* **36:** 2435–2444

Malatynska E, Pinhasov A, Crooke J, Horowitz D, Brenneman DE & Ilyin SE (2006) Levels of mRNA coding for alpha-, beta-, and gamma-synuclein in the brains of newborn, juvenile, and adult rats. *J. Mol. Neurosci.* **29:** 269–277

Mariño G, Ugalde AP, Salvador-Montoliu N, Varela I, Quirós PM, Cadiñanos J, van der Pluijm I, Freije JM & López-Otín C (2008) Premature aging in mice activates a systemic metabolic response involving autophagy induction. *Hum. Mol. Genet.* **17**: 2196-2211.

Martinez-Vicente M & Cuervo AM (2007) Autophagy and neurodegeneration: when the cleaning crew goes on strike. *Lancet neurology* **6:** 352–361

Marx J (2002) Cell biology. Ubiquitin lives up to its name. *Science* **297:** 1792–1794

Massey AC, Zhang C & Cuervo AM (2006) Chaperone-mediated autophagy in aging and disease. *Curr. Top. Dev. Biol.* **73:** 205–235

Matsuda T & Cepko CL (2007) Controlled expression of transgenes introduced by in vivo electroporation. *Proc. Natl. Acad. Sci. U.S.A.* 104: 1027–1032

McDonough H & Patterson C (2003) CHIP: a link between the chaperone and proteasome systems. *Cell Stress Chaperones* **8:** 303–308

Meléndez A, Tallóczy Z, Seaman M, Eskelinen E, Hall DH & Levine B (2003) Autophagy genes are essential for dauer development and life-span extension in C. elegans. *Science* **301:** 1387–1391

Mersseman V, Besold K, Reddehase MJ, Wolfrum U, Strand D, Plachter B & Reyda S (2008) Exogenous introduction of an immunodominant peptide from the non-structural IE1 protein of human cytomegalovirus into the MHC class I presentation pathway by recombinant dense bodies. *J. Gen. Virol.* 89: 369–379

Mizushima N (2007) Autophagy: process and function. *Genes Dev.* **21:** 2861–2873

Mizushima N & Yoshimori T (2007) How to interpret LC3 immunoblotting. *Autophagy* **3:** 542–545

Moosmann B & Behl C (2008) Mitochondrially encoded cysteine predicts animal lifespan. *Aging Cell* **7:** 32–46

Mullen RJ, Buck CR & Smith AM (1992) NeuN, a neuronal specific nuclear protein in vertebrates. *Development* **116:** 201–211

Nandi D, Tahiliani P, Kumar A & Chandu D (2006) The ubiquitin-proteasome system. *J. Biosci.* **31:** 137–155

Navon A & Goldberg AL (2001) Proteins are unfolded on the surface of the ATPase ring before transport into the proteasome. *Mol. Cell* **8:** 1339–1349

N'Diaye E, Kajihara KK, Hsieh I, Morisaki H, Debnath J & Brown EJ (2009) PLIC proteins or ubiquilins regulate autophagy-dependent cell survival during nutrient starvation. *EMBO Rep.* **10:** 173–179

Nichols WW, Murphy DG, Cristofalo VJ, Toji LH, Greene AE & Dwight SA (1977) Characterization of a new human diploid cell strain, IMR-90. *Science* **196:** 60–63

Nicklin P, Bergman P, Zhang B, Triantafellow E, Wang H, Nyfeler B, Yang H, Hild M, Kung C, Wilson C, Myer VE, MacKeigan JP, Porter JA, Wang YK, Cantley LC, Finan PM & Murphy LO (2009) Bidirectional transport of amino acids regulates mTOR and autophagy. *Cell* **136:** 521–534

Nollen EA, Brunsting JF, Song J, Kampinga HH & Morimoto RI (2000) Bag1 functions in vivo as a negative regulator of Hsp70 chaperone activity. *Mol. Cell. Biol.* **20:** 1083–1088

Nollen EA, Kabakov AE, Brunsting JF, Kanon B, Höhfeld J & Kampinga HH (2001) Modulation of in vivo HSP70 chaperone activity by Hip and Bag-1. *J. Biol. Chem.* **276:** 4677–4682

Oberley TD, Swanlund JM, Zhang HJ & Kregel KC (2008) Aging results in increased autophagy of mitochondria and protein nitration in rat hepatocytes following heat stress. *J. Histochem. Cytochem.* **56:** 615–627

Oh-Ishi S, Kizaki T, Yamashita H, Nagata N, Suzuki K, Taniguchi N & Ohno H (1995) Alterations of superoxide dismutase iso-enzyme activity, content, and mRNA expression with aging in rat skeletal muscle. *Mech. Ageing Dev.* **84:** 65–76

Olzmann JA & Chin L (2008) Parkin-mediated K63-linked polyubiquitination: a signal for targeting misfolded proteins to the aggresome-autophagy pathway. *Autophagy* **4:** 85–87

Ono K, Hirohata M & Yamada M (2008) Alpha-synuclein assembly as a therapeutic target of Parkinson's disease and related disorders. *Curr. Pharm. Des.* **14:** 3247–3266

Pagliuca MG, Lerose R, Cigliano S & Leone A (2003) Regulation by heavy metals and temperature of the human BAG-3 gene, a modulator of Hsp70 activity. *FEBS Lett.* **541:** 11–15

Pankiv S, Clausen TH, Lamark T, Brech A, Bruun J, Outzen H, Øvervatn A, Bjørkøy G & Johansen T (2007) p62/SQSTM1 binds directly to Atg8/LC3 to facilitate degradation of ubiquitinated protein aggregates by autophagy. *J. Biol. Chem.* **282:** 24131–24145

Pattingre S, Espert L, Biard-Piechaczyk M & Codogno P (2008) Regulation of macroautophagy by mTOR and Beclin 1 complexes. *Biochimie* **90:** 313–323

Paulson HL (1999) Protein fate in neurodegenerative proteinopathies: polyglutamine diseases join the (mis)fold. *Am. J. Hum. Genet.* **64:** 339–345

Pfaffl MW, Horgan GW & Dempfle L (2002) Relative expression software tool (REST) for group-wise comparison and statistical analysis of relative expression results in real-time PCR. *Nucleic Acids Res.* 30: e36

Polier S, Dragovic Z, Hartl FU & Bracher A (2008) Structural basis for the cooperation of Hsp70 and Hsp110 chaperones in protein folding. *Cell* **133:** 1068–1079

Proikas-Cezanne T, Ruckerbauer S, Stierhof Y, Berg C & Nordheim A (2007) Human WIPI-1 puncta-formation: a novel assay to assess mammalian autophagy. *FEBS Lett.* **581:** 3396–3404

Ramesh Babu J, Lamar Seibenhener M, Peng J, Strom A, Kemppainen R, Cox N, Zhu H, Wooten MC, Diaz-Meco MT, Moscat J & Wooten MW (2008) Genetic inactivation of p62 leads to accumulation of hyperphosphorylated tau and neurodegeneration. *J. Neurochem.* **106:** 107–120

Ravikumar B, Duden R & Rubinsztein DC (2002) Aggregate-prone proteins with polyglutamine and polyalanine expansions are degraded by autophagy. *Hum. Mol. Genet.* **11:** 1107–1117

Rechsteiner M & Rogers SW (1996) PEST sequences and regulation by proteolysis. *Trends Biochem. Sci.* **21:** 267–271

Reits EA, Benham AM, Plougastel B, Neefjes J & Trowsdale J (1997) Dynamics of proteasome distribution in living cells. *EMBO J.* **16:** 6087–6094

Ross CA & Poirier MA (2005) Opinion: What is the role of protein aggregation in neurodegeneration? *Nat. Rev. Mol. Cell Biol.* **6:** 891–898

Rothstein JD, Martin L, Levey AI, Dykes-Hoberg M, Jin L, Wu D, Nash N & Kuncl RW (1994) Localization of neuronal and glial glutamate transporters. *Neuron* **13:** 713–725

Rubinsztein DC (2006) The roles of intracellular protein-degradation pathways in neurodegeneration. *Nature* **443:** 780–786

Rubinsztein DC, DiFiglia M, Heintz N, Nixon RA, Qin Z, Ravikumar B, Stefanis L & Tolkovsky A (2005) Autophagy and its possible roles in nervous system diseases, damage and repair. *Autophagy* **1:** 11–22

Sanz A, Caro P, Gómez J & Barja G (2006) Testing the vicious cycle theory of mitochondrial ROS production: effects of H2O2 and cumene hydroperoxide treatment on heart mitochondria. *J. Bioenerg. Biomembr.* **38:** 121–127

Sarkar S, Davies JE, Huang Z, Tunnacliffe A & Rubinsztein DC (2007) Trehalose, a novel mTOR-independent autophagy enhancer, accelerates the clearance of mutant huntingtin and alpha-synuclein. *J. Biol. Chem.* **282:** 5641–5652

Sarkar S, Ravikumar B, Floto RA & Rubinsztein DC (2009) Rapamycin and mTOR-independent autophagy inducers ameliorate toxicity of polyglutamine-expanded huntingtin and related proteinopathies. *Cell Death Differ.* **16:** 46–56

Sarközi R, Perco P, Hochegger K, Enrich J, Wiesinger M, Pirklbauer M, Eder S, Rudnicki M, Rosenkranz AR, Mayer B, Mayer G & Schramek H (2008) Bortezomib-induced survival signals and genes in human proximal tubular cells. *J. Pharmacol. Exp. Ther.* **327:** 645–656

Scarpa M, Rigo A, Viglino P, Stevanato R, Bracco F & Battistin L (1987) Age dependence of the level of the enzymes involved in the protection against active oxygen species in the rat brain. *Proc. Soc. Exp. Biol. Med.* **185:** 129–133

Scherz-Shouval R, Shvets E, Fass E, Shorer H, Gil L & Elazar Z (2007) Reactive oxygen species are essential for autophagy and specifically regulate the activity of Atg4. *EMBO J.* **26:** 1749–1760

Scheufler C, Brinker A, Bourenkov G, Pegoraro S, Moroder L, Bartunik H, Hartl FU & Moarefi I (2000) Structure of TPR domain-peptide complexes: critical elements in the assembly of the Hsp70-Hsp90 multichaperone machine. *Cell* **101:** 199–210

Schmidt M, Hanna J, Elsasser S & Finley D (2005) Proteasome-associated proteins: regulation of a proteolytic machine. *Biol. Chem.* **386:** 725–737

Schmidt U, Wochnik GM, Rosenhagen MC, Young JC, Hartl FU, Holsboer F & Rein T (2003) Essential role of the unusual DNA-binding motif of BAG-1 for inhibition of the glucocorticoid receptor. *J. Biol. Chem.* 278: 4926–4931

Seo H, Sonntag K & Isacson O (2004) Generalized brain and skin proteasome inhibition in Huntington's disease. *Ann. Neurol.* **56:** 319–328

Sharon M, Taverner T, Ambroggio XI, Deshaies RJ & Robinson CV (2006) Structural organization of the 19S proteasome lid: insights from MS of intact complexes. *PLoS Biol.* **4:** e267

Shay JW & Wright WE (2000) Hayflick, his limit, and cellular ageing. *Nat. Rev. Mol. Cell Biol.* **1:** 72–76

Shibata M, Lu T, Furuya T, Degterev A, Mizushima N, Yoshimori T, MacDonald M, Yankner B & Yuan J (2006) Regulation of intracellular accumulation of mutant Huntingtin by Beclin 1. *J. Biol. Chem.* **281:** 14474–14485

Shimizu S, Kanaseki T, Mizushima N, Mizuta T, Arakawa-Kobayashi S, Thompson CB & Tsujimoto Y (2004) Role of Bcl-2 family proteins in a non-apoptotic programmed cell death dependent on autophagy genes. *Nat. Cell Biol.* **6:** 1221–1228

Shin Y, Klucken J, Patterson C, Hyman BT & McLean PJ (2005) The co-chaperone carboxyl terminus of Hsp70-interacting protein (CHIP) mediates alpha-synuclein degradation decisions between proteasomal and lysosomal pathways. *J. Biol. Chem.* **280:** 23727–23734

Simonsen A, Cumming RC, Brech A, Isakson P, Schubert DR & Finley KD (2008) Promoting basal levels of autophagy in the nervous system enhances longevity and oxidant resistance in adult Drosophila. *Autophagy* **4:** 176–184

Sohal RS & Weindruch R (1996) Oxidative stress, caloric restriction, and aging. *Science* **273:** 59–63

Sohal RS (2002) Oxidative stress hypothesis of aging. *Free Radic. Biol. Med.* **33:** 573–574

Sondermann H, Scheufler C, Schneider C, Hohfeld J, Hartl FU & Moarefi I (2001) Structure of a Bag/Hsc70 complex: convergent functional evolution of Hsp70 nucleotide exchange factors. *Science* **291:** 1553–1557

Soto C (2003) Unfolding the role of protein misfolding in neurodegenerative diseases. *Nat. Rev. Neurosci.* **4:** 49–60

Sowa ME & Harper JW (2006) From loops to chains: unraveling the mysteries of polyubiquitin chain specificity and processivity. *ACS Chem. Biol.* **1:** 20–24

Takayama S & Reed JC (2001) Molecular chaperone targeting and regulation by BAG family proteins. *Nat. Cell Biol.* **3:** E237-41

Takayama S, Sato T, Krajewski S, Kochel K, Irie S, Millan JA & Reed JC (1995) Cloning and functional analysis of BAG-1: a novel Bcl-2-binding protein with anti-cell death activity. *Cell* **80:** 279–284

Tan JMM, Wong ESP, Kirkpatrick DS, Pletnikova O, Ko HS, Tay S, Ho MWL, Troncoso J, Gygi SP, Lee MK, Dawson VL, Dawson TM & Lim K (2008) Lysine 63-linked ubiquitination promotes the formation and autophagic clearance of protein inclusions associated with neurodegenerative diseases. *Hum. Mol. Genet.* **17:** 431–439

Tang Y, Chang H, Hayer-Hartl M & Hartl FU (2007) SnapShot: molecular chaperones, Part II. *Cell* **128:** 412

Tan JMM, Wong ESP, Kirkpatrick DS, Pletnikova O, Ko HS, Tay S, Ho MWL, Troncoso J, Gygi SP, Lee MK, Dawson VL, Dawson TM & Lim K (2008) Lysine 63-linked ubiquitination promotes the formation and autophagic clearance of protein inclusions associated with neurodegenerative diseases. *Hum. Mol. Genet.* **17:** 431–439

Taylor JP, Hardy J & Fischbeck KH (2002) Toxic proteins in neurodegenerative disease. *Science* **296:** 1991–1995

Tenno T, Fujiwara K, Tochio H, Iwai K, Morita EH, Hayashi H, Murata S, Hiroaki H, Sato M, Tanaka K & Shirakawa M (2004) Structural basis for distinct roles of Lys63- and Lys48-linked polyubiquitin chains. *Genes Cells* **9:** 865–875

Thress K, Henzel W, Shillinglaw W & Kornbluth S (1998) Scythe: a novel reaper-binding apoptotic regulator. *EMBO J.* **17:** 6135–6143

Thress K, Song J, Morimoto RI & Kornbluth S (2001) Reversible inhibition of Hsp70 chaperone function by Scythe and Reaper. *EMBO J.* **20:** 1033–1041

Thrower JS, Hoffman L, Rechsteiner M & Pickart CM (2000) Recognition of the polyubiquitin proteolytic signal. *EMBO J.* **19:** 94–102

Touret N, Paroutis P & Grinstein S (2005) The nature of the phagosomal membrane: endoplasmic reticulum versus plasmalemma. *J. Leukoc. Biol.* **77:** 878–885

Troen BR (2003) The biology of aging. *Mt. Sinai J. Med.* **70:** 3–22

Tschopp J, Martinon F & Hofmann K (1999) Apoptosis: Silencing the death receptors. *Curr. Biol.* **9:** R381-4

Urushitani M, Kurisu J, Tsukita K & Takahashi R (2002) Proteasomal inhibition by misfolded mutant superoxide dismutase 1 induces selective motor neuron death in familial amyotrophic lateral sclerosis. *J. Neurochem.* **83:** 1030–1042

Uttenweiler A & Mayer A (2008) Microautophagy in the yeast Saccharomyces cerevisiae. *Methods Mol. Biol.* **445:** 245–259

Vabulas RM & Hartl FU (2005) Protein synthesis upon acute nutrient restriction relies on proteasome function. *Science* **310:** 1960–1963

Vainberg IE, Lewis SA, Rommelaere H, Ampe C, Vandekerckhove J, Klein HL & Cowan NJ (1998) Prefoldin, a chaperone that delivers unfolded proteins to cytosolic chaperonin. *Cell* **93:** 863–873

Varshavsky A (2000) Recent studies of the ubiquitin system and the N-end rule pathway. *Harvey Lect.* **96:** 93–116

Virador VM, Davidson B, Czechowicz J, Mai A, Kassis J & Kohn EC (2009) The anti-apoptotic activity of BAG3 is restricted by caspases and the proteasome. *PLoS ONE* **4:** e5136

Waelter S, Boeddrich A, Lurz R, Scherzinger E, Lueder G, Lehrach H & Wanker EE (2001) Accumulation of mutant huntingtin fragments in aggresome-like inclusion bodies as a result of insufficient protein degradation. *Mol. Biol. Cell* **12:** 1393–1407

Wang H, Liu H, Zhang H, Guan Y & Du Z (2008) Transcriptional upregulation of BAG3 upon proteasome inhibition. *Biochem. Biophys. Res. Commun.* **365:** 381–385

Wickens AP (2001) Ageing and the free radical theory. *Respiration physiology* **128:** 379–391

Wouters BG & Koritzinsky M (2008) Hypoxia signalling through mTOR and the unfolded protein response in cancer. *Nat. Rev. Cancer* **8:** 851–864

Wyttenbach A, Hands S, King MA, Lipkow K & Tolkovsky AM (2008) Amelioration of protein misfolding disease by rapamycin: translation or autophagy? *Autophagy* **4:** 542–545

Yamamoto A, Cremona ML & Rothman JE (2006) Autophagy-mediated clearance of huntingtin aggregates triggered by the insulin-signaling pathway. *J. Cell Biol.* **172:** 719–731

Yorimitsu T & Klionsky DJ (2005) Autophagy: molecular machinery for self-eating. *Cell Death Differ.* **12 Suppl 2:** 1542–1552

Yoshimura T, Kameyama K, Takagi T, Ikai A, Tokunaga F, Koide T, Tanahashi N, Tamura T, Cejka Z & Baumeister W (1993) Molecular characterization of the "26S" proteasome complex from rat liver. *J. Struct. Biol.* **111:** 200–211

Young ARJ, Narita M, Ferreira M, Kirschner K, Sadaie M, Darot JFJ, Tavaré S, Arakawa S, Shimizu S, Watt FM & Narita M (2009) Autophagy mediates the mitotic senescence transition. *Genes Dev.*

Zatloukal K, Stumptner C, Fuchsbichler A, Heid H, Schnoelzer M, Kenner L, Kleinert R, Prinz M, Aguzzi A & Denk H (2002) p62 Is a common component of cytoplasmic inclusions in protein aggregation diseases. *Am. J. Pathol.* **160:** 255–263

Zhang N, Tang Z & Liu C (2008) alpha-Synuclein protofibrils inhibit 26 S proteasome-mediated protein degradation: understanding the cytotoxicity of protein protofibrils in neurodegenerative disease pathogenesis. *J. Biol. Chem.* **283:** 20288–20298

Zhu Q, Wani G, Wang QE, El-mahdy M, Snapka RM & Wani AA (2005) Deubiquitination by proteasome is coordinated with substrate translocation for proteolysis in vivo. *Exp Cell Res* **307:** 436–451

G APPENDIX

G.1 Publications

Gamerdinger M, Hajieva P, Kaya AM, Wolfrum U, Hartl FU & Behl C (2009) Protein quality control during aging involves recruitment of the macroautophagy pathway by BAG3. *EMBO J.* **28**: 889-901

Gamerdinger M, Clement AB & Behl C (2008) Effects of sulindac sulfide on the membrane architecture and the activity of gamma-secretase. *Neuropharmacology* **54**: 998–1005

Gamerdinger M, Clement AB & Behl C (2007) Cholesterol-like effects of selective cyclooxygenase inhibitors and fibrates on cellular membranes and amyloid-beta production. *Mol. Pharmacol.* **72**: 141–151

Kuhlmann CRW, Tamaki R, **Gamerdinger M**, Lessmann V, Behl C, Kempski OS & Luhmann HJ (2007) Inhibition of the myosin light chain kinase prevents hypoxia-induced blood-brain barrier disruption. *J. Neurochem.* **102**: 501–507

Gamerdinger M, Manthey D & Behl C (2006) Oestrogen receptor subtype-specific repression of calpain expression and calpain enzymatic activity in neuronal cells--implications for neuroprotection against Ca^{2+}-mediated excitotoxicity. *J. Neurochem.* **97**: 57–68

G.2 Meeting Abstracts

Gamerdinger M, Hajieva P & Behl C (2009) A switch from BAG1 to BAG3 during ageing triggers the enhanced use of the autophagic-lysosomal system for the degradation of polyubiquitinated proteins. Experimental Biology 2009, APR 18-22, 2009 New Orleans, Louisiana, USA. *FASEB J*. **23**: 668.1

Gamerdinger M, Clement AM & Behl C (2007) Lipid-ordering effects of celecoxib and fenofibrate in cellular membranes may contribute to enhanced amyloid-β production. 37th annual meeting of the Society for Neuroscience (SfN), NOV 03-07, 2007 San Diego, California, USA.

Manthey D, **Gamerdinger M** & Behl C (2005) Estrogen mediates neuroprotection via estrogen receptor α, not beta, in a neuronal in vitro model. 24th Symposium of the Arbeitsgemeinschaft-fur-Neuropsychopharmakologie-und-Pharmakopsychiatrie (AGNP), OCT 05-08, 2005 Munich Germany. *Pharmacopsychiatry* **38**: 263-263

Gamerdinger M, Manthey D & Behl C (2005) Estrogen receptor subtype-specific repression of calpain-activation in neuronal cells. 24th Symposium of the Arbeitsgemeinschaft-fur-Neuropsychopharmakologie-und-Pharmakopsychiatrie (AGNP), Date: OCT 05-08, 2005 Munich Germany. *Pharmacopsychiatry* **38**: 242-242

G.3 Abbreviations

AD	Alzheimer's disease
ADP	Adenosine di-phosphate
ALS	Amyotrophic lateral sclerosis
AMC	Amino-4-methyl coumarin
AIF	Apoptosis inducing factor
Atg	Autophagy-related gene
ATP	Adenosine tri-phosphate
ATPase	Adenosine tri-phosphatase
BafA1	Bafilomycin A1
BAG	Bcl-2-associated athanogene
BAG3-N1	pBAG3-N1 (BAG3 expression plasmid)
BAT3	HLA-B-associated transcript 3
CAIR-1	Carboxyamido-triazole-stressed-1
CER	Cerebellum
CHIP	C-terminal Hsc70-interacting protein
CMA	Chaperone-mediated autophagy
CNS	Central nervous system
Co-IP	Co-immunoprecipitation
Ctrl	Control
CTX	Cortex
d2HEK	HEK293 cell line stably transfected with d2GFP
DAPI	4',6-diamidino-2-phenylindole
DMEM	Dulbecco's Modified Eagle's Medium
DMSO	Dimethyl sulfoxide
DR3	Death receptor 3
EGFP	Enhanced green fluorescent protein
eIF2α	Eukaryotic initiation factor-2α
ER	Endoplasmic reticulum
FTDP-17	Frontotemporal dementia with parkinsonism linked to chromosome 17
GFP	Green fluorescent protein
GLT1	Glial glutamate transporter 1
GR	Glucocorticoid receptor
HBSS	Hanks' balanced salt solution
HEK	Human embryonic kidney
HIP	Hippocampus
Hip	Hsc70/Hsp70-interacting protein

Hop	Hsp70/Hsp90 organizing protein
Hsc70	70-kilodalton heat shock cognate protein
HSF1	Heat shock factor 1
Hsp70	70-kilodalton heat shock protein
IP	Immunoprecipitation
kDa	kilodalton
LAMP2A	Lysosome associate membrane protein type 2A
LC3	Microtubule-associated protein 1 light chain 3
Leu	Leupeptin
LIR	LC3-interacting region
lyHsc73	lysosomal 73-kilodalton heat shock cognate protein
MB	Midbrain
mRNA	Messenger ribonucleic acid
ms	mouse
mTOR	Mammalian target of rapamycin
N1	p-N1 (empty control plasmid)
NAC	Nascent polypeptide-associated complex
NBR1	Neighbor of BRCA1 gene 1
NEF	Nucleotide exchange factors
NeuN	Neuron-specific nuclear protein
nons	nonsense
PB1	Phox and Bem1p
PCR	Polymerase chain reaction
PD	Parkinson’s disease
PE	Phosphatidylethanolamine
Pep.A	Pepstatin A
PLC	Phospholipase C
polyUb	Polyubiquitinated proteins
polyQ	Polyglutamine
PQC	Protein quality control
PXXP	Proline rich domain
rb	rabbit
RFP	Red fluorescent protein
RNA	Ribonucleic acid
ROS	Reactive oxygen species
SDS-PAGE	SDS-polyacrylamide gel electrophoresis
siRNA	Small interfering RNA
SEM	Standard error of the mean

SH3	Src Homology 3
SOD1	Superoxide dismutase 1
SODD	Silencer of death domains
SQSTM1	Sequestosome-1
TDP-43	TAR DNA-binding Protein 43
TEM	Transmission electron microscopy
TNF	Tumour necrosis factor
TPR	Tetra tricopeptide repeat
TX-100	Triton X-100
UBA	Ubiquitin-associated
UBL	Ubiquitin-like
UBQLN1	Ubiquilin 1
UFD	Ubiquitin-fusion degradation
WIPI1	WD40 repeat protein interacting with phosphoinositides 1
ZnF	Zinc finger

G.4 Maps and sequences of constructed plasmids

G.4.1.1 Map of pBAG3-N1

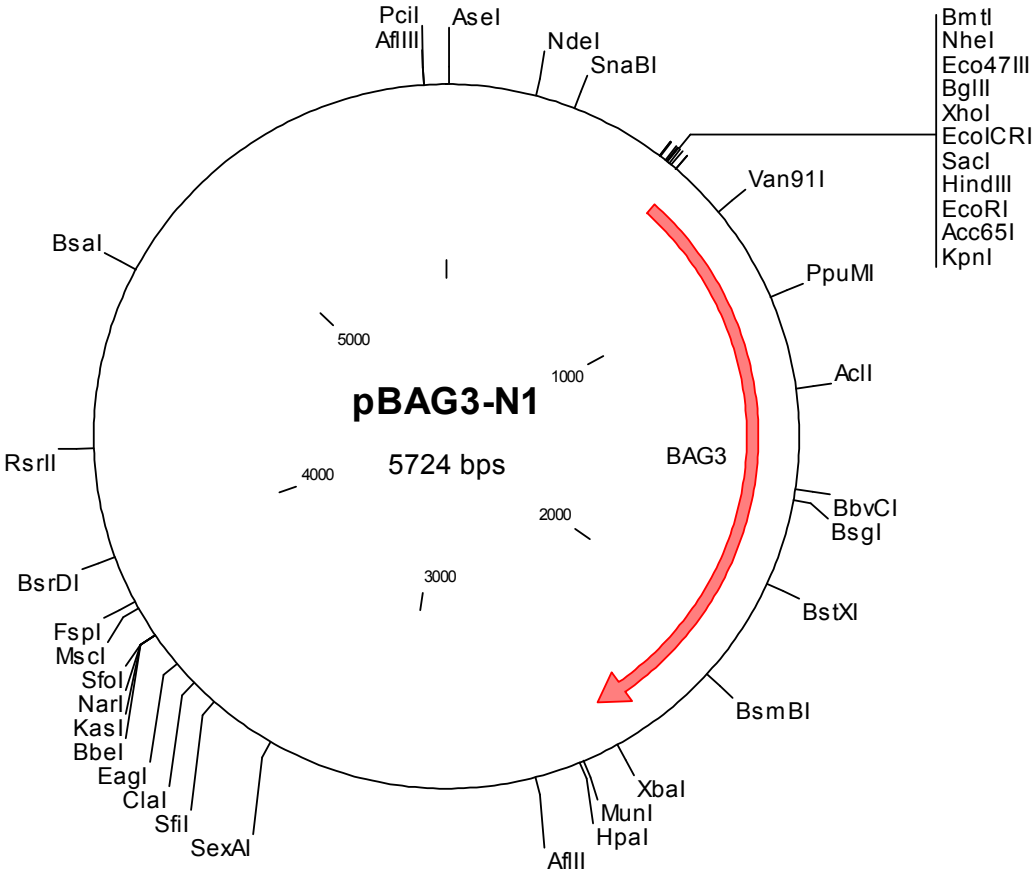

G.4.1.2 Sequence of pBAG3-N1

```
   1  tagttattaa tagtaatcaa ttacggggtc attagttcat agcccatata tggagttccg
  61  cgttacataa cttacggtaa atggcccgcc tggctgaccg cccaacgacc cccgcccatt
 121  gacgtcaata atgacgtatg ttcccatagt aacgccaata gggactttcc attgacgtca
 181  atgggtggag tatttacggt aaactgccca cttggcagta catcaagtgt atcatatgcc
 241  aagtacgccc cctattgacg tcaatgacgg taaatggccc gcctggcatt atgcccagta
 301  catgacctta tgggactttc ctacttggca gtacatctac gtattagtca tcgctattac
 361  catggtgatg cggttttggc agtacatcaa tgggcgtgga tagcggtttg actcacgggg
 421  atttccaagt ctccacccca ttgacgtcaa tgggagtttg ttttggcacc aaaatcaacg
 481  ggactttcca aaatgtcgta acaactccgc cccattgacg caaatgggcg gtaggcgtgt
 541  acggtgggag gtctatataa gcagagctgg tttagtgaac cgtcagatcc gctagcgcta
 601  ccggactcag atctcgagct caagcttcga attctgcagt cgacggtacc gcgggcccgg
 661  gatcatgagc gccgccaccc actcgcccat gatgcaggtg gcgtccggca acggtgaccg
 721  cgacccttg ccccccggat gggagatcaa gatcgacccg cagaccggct ggcccttctt
 781  cgtggaccac aacagccgca ccactacgtg gaacgacccg cgcgtgccct ctgagggccc
```

```
 841  caaggagact ccatcctctg ccaatggccc ttcccgggag ggctctaggc tgccgcctgc
 901  tagggaaggc caccctgtgt acccccagct ccgaccaggc tacattccca ttcctgtgct
 961  ccatgaaggc gctgagaacc ggcaggtgca ccctttccat gtctatcccc agcctgggat
1021  gcagcgattc cgaactgagg cggcagcagc ggctcctcag aggtcccagt cacctctgcg
1081  gggcatgcca gaaaccactc agccagataa acagtgtgga caggtggcag cggcggcggc
1141  agcccagccc ccagcctccc acggacctga gcggtcccag tctccagctg cctctgactg
1201  ctcatcctca tcctcctcgg ccagcctgcc ttcctccggc aggagcagcc tgggcagtca
1261  ccagctcccg cgggggtaca tctccattcc ggtgatacac gagcagaacg ttacccggcc
1321  agcagcccag ccctccttcc accaagccca gaagacgcac tacccagcgc agcaggggga
1381  gtaccagacc caccagcctg tgtaccacaa gatccagggg gatgactggg agccccggcc
1441  cctgcgggcg gcatccccgt tcaggtcatc tgtccagggt gcatcgagcc gggagggctc
1501  accagccagg agcagcacgc cactccactc cccctcgccc atccgtgtgc acaccgtggt
1561  cgacaggcct cagcagccca tgacccatcg agaaactgca cctgtttccc agcctgaaaa
1621  caaaccagaa agtaagccag gcccagttgg accagaactc cctcctggac acatcccaat
1681  tcaagtgatc cgcaaagagg tggattctaa acctgtttcc cagaagcccc cacctccctc
1741  tgagaaggta gaggtgaaag ttccccctgc tccagttcct tgtcctcctc ccagccctgg
1801  cccttctgct gtcccctctt cccccaagag tgtggctaca gaagagaggg cagcccccag
1861  cactgcccct gcagaagcta cacctccaaa accaggagaa gccgaggctc ccccaaaaca
1921  tccaggagtg ctgaaagtgg aagccatcct ggagaaggtg caggggctgg agcaggctgt
1981  agacaacttt gaaggcaaga agactgacaa aaagtacctg atgatcgaag agtatttgac
2041  caaagagctg ctggccctgg attcagtgga ccccgaggga cgagccgatg tgcgtcaggc
2101  caggagagac ggtgtcagga aggttcagac catcttggaa aaacttgaac agaaagccat
2161  tgatgtccca ggtcaagtcc aggtctatga actccagccc agcaaccttg aagcagatca
2221  gccactgcag gcaatcatgg agatgggtgc cgtggcagca gacaagggca agaaaaatgc
2281  tggaaatgca gaagatcccc acacagaaac ccagcagcca gaagccacag cagcagcgac
2341  ttcaaacccc agcagcatga cagacacccc tggtaaccca gcagcaccgt agggccgcga
2401  ctctagatca taatcagcca taccacattt gtagaggttt tacttgcttt aaaaaacctc
2461  ccacacctcc ccctgaacct gaaacataaa atgaatgcaa ttgttgttgt taacttgttt
2521  attgcagctt ataatggtta caaataaagc aatagcatca caaatttcac aaataaagca
2581  ttttttttcac tgcattctag ttgtggtttg tccaaactca tcaatgtatc ttaaggcgta
2641  aattgtaagc gttaatattt tgttaaaatt cgcgttaaat ttttgttaaa tcagctcatt
2701  ttttaaccaa taggccgaaa tcggcaaaat cccttataaa tcaaaagaat agaccgagat
2761  agggttgagt gttgttccag tttggaacaa gagtccacta ttaaagaacg tggactccaa
2821  cgtcaaaggg cgaaaaaccg tctatcaggg cgatggccca ctacgtgaac catcacccta
2881  atcaagtttt ttggggtcga ggtgccgtaa agcactaaat cggaacccta aagggagccc
2941  ccgatttaga gcttgacggg gaaagccggc gaacgtggcg agaaaggaag ggaagaaagc
3001  gaaaggagcg ggcgctaggg cgctggcaag tgtagcggtc acgctgcgcg taaccaccac
3061  acccgccgcg cttaatgcgc cgctacaggg cgcgtcaggt ggcacttttc ggggaaatgt
3121  gcgcggaacc cctatttgtt tatttttcta aatacattca aatatgtatc cgctcatgag
3181  acaataaccc tgataaatgc ttcaataata ttgaaaaagg aagagtcctg aggcggaaag
3241  aaccagctgt ggaatgtgtg tcagttaggg tgtggaaagt ccccaggctc cccagcaggc
3301  agaagtatgc aaagcatgca tctcaattag tcagcaacca ggtgtggaaa gtccccaggc
3361  tccccagcag gcagaagtat gcaaagcatg catctcaatt agtcagcaac catagtcccg
3421  cccctaactc cgcccatccc gcccctaact ccgcccagtt ccgcccattc tccgccccat
3481  ggctgactaa ttttttttat ttatgcagag gccgaggccg cctcggcctc tgagctattc
3541  cagaagtagt gaggaggctt ttttggaggc ctaggctttt gcaaagatcg atcaagagac
3601  aggatgagga tcgtttcgca tgattgaaca agatggattg cacgcaggtt ctccggccgc
3661  ttgggtggag aggctattcg gctatgactg ggcacaacag acaatcggct gctctgatgc
3721  cgccgtgttc cggctgtcag cgcaggggcg cccggttctt tttgtcaaga ccgacctgtc
3781  cggtgccctg aatgaactgc aagacgaggc agcgcggcta tcgtggctgg ccacgacggg
3841  cgttccttgc gcagctgtgc tcgacgttgt cactgaagcg ggaagggact ggctgctatt
3901  gggcgaagtg ccggggcagg atctcctgtc atctcacctt gctcctgccg agaaagtatc
3961  catcatggct gatgcaatgc ggcggctgca tacgcttgat ccggctacct gcccattcga
4021  ccaccaagcg aaacatcgca tcgagcgagc acgtactcgg atggaagccg gtcttgtcga
4081  tcaggatgat ctggacgaag agcatcaggg gctcgcgcca gccgaactgt tcgccaggct
4141  caaggcgagc atgcccgacg gcgaggatct cgtcgtgacc catggcgatg cctgcttgcc
4201  gaatatcatg gtggaaaatg gccgcttttc tggattcatc gactgtggcc ggctgggtgt
4261  ggcggaccgc tatcaggaca tagcgttggc tacccgtgat attgctgaag agcttggcgg
4321  cgaatgggct gaccgcttcc tcgtgcttta cggtatcgcc gctcccgatt cgcagcgcat
4381  cgccttctat cgccttcttg acgagttctt ctgagcggga ctctggggtt cgaaatgacc
4441  gaccaagcga cgcccaacct gccatcacga gatttcgatt ccaccgccgc cttctatgaa
4501  aggttgggct tcggaatcgt tttccgggac gccggctgga tgatcctcca gcgcggggat
4561  ctcatgctgg agttcttcgc ccaccctagg gggaggctaa ctgaaacacg gaaggagaca
```

```
4621  ataccggaag gaacccgcgc tatgacggca ataaaaagac agaataaaac gcacggtgtt
4681  gggtcgtttg ttcataaacg cggggttcgg tcccagggct ggcactctgt cgatacccca
4741  ccgagacccc attggggcca atacgcccgc gtttcttcct ttccccacc ccaccccca
4801  agttcgggtg aaggcccagg gctcgcagcc aacgtcgggg cggcaggccc tgccatagcc
4861  tcaggttact catatatact ttagattgat ttaaaacttc atttttaatt taaaaggatc
4921  taggtgaaga tccttttga taatctcatg accaaaatcc cttaacgtga gttttcgttc
4981  cactgagcgt cagaccccgt agaaaagatc aaaggatctt cttgagatcc ttttttctg
5041  cgcgtaatct gctgcttgca aacaaaaaaa ccaccgctac cagcggtggt ttgtttgccg
5101  gatcaagagc taccaactct ttttccgaag gtaactggct tcagcagagc gcagatacca
5161  aatactgtcc ttctagtgta gccgtagtta ggccaccact tcaagaactc tgtagcaccg
5221  cctacatacc tcgctctgct aatcctgtta ccagtggctg ctgccagtgg cgataagtcg
5281  tgtcttaccg ggttggactc aagacgatag ttaccggata aggcgcagcg gtcgggctga
5341  acgggggggtt cgtgcacaca gcccagcttg gagcgaacga cctacaccga actgagatac
5401  ctacagcgtg agctatgaga aagcgccacg cttcccgaag ggagaaaggc ggacaggtat
5461  ccggtaagcg gcagggtcgg aacaggagag cgcacgaggg agcttccagg gggaaacgcc
5521  tggtatcttt atagtcctgt cgggtttcgc cacctctgac ttgagcgtcg atttttgtga
5581  tgctcgtcag gggggcggag cctatggaaa aacgccagca acgcggcctt tttacggttc
5641  ctggcctttt gctggccttt tgctcacatg ttctttcctg cgttatcccc tgattctgtg
5701  gataaccgta ttaccgccat gcat
```

G.4.2.1 Map of pBAG3.EGFP-N1

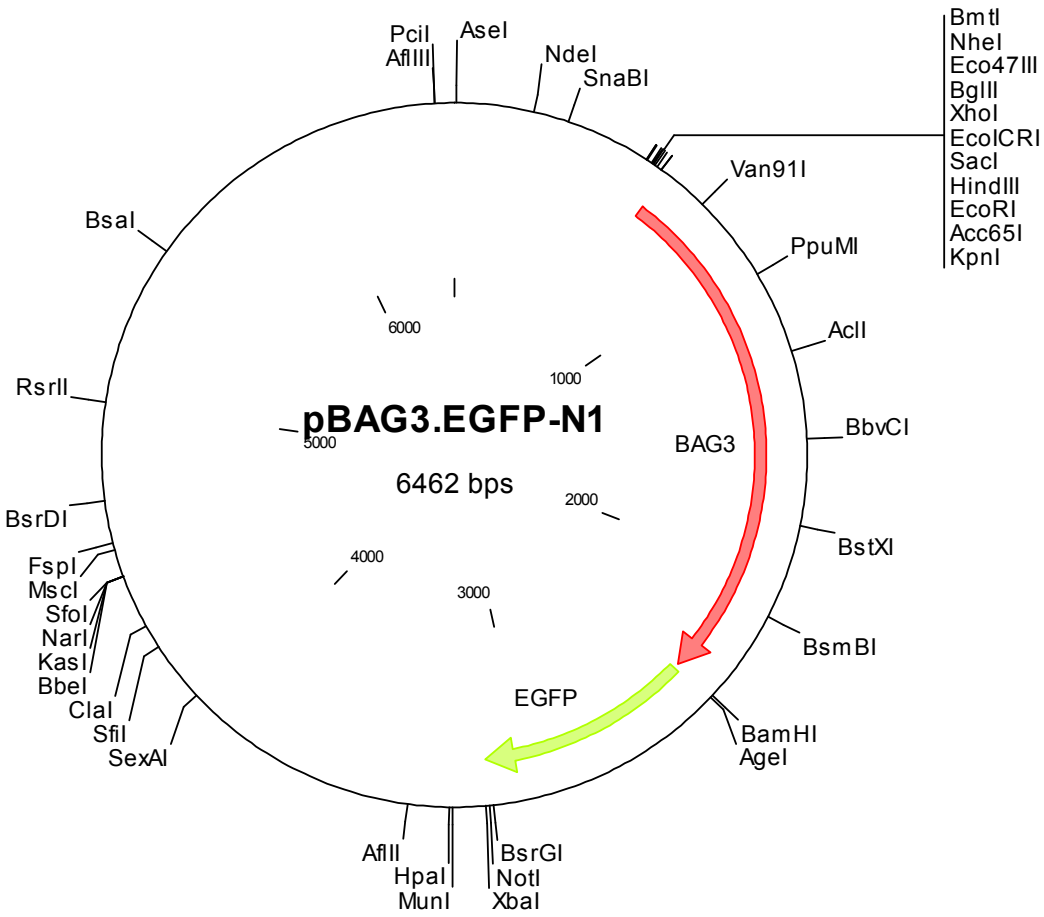

G.4.2.2 Sequence of pBAG3.EGFP-N1

```
   1  tagttattaa tagtaatcaa ttacggggtc attagttcat agcccatata tggagttccg
  61  cgttacataa cttacggtaa atggcccgcc tggctgaccg cccaacgacc cccgcccatt
 121  gacgtcaata atgacgtatg ttcccatagt aacgccaata gggactttcc attgacgtca
 181  atgggtggag tatttacggt aaactgccca cttggcagta catcaagtgt atcatatgcc
 241  aagtacgccc cctattgacg tcaatgacgg taaatggccc gcctggcatt atgcccagta
 301  catgacctta tgggactttc ctacttggca gtacatctac gtattagtca tcgctattac
 361  catggtgatg cggttttggc agtacatcaa tgggcgtgga tagcggtttg actcacgggg
 421  atttccaagt ctccacccca ttgacgtcaa tgggagtttg ttttggcacc aaaatcaacg
 481  ggactttcca aaatgtcgta acaactccgc cccattgacg caaatgggcg gtaggcgtgt
 541  acggtgggag gtctatataa gcagagctgg tttagtgaac cgtcagatcc gctagcgcta
 601  ccggactcag atctcgagct caagcttcga attctgcagt cgacggtacc gcgggcccgg
 661  gatcatgagc gccgccaccc actcgcccat gatgcaggtg gcgtccggca acggtgaccg
 721  cgacccttg ccccccggat gggagatcaa gatcgacccg cagaccggct ggcccttctt
 781  cgtggaccac aacagccgca ccactacgtg gaacgacccg cgcgtgccct ctgagggccc
 841  caaggagact ccatcctctg ccaatggccc ttcccgggag ggctctaggc tgccgcctgc
 901  tagggaaggc caccctgtgt acccccagct ccgaccaggc tacattccca ttcctgtgct
 961  ccatgaaggc gctgagaacc ggcaggtgca ccctttccat gtctatcccc agcctgggat
1021  gcagcgattc cgaactgagg cggcagcagc ggctcctcag aggtcccagt cacctctgcg
1081  gggcatgcca gaaaccactc agccagataa acagtgtgga caggtggcag cggcggcggc
1141  agcccagccc ccagcctccc acggacctga gcggtcccag tctccagctg cctctgactg
1201  ctcatcctca tcctcctcgg ccagcctgcc ttcctccggc aggagcagcc tgggcagtca
1261  ccagctcccg cgggggtaca tctccattcc ggtgatacac gagcagaacg ttacccggcc
1321  agcagcccag ccctccttcc accaagccca gaagacgcac tacccagcgc agcaggggga
1381  gtaccagacc caccagcctg tgtaccacaa gatccagggg gatgactggg agccccggcc
1441  cctgcgggcg gcatccccgt tcaggtcatc tgtccagggt gcatcgagcc gggagggctc
1501  accagccagg agcagcacgc cactccactc cccctcgccc atccgtgtgc acaccgtggt
1561  cgacaggcct cagcagccca tgacccatcg agaaactgca cctgtttccc agcctgaaaa
1621  caaaccagaa agtaagccag gcccagttgg accagaactc cctcctggac acatcccaat
1681  tcaagtgatc cgcaaagagg tggattctaa acctgtttcc cagaagcccc cacctccctc
1741  tgagaaggta gaggtgaaag ttccccctgc tccagttcct tgtcctcctc ccagccctgg
1801  cccttctgct gtcccctctt cccccaagag tgtggctaca gaagagaggg cagcccccag
1861  cactgccccc gcagaagcta cacctccaaa accaggagaa gccgaggctc ccccaaaaca
1921  tccaggagtg ctgaaagtgg aagccatcct ggagaaggta caggggctgg agcaggctgt
1981  agacaacttt gaaggcaaga agactgacaa aaagtacctg atgatcgaag agtatttgac
2041  caaagagctg ctggccctgg attcagtgga ccccgaggga cgagccgatg tgcgtcaggc
2101  caggagagac ggtgtcagga aggttcagac catcttggaa aaacttgaac agaaagccat
2161  tgatgtccca ggtcaagtcc aggtctatga actccagccc agcaaccttg aagcagatca
2221  gccactgcag gcaatcatgg agatgggtgc cgtggcagca gacaagggca agaaaaatgc
2281  tggaaatgca gaagatcccc acacagaaac ccagcagcca gaagccacag cagcagcgac
2341  ttcaaacccc agcagcatga cagacacccc tggtaaccca gcagcaccgg atccaccggt
2401  cgccaccatg gtgagcaagg gcgaggagct gttcaccggg gtggtgccca tcctggtcga
2461  gctggacggc gacgtaaacg gccacaagtt cagcgtgtcc ggcgagggcg agggcgatgc
2521  cacctacggc aagctgaccc tgaagttcat ctgcaccacc ggcaagctgc ccgtgccctg
2581  gcccaccctc gtgaccaccc tgacctacgg cgtgcagtgc ttcagccgct accccgacca
2641  catgaagcag cacgacttct tcaagtccgc catgcccgaa ggctacgtcc aggagcgcac
2701  catcttcttc aaggacgacg gcaactacaa gacccgcgcc gaggtgaagt tcgagggcga
2761  caccctggtg aaccgcatcg agctgaaggg catcgacttc aaggaggacg gcaacatcct
2821  ggggcacaag ctggagtaca actacaacag ccacaacgtc tatatcatgg ccgacaagca
2881  gaagaacggc atcaaggtga acttcaagat ccgccacaac atcgaggacg gcagcgtgca
2941  gctcgccgac cactaccagc agaacacccc catcggcgac ggccccgtgc tgctgcccga
3001  caaccactac ctgagcaccc agtccgccct gagcaaagac cccaacgaga agcgcgatca
3061  catggtcctg ctggagttcg tgaccgccgc cgggatcact ctcggcatgg acgagctgta
3121  caagtaaagc ggccgcgact ctagatcata atcagccata ccacatttgt agaggtttta
3181  cttgctttaa aaaacctccc acacctcccc ctgaacctga aacataaaat gaatgcaatt
3241  gttgttgtta acttgtttat tgcagcttat aatggttaca aataaagcaa tagcatcaca
3301  aatttcacaa ataaagcatt tttttcactg cattctagtt gtggtttgtc caaactcatc
3361  aatgtatctt aaggcgtaaa ttgtaagcgt taatattttg ttaaaattcg cgttaaattt
3421  ttgttaaatc agctcatttt ttaaccaata ggccgaaatc ggcaaaatcc cttataaatc
3481  aaaagaatag accgagatag ggttgagtgt tgttccagtt tggaacaaga gtccactatt
3541  aaagaacgtg gactccaacg tcaaagggcg aaaaaccgtc tatcagggcg atggcccact
```

```
3601  acgtgaacca tcaccctaat caagtttttt ggggtcgagg tgccgtaaag cactaaatcg
3661  gaaccctaaa gggagccccc gatttagagc ttgacgggga aagccggcga acgtggcgag
3721  aaaggaaggg aagaaagcga aaggagcggg cgctagggcg ctggcaagtg tagcggtcac
3781  gctgcgcgta accaccacac ccgccgcgct taatgcgccg ctacagggcg cgtcaggtgg
3841  cacttttcgg ggaaatgtgc gcggaacccc tatttgttta tttttctaaa tacattcaaa
3901  tatgtatccg ctcatgagac aataaccctg ataaatgctt caataatatt gaaaaaggaa
3961  gagtcctgag gcggaaagaa ccagctgtgg aatgtgtgtc agttagggtg tggaaagtcc
4021  ccaggctccc cagcaggcag aagtatgcaa agcatgcatc tcaattagtc agcaaccagg
4081  tgtggaaagt ccccaggctc cccagcaggc agaagtatgc aaagcatgca tctcaattag
4141  tcagcaacca tagtcccgcc cctaactccg cccatcccgc ccctaactcc gcccagttcc
4201  gcccattctc cgccccatgg ctgactaatt ttttttattt atgcagaggc cgaggccgcc
4261  tcggcctctg agctattcca gaagtagtga ggaggctttt ttggaggcct aggcttttgc
4321  aaagatcgat caagagacag gatgaggatc gtttcgcatg attgaacaag atggattgca
4381  cgcaggttct ccggccgctt gggtggagag gctattcggc tatgactggg cacaacagac
4441  aatcggctgc tctgatgccg ccgtgttccg gctgtcagcg caggggcgcc cggttctttt
4501  tgtcaagacc gacctgtccg gtgccctgaa tgaactgcaa gacgaggcag cgcggctatc
4561  gtggctggcc acgacgggcg ttccttgcgc agctgtgctc gacgttgtca ctgaagcggg
4621  aagggactgg ctgctattgg gcgaagtgcc ggggcaggat ctcctgtcat ctcaccttgc
4681  tcctgccgag aaagtatcca tcatggctga tgcaatgcgg cggctgcata cgcttgatcc
4741  ggctacctgc ccattcgacc accaagcgaa acatcgcatc gagcgagcac gtactcggat
4801  ggaagccggt cttgtcgatc aggatgatct ggacgaagag catcaggggc tcgcgccagc
4861  cgaactgttc gccaggctca aggcgagcat gcccgacggc gaggatctcg tcgtgaccca
4921  tggcgatgcc tgcttgccga atatcatggt ggaaaatggc cgcttttctg gattcatcga
4981  ctgtggccgg ctgggtgtgg cggaccgcta tcaggacata gcgttggcta cccgtgatat
5041  tgctgaagag cttggcggcg aatgggctga ccgcttcctc gtgctttacg gtatcgccgc
5101  tcccgattcg cagcgcatcg ccttctatcg ccttcttgac gagttcttct gagcgggact
5161  ctggggttcg aaatgaccga ccaagcgacg cccaacctgc catcacgaga tttcgattcc
5221  accgccgcct tctatgaaag gttgggcttc ggaatcgttt tccgggacgc cggctggatg
5281  atcctccagc gcggggatct catgctggag ttcttcgccc accctagggg gaggctaact
5341  gaaacacgga aggagacaat accggaagga acccgcgcta tgacggcaat aaaaagacag
5401  aataaaacgc acggtgttgg gtcgtttgtt cataaacgcg gggttcggtc ccagggctgg
5461  cactctgtcg ataccccacc gagaccccat tggggccaat acgcccgcgt ttcttccttt
5521  tccccacccc acccccccaag ttcgggtgaa ggcccagggc tcgcagccaa cgtcggggcg
5581  gcaggccctg ccatagcctc aggttactca tatatacttt agattgattt aaaacttcat
5641  ttttaattta aaaggatcta ggtgaagatc ctttttgata atctcatgac caaaatccct
5701  taacgtgagt tttcgttcca ctgagcgtca gaccccgtag aaaagatcaa aggatcttct
5761  tgagatcctt tttttctgcg cgtaatctgc tgcttgcaaa caaaaaaacc accgctacca
5821  gcggtggttt gtttgccgga tcaagagcta ccaactcttt ttccgaaggt aactggcttc
5881  agcagagcgc agataccaaa tactgtcctt ctagtgtagc cgtagttagg ccaccacttc
5941  aagaactctg tagcaccgcc tacatacctc gctctgctaa tcctgttacc agtggctgct
6001  gccagtggcg ataagtcgtg tcttaccggg ttggactcaa gacgatagtt accggataag
6061  gcgcagcggt cgggctgaac gggggttcg tgcacacagc ccagcttgga gcgaacgacc
6121  tacaccgaac tgagatacct acagcgtgag ctatgagaaa gcgccacgct tcccgaaggg
6181  agaaaggcgg acaggtatcc ggtaagcggc agggtcggaa caggagagcg cacgagggag
6241  cttccagggg gaaacgcctg gtatctttat agtcctgtcg ggtttcgcca cctctgactt
6301  gagcgtcgat ttttgtgatg ctcgtcaggg gggcggagcc tatggaaaaa cgccagcaac
6361  gcggcctttt tacggttcct ggccttttgc tggccttttg ctcacatgtt ctttcctgcg
6421  ttatcccctg attctgtgga taaccgtatt accgccatgc at
```

G.4.3.1 Map of p25QHtt.EGFP-N1

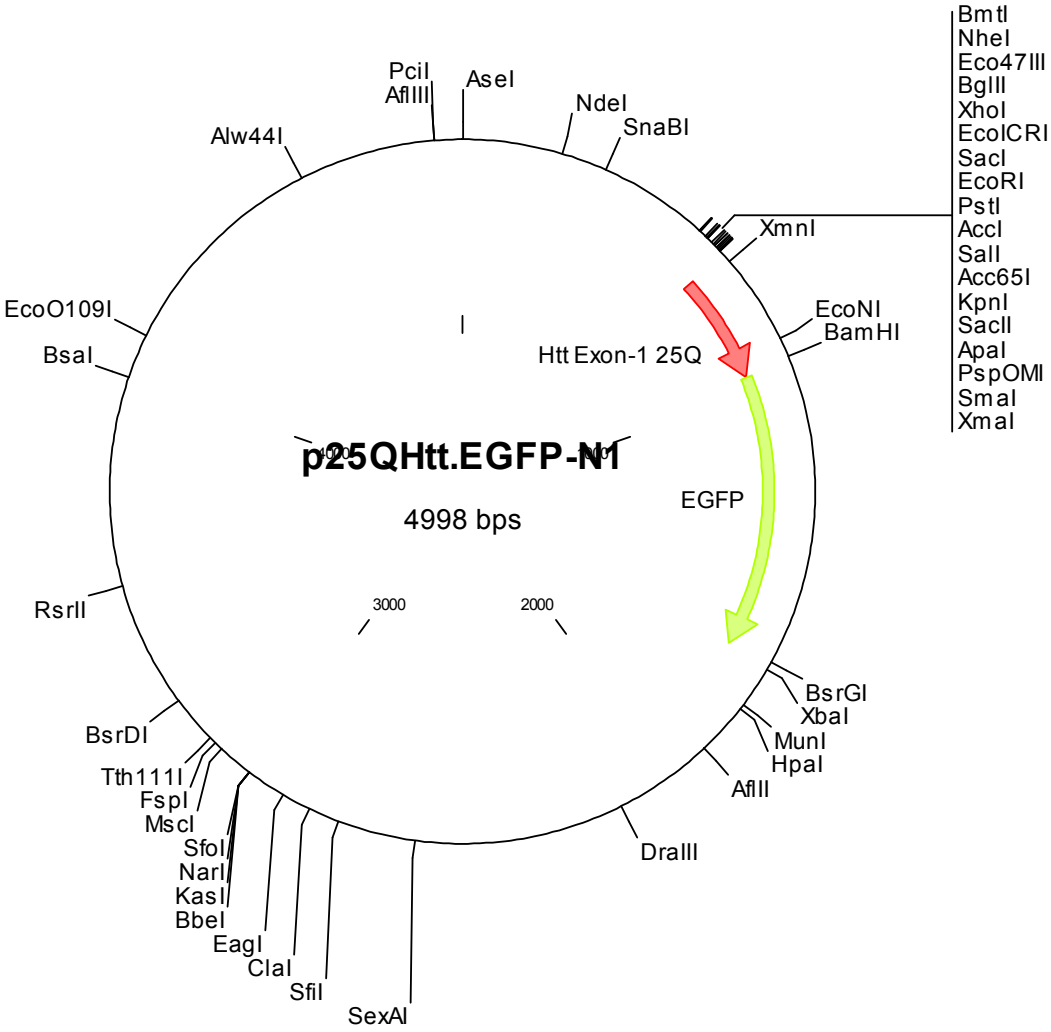

G.4.3.2 Sequence of p25QHtt.EGFP-N1

```
   1  attaatagta atcaattacg gggtcattag ttcatagccc atatatggag ttccgcgtta
  61  cataacttac ggtaaatggc ccgcctggct gaccgcccaa cgacccccgc ccattgacgt
 121  caataatgac gtatgttccc atagtaacgc caatagggac tttccattga cgtcaatggg
 181  tggagtattt acggtaaact gcccacttgg cagtacatca agtgtatcat atgccaagta
 241  cgcccccta tgacgtcaat gacggtaaat ggcccgcctg gcattatgcc cagtacatga
 301  ccttatggga ctttcctact tggcagtaca tctacgtatt agtcatcgct attaccatgg
 361  tgatgcggtt ttggcagtac atcaatgggc gtggatagcg gtttgactca cggggatttc
 421  caagtctcca ccccattgac gtcaatggga gtttgttttg gcaccaaaat caacgggact
 481  ttccaaaatg tcgtaacaac tccgccccat tgacgcaaat gggcggtagg cgtgtacggt
 541  gggaggtcta tataagcaga gctggtttag tgaaccgtca gatccgctag cgctaccgga
 601  ctcagatctc gagctcaagc ttcgaattct gcagtcgacg gtaccgcggg cccgggatca
 661  tggcgaccct ggaaaagctg atgaaggcct tcgagtccct caaaagcttc caacagcagc
 721  aacagcaaca acagcagcaa cagcaacaac agcagcaaca gcaacaacag cagcaacagc
 781  aacaaccgcc accacctccc cctccacccc cacctcctca acttcctcaa cctcctccac
 841  aggcacagcc tctgctgcct cagccacaac ctcctccacc tccacctcca cctcctccag
 901  gcccagctgt ggctgaggag cctctgcacc gacctggatc cctggtgagc aagggcgagg
 961  agctgttcac cggggtggtg cccatcctgg tcgagctgga cggcgacgta aacggccaca
1021  agttcagcgt gtccggcgag ggcgagggcg atgccaccta cggcaagctg accctgaagt
1081  tcatctgcac caccggcaag ctgcccgtgc cctggcccac cctcgtgacc accctgacct
```

```
1141  acggcgtgca gtgcttcagc cgctaccccg accacatgaa gcagcacgac ttcttcaagt
1201  ccgccatgcc cgaaggctac gtccaggagc gcaccatctt cttcaaggac gacggcaact
1261  acaagacccg cgccgaggtg aagttcgagg gcgacaccct ggtgaaccgc atcgagctga
1321  agggcatcga cttcaaggag gacggcaaca tcctggggca caagctggag tacaactaca
1381  acagccacaa cgtctatatc atggccgaca agcagaagaa cggcatcaag gtgaacttca
1441  agatccgcca caacatcgag gacggcagcg tgcagctcgc cgaccactac cagcagaaca
1501  cccccatcgg cgacggcccc gtgctgctgc ccgacaacca ctacctgagc acccagtccg
1561  ccctgagcaa agaccccaac gagaagcgcg atcacatggt cctgctggag ttcgtgaccg
1621  ccgccgggat cactctcggc atggacgagc tgtacaagta aggccgcgac tctagatcat
1681  aatcagccat accacatttg tagaggtttt acttgcttta aaaaacctcc cacacctccc
1741  cctgaacctg aaacataaaa tgaatgcaat tgttgttgtt aacttgttta ttgcagctta
1801  taatggttac aaataaagca atagcatcac aaatttcaca aataaagcat ttttttcact
1861  gcattctagt tgtggtttgt ccaaactcat caatgtatct taaggcgtaa attgtaagcg
1921  ttaatatttt gttaaaattc gcgttaaatt tttgttaaat cagctcattt tttaaccaat
1981  aggccgaaat cggcaaaatc ccttataaat caaaagaata gaccgagata gggttgagtg
2041  ttgttccagt ttggaacaag agtccactat taaagaacgt ggactccaac gtcaaagggc
2101  gaaaaaccgt ctatcagggc gatggcccac tacgtgaacc atcaccctaa tcaagttttt
2161  tggggtcgag gtgccgtaaa gcactaaatc ggaaccctaa agggagcccc cgatttagag
2221  cttgacgggg aaagccggcg aacgtggcga gaaaggaagg gaagaaagcg aaaggagcgg
2281  gcgctagggc gctggcaagt gtagcggtca cgctgcgcgt aaccaccaca cccgccgcgc
2341  ttaatgcgcc gctacagggc gcgtcaggtg gcacttttcg gggaaatgtg cgcggaaccc
2401  ctatttgttt atttttctaa atacattcaa atatgtatcc gctcatgaga caataaccct
2461  gataaatgct tcaataatat tgaaaaagga agagtcctga ggcggaaaga accagctgtg
2521  gaatgtgtgt cagttagggt gtggaaagtc cccaggctcc ccagcaggca gaagtatgca
2581  aagcatgcat ctcaattagt cagcaaccag gtgtggaaag tccccaggct ccccagcagg
2641  cagaagtatg caaagcatgc atctcaatta gtcagcaacc atagtcccgc ccctaactcc
2701  gcccatcccg cccctaactc cgcccagttc cgcccattct ccgccccatg gctgactaat
2761  ttttttttatt tatgcagagg ccgaggccgc ctcggcctct gagctattcc agaagtagtg
2821  aggaggcttt tttggaggcc taggcttttg caaagatcga tcaagagaca ggatgaggat
2881  cgtttcgcat gattgaacaa gatggattgc acgcaggttc tccggccgct tgggtggaga
2941  ggctattcgg ctatgactgg gcacaacaga caatcggctg ctctgatgcc gccgtgttcc
3001  ggctgtcagc gcaggggcgc ccggttcttt ttgtcaagac cgacctgtcc ggtgccctga
3061  atgaactgca agacgaggca gcgcggctat cgtggctggc cacgacgggc gttccttgcg
3121  cagctgtgct cgacgttgtc actgaagcgg gaagggactg gctgctattg ggcgaagtgc
3181  cggggcagga tctcctgtca tctcaccttg ctcctgccga gaaagtatcc atcatggctg
3241  atgcaatgcg gcggctgcat acgcttgatc cggctacctg cccattcgac caccaagcga
3301  aacatcgcat cgagcgagca cgtactcgga tggaagccgg tcttgtcgat caggatgatc
3361  tggacgaaga gcatcagggg ctcgcgccag ccgaactgtt cgccaggctc aaggcgagca
3421  tgcccgacgg cgaggatctc gtcgtgaccc atggcgatgc ctgcttgccg aatatcatgg
3481  tggaaaatgg ccgcttttct ggattcatcg actgtggccg gctgggtgtg gcggaccgct
3541  atcaggacat agcgttggct acccgtgata ttgctgaaga gcttggcggc gaatgggctg
3601  accgcttcct cgtgctttac ggtatcgccg ctcccgattc gcagcgcatc gccttctatc
3661  gccttcttga cgagttcttc tgagcgggac tctggggttc gaaatgaccg accaagcgac
3721  gcccaacctg ccatcacgag atttcgattc caccgccgcc ttctatgaaa ggttgggctt
3781  cggaatcgtt ttccgggacg ccggctggat gatcctccag cgcggggatc tcatgctgga
3841  gttcttcgcc caccctaggg ggaggctaac tgaaacacgg aaggagacaa taccggaagg
3901  aacccgcgct atgacggcaa taaaaagaca gaataaaacg cacggtgttg ggtcgtttgt
3961  tcataaacgc ggggttcggt cccagggctg gcactctgtc gataccccac cgagacccca
4021  ttggggccaa tacgcccgcg tttcttcctt ttccccaccc cacccccaa gttcgggtga
4081  aggcccaggg ctcgcagcca acgtcggggc ggcaggccct gccatagcct caggttactc
4141  atatatactt tagattgatt taaaacttca tttttaattt aaaaggatct aggtgaagat
4201  ccttttttgat aatctcatga ccaaaatccc ttaacgtgag ttttcgttcc actgagcgtc
4261  agaccccgta gaaaagatca aaggatcttc ttgagatcct ttttttctgc gcgtaatctg
4321  ctgcttgcaa acaaaaaaac caccgctacc agcggtggtt tgtttgccgg atcaagagct
4381  accaactctt tttccgaagg taactggctt cagcagagcg cagataccaa atactgtcct
4441  tctagtgtag ccgtagttag gccaccactt caagaactct gtagcaccgc ctacatacct
4501  cgctctgcta atcctgttac cagtggctgc tgccagtggc gataagtcgt gtcttaccgg
4561  gttggactca agacgatagt taccggataa ggcgcagcgg tcgggctgaa cgggggggttc
4621  gtgcacacag cccagcttgg agcgaacgac ctacaccgaa ctgagatacc tacagcgtga
4681  gctatgagaa agcgccacgc ttcccgaagg gagaaaggcg gacaggtatc cggtaagcgg
4741  cagggtcgga acaggagagc gcacgaggga gcttccaggg ggaaacgcct ggtatcttta
4801  tagtcctgtc gggtttcgcc acctctgact tgagcgtcga tttttgtgat gctcgtcagg
4861  ggggcggagc ctatggaaaa acgccagcaa cgcggccttt ttacggttcc tggccttttg
```

```
4921  ctggcctttt gctcacatgt tctttcctgc gttatcccct gattctgtgg ataaccgtat
4981  taccgccatg cattagtt
```

G.4.4.1 Map of p103QHtt.EGFP-N1

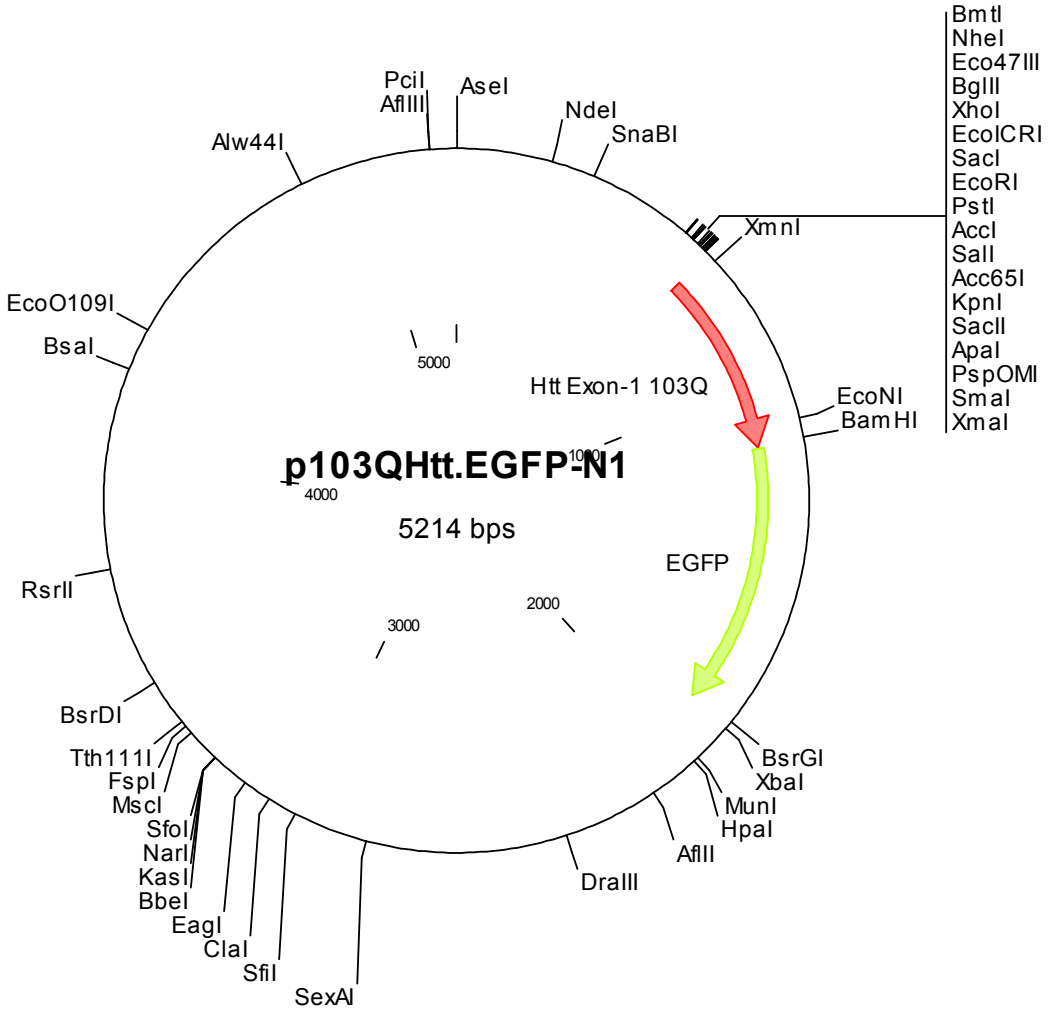

G.4.4.2 Sequence of p103QHtt.EGFP-N1

```
   1  attaatagta atcaattacg gggtcattag ttcatagccc atatatggag ttccgcgtta
  61  cataacttac ggtaaatggc ccgcctggct gaccgcccaa cgacccccgc ccattgacgt
 121  caataatgac gtatgttccc atagtaacgc caatagggac tttccattga cgtcaatggg
 181  tggagtattt acggtaaact gcccacttgg cagtacatca agtgtatcat atgccaagta
 241  cgcccccta tgacgtcaat gacggtaaat ggcccgcctg gcattatgcc cagtacatga
 301  ccttatggga ctttcctact tggcagtaca tctacgtatt agtcatcgct attaccatgg
 361  tgatgcggtt ttggcagtac atcaatgggc gtggatagcg gtttgactca cggggatttc
 421  caagtctcca ccccattgac gtcaatggga gtttgttttg gcaccaaaat caacgggact
 481  ttccaaaatg tcgtaacaac tccgccccat tgacgcaaat gggcggtagg cgtgtacggt
 541  gggaggtcta tataagcaga gctggtttag tgaaccgtca gatccgctag cgctaccgga
 601  ctcagatctc gagctcaagc ttcgaattct gcagtcgacg gtaccgcggg cccgggatca
 661  tggcgaccct ggaaaagctg atgaaggcct tcgagtccct caaaagcttc caacagcagc
 721  aacagcaaca acagcagcaa cagcaacaac agcagcaaca gcaacaacag cagcaacagc
 781  aacaacagca gcaacagcaa caacagcagc aacagcaaca acagcagcaa cagcaacaac
```

```
 841  agcagcaaca gcaacaacag cagcaacagc aacaacagca gcaacagcaa caacagcagc
 901  aacagcaaca acagcagcaa cagcaacaac agcagcaaca gcaacaacag cagcaacagc
 961  aacaacagca gcaacagcaa caacagcagc aacagcaaca accgccacca cctccccctc
1021  caccccacc tcctcaactt cctcaacctc ctccacaggc acagcctctg ctgcctcagc
1081  cacaacctcc tccacctcca cctccacctc ctccaggccc agctgtggct gaggagcctc
1141  tgcaccgacc tggatccctg gtgagcaagg gcgaggagct gttcaccggg gtggtgccca
1201  tcctggtcga gctggacggc gacgtaaacg gccacaagtt cagcgtgtcc ggcgagggcg
1261  agggcgatgc cacctacggc aagctgaccc tgaagttcat ctgcaccacc ggcaagctgc
1321  ccgtgccctg gcccaccctc gtgaccaccc tgacctacgg cgtgcagtgc ttcagccgct
1381  accccgacca catgaagcag cacgacttct tcaagtccgc catgcccgaa ggctacgtcc
1441  aggagcgcac catcttcttc aaggacgacg gcaactacaa gacccgcgcc gaggtgaagt
1501  tcgagggcga caccctggtg aaccgcatcg agctgaaggg catcgacttc aaggaggacg
1561  gcaacatcct ggggcacaag ctggagtaca actacaacag ccacaacgtc tatatcatgg
1621  ccgacaagca gaagaacggc atcaaggtga acttcaagat ccgccacaac atcgaggacg
1681  gcagcgtgca gctcgccgac cactaccagc agaacacccc catcggcgac ggccccgtgc
1741  tgctgcccga caaccactac ctgagcaccc agtccgccct gagcaaagac cccaacgaga
1801  agcgcgatca catggtcctg ctggagttcg tgaccgccgc cgggatcact ctcggcatgg
1861  acgagctgta caagtaaggc cgcgactcta gatcataatc agccatacca catttgtaga
1921  ggttttactt gctttaaaaa acctcccaca cctccccctg aacctgaaac ataaaatgaa
1981  tgcaattgtt gttgttaact tgtttattgc agcttataat ggttacaaat aaagcaatag
2041  catcacaaat ttcacaaata aagcattttt ttcactgcat tctagttgtg gtttgtccaa
2101  actcatcaat gtatcttaag gcgtaaattg taagcgttaa tattttgtta aaattcgcgt
2161  taaatttttg ttaaatcagc tcatttttta accaataggc cgaaatcggc aaaatcccтt
2221  ataaatcaaa agaatagacc gagatagggt tgagtgttgt tccagtttgg aacaagagtc
2281  cactattaaa gaacgtggac tccaacgtca aagggcgaaa aaccgtctat cagggcgatg
2341  gcccactacg tgaaccatca ccctaatcaa gtttttgggg gtcgaggtgc cgtaaagcac
2401  taaatcggaa ccctaaaggg agcccccgat ttagagcttg acggggaaag ccggcgaacg
2461  tggcgagaaa ggaagggaag aaagcgaaag gagcgggcgc tagggcgctg gcaagtgtag
2521  cggtcacgct gcgcgtaacc accacacccg ccgcgcttaa tgcgccgcta cagggcgcgt
2581  caggtggcac ttttcgggga aatgtgcgcg gaacccctat ttgtttattt ttctaaatac
2641  attcaaatat gtatccgctc atgagacaat aaccctgata aatgcttcaa taatattgaa
2701  aaaggaagag tcctgaggcg gaaagaacca gctgtggaat gtgtgtcagt tagggtgtgg
2761  aaagtcccca ggctccccag caggcagaag tatgcaaagc atgcatctca attagtcagc
2821  aaccaggtgt ggaaagtccc caggctcccc agcaggcaga agtatgcaaa gcatgcatct
2881  caattagtca gcaaccatag tcccgccccт aactccgccc atcccgcccc taactccgcc
2941  cagttccgcc cattctccgc cccatggctg actaatttтt tttatttatg cagaggccga
3001  ggccgcctcg gcctctgagc tattccagaa gtagtgagga ggcttttttg gaggcctagg
3061  cttttgcaaa gatcgatcaa gagacaggat gaggatcgtt tcgcatgatt gaacaagatg
3121  gattgcacgc aggttctccg gccgcttggg tggagaggct attcggctat gactgggcac
3181  aacagacaat cggctgctct gatgccgccg tgttccggct gtcagcgcag gggcgcccgg
3241  ttctтttttgt caagaccgac ctgtccggtg ccctgaatga actgcaagac gaggcagcgc
3301  ggctatcgtg gctggccacg acgggcgttc cttgcgcagc tgtgctcgac gttgtcactg
3361  aagcgggaag ggactggctg ctattgggcg aagtgccggg gcaggatctc ctgtcatctc
3421  accttgctcc tgccgagaaa gtatccatca tggctgatgc aatgcggcgg ctgcatacgc
3481  ttgatccggc tacctgccca ttcgaccacc aagcgaaaca tcgcatcgag cgagcacgta
3541  ctcggatgga agccggtctt gtcgatcagg atgatctgga cgaagagcat caggggctcg
3601  cgccagccga actgttcgcc aggctcaagg cgagcatgcc cgacggcgag gatctcgtcg
3661  tgacccatgg cgatgcctgc ttgccgaata tcatggtgga aaatggccgc ttttctggat
3721  tcatcgactg tggccggctg ggtgtggcgg accgctatca ggacatagcg ttggctaccc
3781  gtgatattgc tgaagagctt ggcggcgaat gggctgaccg cttcctcgtg ctttacggta
3841  tcgccgctcc cgattcgcag cgcatcgcct tctatcgcct tcttgacgag ttcttctgag
3901  cgggactctg gggttcgaaa tgaccgacca agcgacgccc aacctgccat cacgagattt
3961  cgattccacc gccgccttct atgaaaggtt gggcttcgga atcgttttcc gggacgccgg
4021  ctggatgatc ctccagcgcg gggatctcat gctggagttc ttcgcccacc ctagggggag
4081  gctaactgaa acacggaagg agacaatacc ggaaggaacc cgcgctatga cggcaataaa
4141  aagacagaat aaaacgcacg gtgttgggtc gtttgttcat aaacgcgggg ttcggtccca
4201  gggctggcac tctgtcgata ccccaccgag accccattgg ggccaatacg cccgcgtttc
4261  ttccttttcc ccaccccacc ccccaagttc gggtgaaggc ccagggctcg cagccaacgt
4321  cggggcggca ggccctgcca tagcctcagg ttactcatat atactttaga ttgatttaaa
4381  acttcatttt taatttaaaa ggatctaggt gaagatcctt tttgataatc tcatgaccaa
4441  aatcccttaa cgtgagtttt cgttccactg agcgtcagac cccgtagaaa agatcaaagg
4501  atcttcttga gatccttttt ttctgcgcgt aatctgctgc ttgcaaacaa aaaaaccacc
4561  gctaccagcg gtggtttgtt tgccggatca agagctacca actcтttttc cgaaggtaac
```

```
4621  tggcttcagc agagcgcaga taccaaatac tgtccttcta gtgtagccgt agttaggcca
4681  ccacttcaag aactctgtag caccgcctac atacctcgct ctgctaatcc tgttaccagt
4741  ggctgctgcc agtggcgata agtcgtgtct taccgggttg gactcaagac gatagttacc
4801  ggataaggcg cagcggtcgg gctgaacggg gggttcgtgc acacagccca gcttggagcg
4861  aacgacctac accgaactga gatacctaca gcgtgagcta tgagaaagcg ccacgcttcc
4921  cgaagggaga aaggcggaca ggtatccggt aagcggcagg gtcggaacag gagagcgcac
4981  gagggagctt ccagggggaa acgcctggta tctttatagt cctgtcgggt ttcgccacct
5041  ctgacttgag cgtcgatttt tgtgatgctc gtcaggggggg cggagcctat ggaaaaacgc
5101  cagcaacgcg gccttttttac ggttcctggc cttttgctgg ccttttgctc acatgttctt
5161  tcctgcgtta tcccctgatt ctgtggataa ccgtattacc gccatgcatt agtt
```

G.4.5.1 Map of p-N1

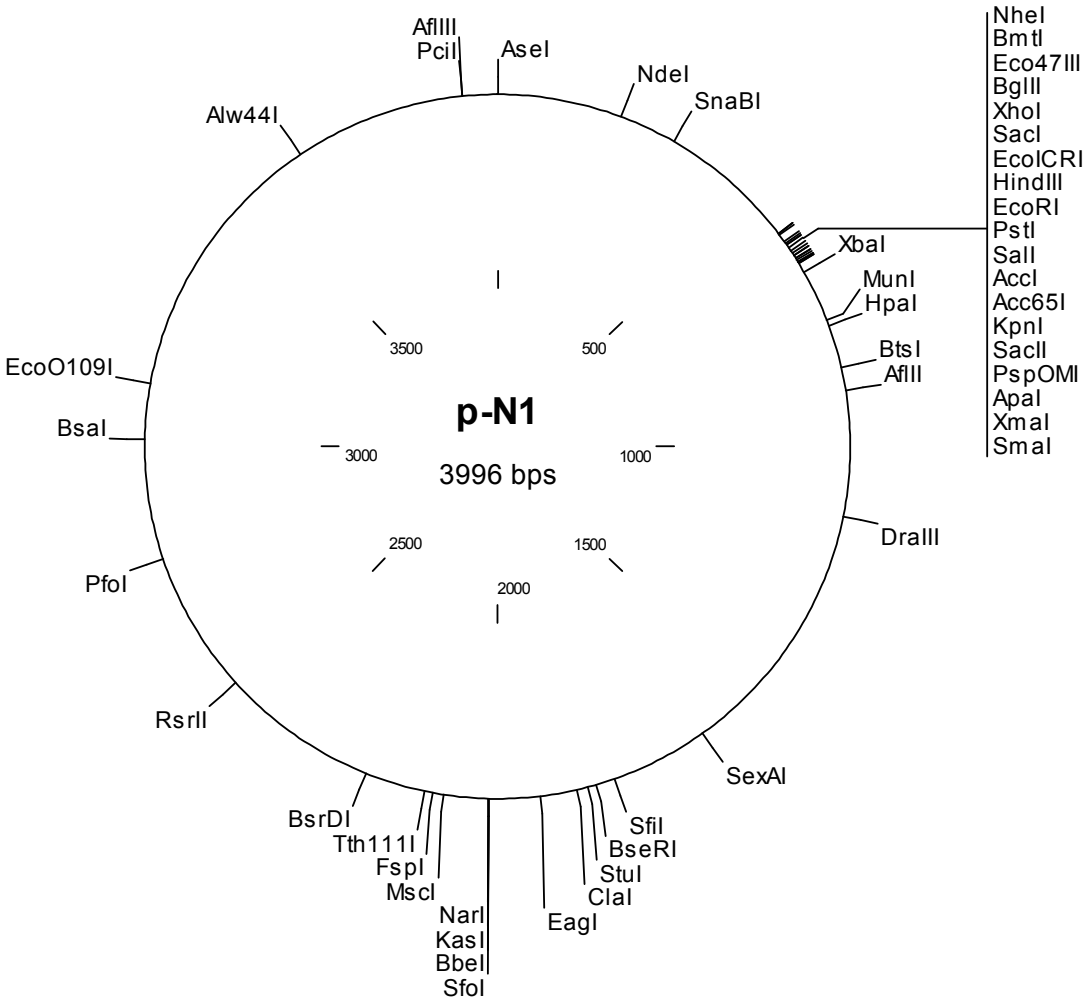

G.4.5.2 Sequence of p-N1

```
   1  gctagcgcta ccggactcag atctcgagct caagcttcga attctgcagt cgacggtacc
  61  gcgggcccgg gatcggccgc gactctagat cataatcagc cataccacat ttgtagaggt
 121  tttacttgct ttaaaaaacc tcccacacct ccccctgaac ctgaaacata aaatgaatgc
 181  aattgttgtt gttaacttgt ttattgcagc ttataatggt tacaaataaa gcaatagcat
```

```
 241  cacaaatttc acaaataaag cattttttc actgcattct agttgtggtt tgtccaaact
 301  catcaatgta tcttaaggcg taaattgtaa gcgttaatat tttgttaaaa ttcgcgttaa
 361  atttttgtta aatcagctca ttttttaacc aataggccga aatcggcaaa atcccttata
 421  aatcaaaaga atagaccgag atagggttga gtgttgttcc agtttggaac aagagtccac
 481  tattaaagaa cgtggactcc aacgtcaaag ggcgaaaaac cgtctatcag ggcgatggcc
 541  cactacgtga accatcaccc taatcaagtt ttttggggtc gaggtgccgt aaagcactaa
 601  atcggaaccc taaagggagc ccccgattta gagcttgacg gggaaagccg gcgaacgtgg
 661  cgagaaagga agggaagaaa gcgaaaggag cgggcgctag ggcgctggca agtgtagcgg
 721  tcacgctgcg cgtaaccacc acacccgccg cgcttaatgc gccgctacag ggcgcgtcag
 781  gtggcacttt tcggggaaat gtgcgcggaa cccctatttg tttatttttc taaatacatt
 841  caaatatgta tccgctcatg agacaataac cctgataaat gcttcaataa tattgaaaaa
 901  ggaagagtcc tgaggcggaa agaaccagct gtggaatgtg tgtcagttag ggtgtggaaa
 961  gtccccaggc tccccagcag gcagaagtat gcaaagcatg catctcaatt agtcagcaac
1021  caggtgtgga aagtccccag gctccccagc aggcagaagt atgcaaagca tgcatctcaa
1081  ttagtcagca accatagtcc cgcccctaac tccgcccatc ccgcccctaa ctccgcccag
1141  ttccgcccat tctccgcccc atggctgact aatttttttt atttatgcag aggccgaggc
1201  cgcctcggcc tctgagctat tccagaagta gtgaggaggc ttttttggag gcctaggctt
1261  ttgcaaagat cgatcaagag acaggatgag gatcgtttcg catgattgaa caagatggat
1321  tgcacgcagg ttctccggcc gcttgggtgg agaggctatt cggctatgac tgggcacaac
1381  agacaatcgg ctgctctgat gccgccgtgt tccggctgtc agcgcagggg cgcccggttc
1441  tttttgtcaa gaccgacctg tccggtgccc tgaatgaact gcaagacgag gcagcgcggc
1501  tatcgtggct ggccacgacg ggcgttcctt gcgcagctgt gctcgacgtt gtcactgaag
1561  cgggaaggga ctggctgcta ttgggcgaag tgccggggca ggatctcctg tcatctcacc
1621  ttgctcctgc cgagaaagta tccatcatgg ctgatgcaat gcggcggctg catacgcttg
1681  atccggctac ctgcccattc gaccaccaag cgaaacatcg catcgagcga gcacgtactc
1741  ggatggaagc cggtcttgtc gatcaggatg atctggacga agagcatcag gggctcgcgc
1801  cagccgaact gttcgccagg ctcaaggcga gcatgcccga cggcgaggat ctcgtcgtga
1861  cccatggcga tgcctgcttg ccgaatatca tggtggaaaa tggccgcttt tctggattca
1921  tcgactgtgg ccggctgggt gtggcggacc gctatcagga catagcgttg gctacccgtg
1981  atattgctga agagcttggc ggcgaatggg ctgaccgctt cctcgtgctt tacggtatcg
2041  ccgctcccga ttcgcagcgc atcgccttct atcgccttct tgacgagttc ttctgagcgg
2101  gactctgggg ttcgaaatga ccgaccaagc gacgcccaac ctgccatcac gagatttcga
2161  ttccaccgcc gccttctatg aaaggttggg cttcggaatc gttttccggg acgccggctg
2221  gatgatcctc cagcgcgggg atctcatgct ggagttcttc gcccacccta gggggaggct
2281  aactgaaaca cggaaggaga caataccgga aggaacccgc gctatgacgg caataaaaag
2341  acagaataaa acgcacggtg ttgggtcgtt tgttcataaa cgcggggttc ggtcccaggg
2401  ctggcactct gtcgataccc caccgagacc ccattggggc caatacgccc gcgtttcttc
2461  cttttcccca ccccaccccc caagttcggg tgaaggccca gggctcgcag ccaacgtcgg
2521  ggcggcaggc cctgccatag cctcaggtta ctcatatata ctttagattg atttaaaact
2581  tcatttttaa tttaaaagga tctaggtgaa gatccttttt gataatctca tgaccaaaat
2641  cccttaacgt gagttttcgt tccactgagc gtcagacccc gtagaaaaga tcaaaggatc
2701  ttcttgagat cctttttttc tgcgcgtaat ctgctgcttg caaacaaaaa aaccaccgct
2761  accagcggtg gtttgtttgc cggatcaaga gctaccaact ctttttccga aggtaactgg
2821  cttcagcaga gcgcagatac caaatactgt ccttctagtg tagccgtagt taggccacca
2881  cttcaagaac tctgtagcac cgcctacata cctcgctctg ctaatcctgt taccagtggc
2941  tgctgccagt ggcgataagt cgtgtcttac cgggttggac tcaagacgat agttaccgga
3001  taaggcgcag cggtcgggct gaacgggggg ttcgtgcaca cagcccagct tggagcgaac
3061  gacctacacc gaactgagat acctacagcg tgagctatga gaaagcgcca cgcttcccga
3121  agggagaaag gcggacaggt atccggtaag cggcagggtc ggaacaggag agcgcacgag
3181  ggagcttcca gggggaaacg cctggtatct ttatagtcct gtcgggtttc gccacctctg
3241  acttgagcgt cgatttttgt gatgctcgtc agggggggcgg agcctatgga aaaacgccag
3301  caacgcggcc tttttacggt tcctggcctt ttgctggcct tttgctcaca tgttctttcc
3361  tgcgttatcc cctgattctg tggataaccg tattaccgcc atgcattagt tattaatagt
3421  aatcaattac ggggtcatta gttcatagcc catatatgga gttccgcgtt acataactta
3481  cggtaaatgg cccgcctggc tgaccgccca acgacccccg cccattgacg tcaataatga
3541  cgtatgttcc catagtaacg ccaataggga ctttccattg acgtcaatgg gtggagtatt
3601  tacggtaaac tgcccacttg gcagtacatc aagtgtatca tatgccaagt acgcccccta
3661  ttgacgtcaa tgacggtaaa tggcccgcct ggcattatgc ccagtacatg accttatggg
3721  actttcctac ttggcagtac atctacgtat tagtcatcgc tattaccatg gtgatgcggt
3781  tttggcagta catcaatggg cgtggatagc ggtttgactc acggggattt ccaagtctcc
3841  accccattga cgtcaatggg agtttgtttt ggcaccaaaa tcaacgggac tttccaaaat
3901  gtcgtaacaa ctccgcccca ttgacgcaaa tgggcggtag gcgtgtacgg tgggaggtct
3961  atataagcag agctggttta gtgaaccgtc agatcc
```